



**Investigation of the biosynthesis of lutein epoxide  
and the roles of  $\alpha$ -branch carotenoids in  
photoprotection and photoacclimation**

Inaugural-Dissertation

Zur

Erlangung des Doktorgrades der

Mathematisch-Naturwissenschaftlichen Fakultät

der Heinrich-Heine-Universität Düsseldorf

vorgelegt von

**Rosanna Caliandro**

aus **Bari**

**November 2011**

Aus dem Institut für Bio- und Geowissenschaften 2:  
Pflanzenwissenschaften (IBG-2), Forschungszentrum Jülich GmbH

Gedruckt mit Genehmigung der  
Mathematisch-Naturwissenschaftlichen Fakultät der  
Heinrich-Heine-Universität Düsseldorf

Referent: Prof. Dr. Ulrich Schurr  
Koreferent: Prof. Dr. Peter Jahns  
Tag der mündlichen Prüfung:

## **Selbstständigkeitserklärung**

Hiermit erkläre ich, dass ich die vorliegende Dissertation eigenständig und ohne fremde Hilfe angefertigt habe. Arbeiten Dritter wurden entsprechend zitiert. Diese Dissertation wurde bisher in dieser oder ähnlicher Form noch bei keiner anderen Institution eingereicht. Ich habe bisher keine erfolglosen Promotionsversuche unternommen.

Jülich, den 21.11.2011

---

Rosanna Caliandro

## **Statement of authorship**

I hereby certify that this dissertation is the result of my own work. No other person's work has been used without due acknowledgement. This dissertation has not been submitted in the same or similar form to other institutions. I have not previously failed a doctoral examination procedure.

To my father

*“Fatti non foste a viver come bruti,  
ma per seguir virtute e canoscenza”*

*Dante Alighieri*

## Publications during the PhD

Matsubara, S., Chen, Y.-C., Caliandro, R., Govindjee, Clegg, R.M. (2011). Photosystem II fluorescence lifetime imaging in avocado leaves: Contributions of the lutein-epoxide and violaxanthin cycles to fluorescence quenching. *Journal of Photochemistry and Photobiology B: Biology* doi:10.1016/j.photobiol.2011.01.003

Caliandro, R., Nagel, A.K., Kastenholz, B.-J., Bassi, R., Pogson, B. J., Schurr, U., Matsubara, S. (submitted). Effects of altered  $\alpha$ - and  $\beta$ - branch carotenoid biosynthesis on acclimation of *Arabidopsis* to photo-oxidative stress induced by short sunflecks

## Presentations at international conferences

Poster presentation at the 15th International Congress on Photosynthesis in Beijing:

Caliandro, R., Bassi, R., Pogson, B. J., Schurr, U., Matsubara, S. (2010) "Roles of the  $\alpha$ -branch carotenoids in photoprotection and photoacclimation under fluctuating light "

Poster presentation at the Botanikertagung 2011 in Berlin:

Caliandro, R., Wiese-Klinkenberg, A., Janzik, I., Schurr, U., Matsubara, S. (2011) "Investigation of the role of zeaxanthin epoxidase in the lutein epoxide cycle"

## Summary

Carotenoids (carotenes and xanthophylls) are essential components of the photosynthetic apparatus and play important roles in protein assembly, light harvesting and photoprotection. The carotenoid composition in higher-plant photosystems has been conserved throughout evolution, suggesting indispensable functions for each pigment. All higher plants can accumulate  $\beta$ -carotene ( $\beta$ -car), zeaxanthin (Z), antheraxanthin (A), violaxanthin (V) and neoxanthin (N) (synthesized in the  $\beta$ -branch of the carotenoid biosynthetic pathway) as well as lutein (L) (synthesized in the  $\alpha$ -branch) in leaves. Two additional carotenoids,  $\alpha$ -carotene ( $\alpha$ -car) and lutein epoxide (Lx), have been found in some taxa, especially rich in shade leaves of tropical rainforest plants.

Violaxanthin and Lx are involved in the operation of the V-cycle and Lx-cycle (xanthophyll cycles), which play an important role in regulation of light harvesting and photoprotection. In high-light condition, V and Lx are de-epoxidised by the enzyme V de-epoxidase (VDE), leading to the formation of Z and L, respectively. In the absence of high light, Z is converted back to V by the membrane-associated enzyme Z epoxidase (ZEP), which is thought to be responsible also for the conversion of L to Lx in the species having Lx in leaves.

In order to investigate the role of ZEP in both xanthophyll cycles, cDNA of one of the two putative ZEP isoforms (*ImZep1*) was isolated from leaves of *Inga marginata*, a tropical legume tree that accumulates large amounts of Lx in shade leaves. For *in-vitro* studies on enzyme activity, two different expression systems have been tried for heterologous expression of *ImZep1*: *Rhodobacter capsulatus* and *Escherichia coli*. Due to its physiological properties, *R. capsulatus* is particularly suited for expression of membrane proteins. However, ZEP proteins could not be detected in this expression system. On the other hand, ZEP protein of *I. marginata* could be successfully expressed in the *E. coli* expression system.

*ImZep1* was then expressed in a ZEP-deficient mutant (*npq2* mutant) and a L-overaccumulating mutant (*szl1npq1* mutant) of *Arabidopsis thaliana* to examine *in vivo* the activity and substrate specificity of its gene product. No Lx has been detected in any of the transgenic lines, although the functionality of the enzyme inserted was confirmed by the accumulation of N, V and A which are synthesized by epoxidation of Z and further reactions in the downstream. One of the transgenic lines, 20.72, showing dark retention of Z due to somewhat lower activity of ImZEP1, revealed a role of Z in a slowly reversible component of NPQ (qI).

The functions of  $\alpha$ -branch carotenoids (L and  $\alpha$ -car) in photoprotection and photoacclimation were also investigated in this work by using the *A. thaliana* mutants *lut2*, *lut5*, *npq1* and *szl1npq1*. The plants of *lut2* have no L but increased amounts of  $\beta$ -branch carotenoids; *lut5* plants accumulate  $\alpha$ -car at the expense of  $\beta$ -car and xanthophylls; *npq1* is deficient in VDE activity and thus cannot synthesize Z; *szl1npq1* is characterized by low levels of all  $\beta$ -branch carotenoids and remarkably high accumulation of L along with the presence of  $\alpha$ -car.

Photo-oxidative stress was applied to these mutants and wild-type plants (wt) by exposing to short-lasting sunflecks, a type of light stress frequently found in shade environments. A reduction of chlorophyll (Chl) content was observed in all plants, but more severely in those having high  $\alpha$ - to  $\beta$ -branch carotenoid composition ( $\alpha/\beta$ -ratio) (*lut5*, *szl1npq1*). The decrease in Chl amount was accompanied by an increase in xanthophylls in the mutants with high  $\alpha/\beta$ -ratios (*lut5*, *szl1npq1*) or without xanthophyll-cycle operation (*npq1*, *szl1npq1*). The PsbS protein level increased in all sunfleck plants but *lut2*. No change in NPQ were observed in *npq1*, *szl1npq1* plants after the sunfleck treatment, while, in the same condition, wt and *lut5* showed enhanced NPQ capacity together with decrease in leaf mass per area. The sunflecks decelerated primary root growth in wt and *npq1* having normal  $\alpha/\beta$ -ratios, but suppressed lateral root formation in *lut5* and *szl1npq1* having high  $\alpha/\beta$ -ratios. The results highlighted the importance of proper regulation of the  $\alpha$ - and  $\beta$ -branch carotenoid pathways for whole-plant acclimation, not only leaf photoprotection, under photo-oxidative stress.

## Zusammenfassung

Carotinoide (Carotine und Xanthophylle) sind essentielle Komponenten des Photosyntheseapparates und spielen eine wichtige Rolle beim Zusammenbau von Proteinen, der Lichtsammlung und der Photoprotektion. Die Zusammensetzung der Carotinoide der Photosysteme höherer Pflanzen blieb im Laufe der Evolution erhalten, was auf eine unverzichtbare Aufgabe der einzelnen Pigmente schließen lässt. Alle höheren Pflanzen können  $\beta$ -Carotin ( $\beta$ -car), Zeaxanthin (Z), Antheraxanthin (A), Violaxanthin (V) und Neoxanthin (N) (synthetisiert im  $\beta$ -Zweig der Carotinoid-Biosynthese) sowie Lutein (L) (synthetisiert im  $\alpha$ -Zweig der Carotinoid-Biosynthese) in Blättern akkumulieren. Zwei weitere Carotinoide,  $\alpha$ -Carotin ( $\alpha$ -car) und Lutein-Epoxid (Lx), wurden in einigen Taxa gefunden, besonders hohe Konzentrationen wurden in Schattenblättern von Pflanzen tropischer Regenwälder entdeckt.

Violaxanthin und Lx sind an dem Ablauf des V-Zyklus und Lx-Zyklus (Xanthophyllzyklen) beteiligt, die in der Regulation der Lichtsammlung und der Photoprotektion eine wichtige Rolle spielen. Bei hohen Lichtstärken werden V und Lx durch das Enzym V-Deepoxidase (VDE) deepoxidiert, wodurch Z und L gebildet werden. In schwachem Licht wird Z durch die Katalyse des membrangebundenen Enzyms Z-Epoxidase (ZEP) wieder zu V umgewandelt, das wahrscheinlich auch für die Umwandlung von L zu Lx in Spezies mit Lx-haltigen Blättern verantwortlich ist.

Um die Bedeutung von ZEP in beiden Xanthophyllzyklen zu untersuchen, wurde cDNA von einem der beiden mutmaßlichen ZEP Isoformen (*ImZep1*) aus den Blättern von *Inga marginata*, einem tropischen Leguminosebaum mit großen Mengen an Lx in Schattenblättern, isoliert. Für *in-vitro* Untersuchungen der Enzymaktivitäten wurden zwei unterschiedliche Expressionssysteme für die heterologe Expression von *ImZep1* eingesetzt: *Rhodobacter capsulatus* und *Escherichia coli*. Aufgrund der physiologischen Eigenschaften ist *R. capsulatus* insbesondere für die Expression von Membranproteinen geeignet. Allerdings konnte das ZEP Protein nicht mit diesem Expressionssystem detektiert werden. Dagegen konnte das ZEP Protein von *I. marginata* im *E. coli*-Expressionssystem erfolgreich exprimiert werden.

*ImZep1* wurde dann in einem ZEP-Mangel Mutanten (*npq2* Mutant) und in einem L-überakkumulierenden Mutanten (*sz1npq1* mutant) von *Arabidopsis thaliana* exprimiert, um die *in-vivo* Aktivität und Substratspezifität von dessen Genprodukt zu untersuchen. In keinem der transgenen Linien wurde Lx gefunden, obwohl die Funktionalität des eingebrachten Enzyms durch

die Akkumulation von N, V und A bestätigt wurde, die durch die Epoxidation von Z synthetisiert werden, sowie durch weitere Reaktionen im Downstream. Einer der transgenen Linien, 20.72, die eine Speicherung von Z im Dunkeln aufgrund der etwas niedrigeren Aktivität von *lmZEP1* aufwies, zeigte dass Z in einer langsamen reversiblen Komponente von NPQ (qI) involviert ist.

Die Rolle der Carotinoide des  $\alpha$ -Zweigs (L und  $\alpha$ -car) bei der Photoprotektion und Photoaklimation wurden auch in dieser Arbeit untersucht, wobei die *A. thaliana* Mutanten *lut2*, *lut5*, *npq1* und *szl1npq1* verwendet wurden. Die Pflanzen von *lut2* haben kein L, jedoch höhere Mengen an Carotinoide des  $\beta$ -Zweigs; *lut5* Pflanzen akkumulieren  $\alpha$ -car auf Kosten von  $\beta$ -car und Xanthophylle; *npq1* hat eine unzureichende VDE-Aktivität und kann deshalb kein Z synthetisieren; *szl1npq1* wird durch niedrige Gehalte aller Carotinoiden des  $\beta$ -Zweigs und außergewöhnlich hoher Akkumulation von L in der Anwesenheit von  $\alpha$ -car charakterisiert.

Photooxidativer Stress wurde an diesen Mutanten und Wildtyp-Pflanzen (wt) angewandt, indem sie kurzzeitig Licht ausgesetzt wurden. Diese Art von Lichtstress tritt regelmäßig in schattigen Umgebungen auf. Eine Reduktion des Chlorophyll(Chl)-Gehaltes wurde in allen Pflanzen beobachtet, besonders in denen, die hohe  $\alpha$ - zu  $\beta$ -Zweig Carotinoid Verhältnisse ( $\alpha/\beta$ -Verhältnis) aufweisen (*lut5*, *szl1npq1*). Eine Abnahme der Chl-Menge wurde entweder von einer Zunahme der Xanthophylle in den Mutanten mit hohen  $\alpha/\beta$ -Verhältnissen begleitet (*lut5*, *szl1npq1*) oder ohne Xanthophyllzyklus-Abläufen (*npq1*, *szl1npq1*). Der PsbS Proteingrad stieg in allen kurzzeitig mit Licht exponierten Pflanzen an, abgesehen von *lut2*. Keine Änderung des NPQ konnte in *npq1*, *szl1npq1* Pflanzen nach der kurzen Lichtexposition beobachtet werden, während unter den gleichen Bedingungen wt und *lut5* eine erweiterte NPQ Kapazität zusammen mit einer Abnahme der Blattmasse pro Fläche aufwiesen. Die kurze Lichtexposition verlangsamte das primäre Wurzelwachstum in wt und *npq1* mit normalen  $\alpha/\beta$ -Verhältnissen, wohingegen in *lut5* und *szl1npq1* mit hohen  $\alpha/\beta$ -Verhältnissen die laterale Wurzelbildung unterdrückt wurde. Die Ergebnisse verdeutlichen die Bedeutung einer korrekten Regulation der  $\alpha$ - und  $\beta$ -Zweige der Carotinoidbildung für die Akklimatisierung der gesamten Pflanze, und nicht nur für die Photoprotektion der Blätter unter photooxidativem Stress.

## Table of Content

|   |    |
|---|----|
| 1 Introduction .....  | 1  |
| 1.1 Photosynthesis .....  | 1  |
| 1.2 Photosystems .....  | 2  |
| 1.3 High Light stress and photoprotection.....  | 3  |
| 1.4 Mechanism of non-photochemical quenching (NPQ).....                                   | 4  |
| 1.5 Carotenoids in photosynthesis.....  | 5  |
| 1.6 Lutein epoxide cycle .....  | 9  |
| 1.7 Zeaxanthin epoxidase.....   | 10 |
| 1.8 Motivation .....  | 13 |
| 2 Materials and Methods.....  | 14 |
| 2.1 Chemicals.....  | 17 |
| 2.2 Cultivation of biological material .....  | 18 |
| 2.2.1 Phototropic growth of <i>R. capuslatus</i> under high light condition .....         | 18 |
| 2.2.2 Cultivation of <i>E. coli</i> and <i>A. tumefaciens</i> strains .....               | 19 |
| 2.2.3 Plant material .....  | 19 |
| 2.2.4 Light treatments .....  | 20 |
| 2.2.4.a Sunfleck treatment .....  | 20 |
| 2.2.4.b High-light treatment .....  | 21 |
| 2.3 Molecular biological methods.....   | 21 |
| 2.3.1 RNA isolation from leaves of <i>A. thaliana</i> and <i>I. marginata</i> plants..... | 21 |
| 2.3.2 cDNA synthesis .....  | 21 |
| 2.3.3 Genomic DNA isolation from <i>A. thaliana</i> transformed plants .....              | 21 |
| 2.3.4 PCR (Polymerase Chain Reaction) .....   | 22 |
| 2.3.5 RACE-PCR (Rapid Amplification of cDNA Ends) .....                                   | 23 |
| 2.3.6 DNA extraction from agarose gel .....   | 23 |
| 2.3.7 Purification of PCR products.....   | 24 |
| 2.3.8 Cloning of PCR products .....   | 24 |
| 2.3.8.a TOPO TA cloning system .....  | 24 |
| 2.3.8.b Cloning into pGWB2 vector via Gateway sites .....                                 | 24 |
| 2.3.8.c Cloning into pUC18 vector .....   | 24 |
| 2.3.8.d Cloning into pRhotHi-2 vector .....   | 24 |

|   |    |
|---|----|
| 2.3.8.e Transformation of <i>E. coli</i> DH5- $\alpha$ .....  | 25 |
| 2.3.8.f Transformation of <i>E. coli</i> strain S17-1 and BL21 (DE3) cells.....                                       | 25 |
| 2.3.8.g Induced gene expression in <i>E. coli</i> BL21 (DE3).....   | 26 |
| 2.3.8.h Conjugation transfer of plasmidic DNA from <i>E. coli</i> to <i>R. capsulatus</i> (Elhai and Wolk 1988) ..... | 26 |
| 2.3.8.i Transformation of <i>A. tumefaciens</i> GV3101 .....  | 26 |
| 2.3.8.j Colony PCR .....  | 27 |
| 2.3.8.k Plasmid mini preparation .....  | 27 |
| 2.3.8.l Sequence analysis of nucleotides .....  | 27 |
| 2.3.9 Northern Blotting.....  | 27 |
| 2.3.10 DIG (Digoxigenin) labeling of probes.....  | 28 |
| 2.3.11 Real-time-PCR analysis of <i>R. capsulatus</i> transformed cells.....  | 29 |
| 2.3.11.a RNA extraction from <i>R. capsulatus</i> .....   | 29 |
| 2.3.11.b Reverse transcription from extracted RNA and real-time PCR .....   | 29 |
| 2.4 Transformation of <i>A. thaliana</i> .....  | 31 |
| 2.4.1 Floral dipping transformation.....  | 31 |
| 2.4.2 Seed sterilization .....  | 31 |
| 2.4.3 Seeds germination on selective agarose plates .....   | 31 |
| 2.5 Biochemical methods .....   | 32 |
| 2.5.1 Western blot of <i>R. capsulatus</i> proteins .....   | 32 |
| 2.5.1.a Protein isolation from <i>R. capsulatus</i> (Katzke <i>et al.</i> 2009).....                                  | 32 |
| 2.5.1.b SDS polyacrylamid gelelectrophoresis (SDS-PAGE) .....   | 32 |
| 2.5.1.c Coomassie blue staining (Merril 1990) .....   | 33 |
| 2.5.1.d Protein transfer to polyvinylidenfluorid (PVDF) membrane .....  | 33 |
| 2.5.1.e Immunodetection of proteins.....  | 33 |
| 2.5.1.f Staining of PVDF membrane .....   | 34 |
| 2.5.2 Western blot of <i>A. thaliana</i> proteins.....  | 34 |
| 2.5.2.a Protein isolation from <i>A. thaliana</i> leaves .....  | 34 |
| 2.5.2.b SDS PAGE.....   | 34 |
| 2.5.2.c Protein transfer to a nitrocellulose membrane .....   | 35 |
| 2.5.2.d Immunodetection of the proteins .....   | 35 |
| 2.6 Photometric determination of total chlorophyll.....   | 35 |
| 2.7 HPLC (High Performance Liquid Chromatography) analysis .....  | 36 |

|   |    |
|---|----|
| 2.8 Plant physiological methods .....   | 37 |
| 2.8.1 Chlorophyll <i>a</i> fluorescence analysis .....  | 37 |
| 2.8.2 Analysis of leaf growth with GROWSCREEN FLUORO (Jansen <i>et al.</i> 2009) .....  | 37 |
| 2.8.3 Analysis of root growth with GROWSCREEN-ROOT (Nagel <i>et al.</i> 2009).....  | 38 |
| 2.8.4 Determination of leaf dry mass .....  | 38 |
| 2.8.5 Seed harvesting from sunfleck treated plants .....  | 38 |
| 2.9 Statistical data analysis .....   | 39 |
| 3 Results .....   | 40 |
| 3.1 Investigation of the role of <i>I. marginata</i> ZEP (ImZEP) in the Lx-cycle and its regulation in the V-cycle .....                      | 40 |
| 3.1.1 Isolation of the Zep isoform 1 ( <i>ImZep1</i> ) cDNA from <i>I. marginata</i> leaves .....   | 40 |
| 3.1.2 Isolation of <i>ImZep1</i> splice variant ( <i>ImZep1_splice</i> ) from <i>I. marginata</i> leaves .....                                | 46 |
| 3.1.3 Heterologous Expression of <i>I. marginata</i> and <i>A. thaliana</i> Zep in <i>R. capsulatus</i> and <i>E. coli</i> .....              | 46 |
| 3.1.4 <i>ImZep1</i> heterologous expression in <i>A. thaliana npq2</i> mutants .....  | 50 |
| 3.1.5 <i>ImZep1</i> heterologous expression in <i>A. thaliana szl1npq1</i> mutants .....  | 56 |
| 3.1.6 Investigation <i>in vivo</i> of ImZEP1 activity in the transgenic lines 20.72 and 24.75.....  | 58 |
| 3.2 Roles of $\alpha$ -branch carotenoids in photoprotection and photoacclimation under fluctuating light.....                                | 65 |
| 3.2.1 Effect of sunfleck treatment on the pigment composition of wt, <i>lut2</i> , <i>lut5</i> , <i>npq1</i> and <i>szl1npq1</i> mutants..... | 66 |
| 3.2.2 PSII activity and PsbS protein level under sunfleck condition.....  | 71 |
| 3.2.3 Growth analysis of wt and carotenoid mutants under fluctuating light .....  | 75 |
| 4 Discussion.....   | 80 |
| 4.1 Does ZEP synthesize Lx? .....   | 80 |
| 4.2 Regulation of ImZEP activity.....   | 82 |
| 4.3 Effect of Z retention in the transgenic line 20.72 .....  | 84 |
| 4.4 Role of L and $\alpha$ -carotene in photoprotection under fluctuating light .....   | 86 |
| 4.4.1 Responses of the pigment composition to fluctuating light .....   | 88 |
| 4.4.2 Effect of fluctuating light on PSII .....   | 90 |
| 4.4.3 Effect of fluctuating light on growth .....   | 92 |
| 5 Conclusion .....  | 95 |
| 6 Reference .....   | 96 |

|   |     |
|---|-----|
| 8 List of abbreviations.....                  | 108 |
| 9 Supplementary material .....                | 111 |
| 9.1 <i>ImZep1</i> cDNA sequence.....          | 111 |
| 9.2 <i>ImZep1_splice</i> cDNA sequence.....   | 112 |
| 9.3 <i>ImZep2</i> partial cDNA sequence ..... | 112 |
| 10 List of tables and figures .....           | 113 |

# 1 Introduction

## 1.1 Photosynthesis

Photosynthesis is the process by which plants use light energy to drive the synthesis of organic compounds. Beside light, as energy source, water and carbon dioxide from the atmosphere are required for this process. The organic compounds produced by photosynthesis include carbohydrate, lipids and proteins, all of which serve as food for all living creatures (Bacon Ke 2001).

The photosynthetic reactions occur inside chloroplasts. The entire process is divided into two stages - the "light reactions", which consist of electron and proton transfer reactions, and the "dark reactions", which consist of the biosynthesis of carbohydrate from CO<sub>2</sub>.

The light reactions take place in a complex membrane system located inside the chloroplasts: the thylakoids. Two photosystems, photosystem I (PSI) and photosystem II (PSII), are embedded in the thylakoids, linked by the cytochrome *b<sub>6</sub>f* complex and by mobile electron carriers. The light energy is captured by the PSI and PSII antenna systems (light harvesting complexes, LHC), containing chlorophylls and carotenoids, and then transferred to the photosynthetic reaction centers (RC). Electrons are derived from water molecules in the oxygen evolving complex of PSII, with production of molecular oxygen, and transported through cytochrome *b<sub>6</sub>f* and PSI to ultimately reduce NADP<sup>+</sup> to NADPH. The reactions in the electron transport are coupled with production of proton in the chloroplast lumen (water splitting) and transport of proton from the stroma to the lumen at cytochrome *b<sub>6</sub>f*, leading to generation of a proton gradient across the thylakoid membranes ( $\Delta pH$ ) which is necessary for the synthesis of ATP (Govindjee *et al.* 2010).

## 1.2 Photosystems

The PSII is a multisubunit complex consisting of more than 20 different proteins. It is composed of a central reaction center core surrounded by a light-harvesting antenna system. The RC is formed by D1 and D2 proteins which bind all the cofactors of the electron transport within the PSII. Two core antenna complexes, CP47 and CP43 chlorophyll (Chl) *a* and carotene binding proteins, are linked to the RC and can be distinguished from the major light harvesting complex of PSII (LHCII), which consists of Chl *a/b* and xanthophyll binding proteins (Lhcb1, Lhcb2 and Lhcb3) organized in homo or heterotrimers. In addition, monomeric minor antenna complexes CP29, CP26 and CP24 (Lhcb4, Lhcb5 and Lhcb6, respectively) are located between the core complex and LHCII (Fig. 1.1.1) (Green and Durnford 1996; Hakamer *et al.* 1997; Govindjee *et al.* 2010).

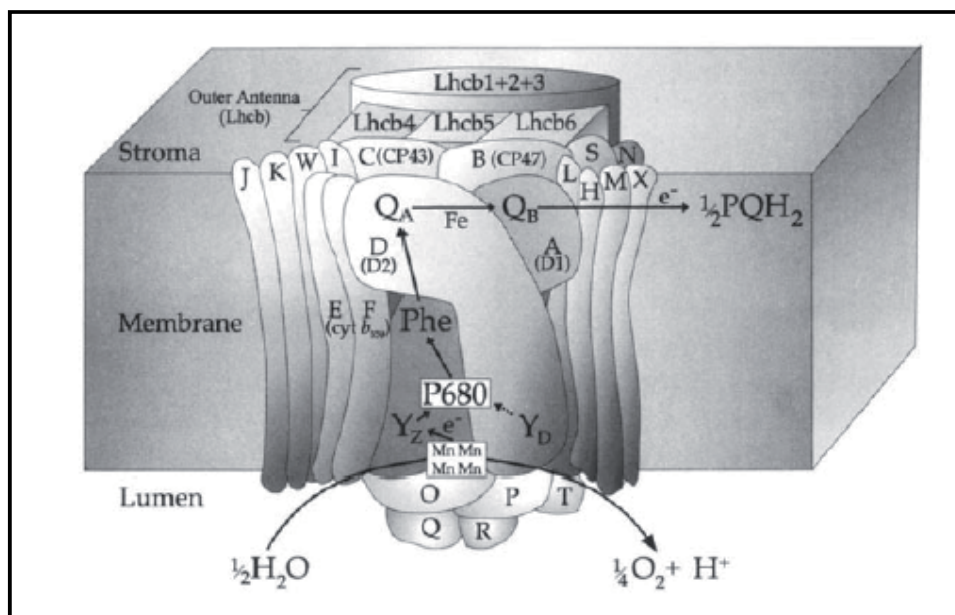


**Figure 1.2.1: Photosystem II (modified from Hakamer *et al.* 1997).** Organization of the protein subunits of LHC and reaction center of PSII (see text for explanation). The electron transport is marked with arrows. Cofactors involved in the electron flow through PSII are shown: Y<sub>z</sub> and Y<sub>d</sub>, tyrosine residues of D1 protein; P680, PSII primary electron donor; Phe, pheophytin; Q<sub>A</sub> and Q<sub>B</sub>, plastoquinone molecules; PQH<sub>2</sub>, reduced plastoquinone

The core complex of PSI consists of 12 protein subunits and two high molecular mass subunits, PsaA and PsaB which form a dimer and bind the majority of pigments (Amunts *et al.* 2010). The outer light harvesting antenna, LHCI, is composed of 4-6 proteins (Lhca proteins) bound to one side of each PSI core unit (Jensen *et al.* 2007).

### 1.3 High Light stress and photoprotection

Even though light is necessary as energy source for the activation of the electron transport chain, the efficiency of photosynthesis ( $\Phi_{\text{PSII}}$ , often measured as Chl fluorescence ratios) can be significantly reduced when plants are exposed to high light. When light is in excess of that required for driving photosynthesis, it causes damage mainly to PSII by forming highly toxic reactive oxygen species. This (photo-)oxidative stress brings to the damage to the PSII RC, in particular of the D1 protein (Aro *et al.* 1993).

Both PSII and PSI are sites for the generation of reactive oxygen species (ROS) in chloroplasts; at PSII level over-reduction of the photosynthetic electron transport chain, caused by excess light, brings to the formation of triplet chlorophyll ( $^3\text{Chl}^*$ ) which can transfer its excitation energy to molecular oxygen, forming singlet oxygen ( $^1\text{O}_2$ ) (Triantaphyllidès and Havaux 2009; Sirikhachornkit and Niyogi 2010). In high light condition, direct photoreduction of  $\text{O}_2$  to superoxide radical ( $\text{O}_2^-$ ) occurs in PSI through its reduced electron transport components;  $\text{O}_2^-$  is then disproportionated to produce hydrogen peroxide ( $\text{H}_2\text{O}_2$ ) and  $\text{O}_2$  by the enzyme superoxide dismutase (SOD). In the presence of transition metal ions,  $\text{H}_2\text{O}_2$  may be reduced to the highly reactive hydroxyl radical ( $\text{OH}^*$ ) (Asada 1999; Apel and Hirt 2004).

In order to prevent the (photo-)oxidative damage plants have evolved multiple photoprotective mechanisms, for example avoiding absorption of excessive light by movement of leaves or chloroplasts, or within the chloroplast, by regulating light harvesting and electron transport to balance the absorption and utilization of light energy. Thermal dissipation of excess absorbed light energy plays a key role in regulating light harvesting for PSII; this process involves de-excitation of excited Chl and is measured as non-photochemical quenching (NPQ) of Chl *a* fluorescence (Niyogi 1999).

Even though these mechanisms can partly prevent production of ROS, ROS scavenging mechanisms are necessary to minimize oxidative damage. Enzymatic antioxidants include SOD, which dismutate  $\text{O}_2^-$  to  $\text{H}_2\text{O}_2$ , ascorbate peroxidase (APX), glutathione peroxidase (GPX) and catalase (CAT), which subsequently detoxify  $\text{H}_2\text{O}_2$ . The enzymes APX and GPX utilize, respectively, ascorbate and glutathione as reducing agent to convert  $\text{H}_2\text{O}_2$  into water. Beside ascorbate and glutathione (hydrophilic antioxidants), non-enzymatic ROS scavenging mechanisms involve also hydrophobic molecules such as tocopherol, flavonoids, alkaloids and carotenoids (Apel and Hirt 2004).

## 1.4 Mechanism of non-photochemical quenching (NPQ)

Absorption of light brings Chl molecules to the singlet excited state ( $^1\text{Chl}^*$ ) which can return to the ground state via several pathways. The excitation energy can be transferred to reaction centers and used to drive photochemistry, re-emitted as Chl fluorescence, de-excited by thermal dissipation processes, or it can decay via the triplet state ( $^3\text{Chl}^*$ ). As  $^3\text{Chl}^*$  has a long lifetime (ms), it can transfer energy to ground-state  $\text{O}_2$  and generate  $^1\text{O}_2$ . As a photoprotective strategy, plants are able to dissipate the excess absorbed light as heat through the NPQ process (Müller *et al.* 2001).

The NPQ is conventionally divided into three components, depending on the kinetic characteristics and processes involved:  $\Delta\text{pH}$ -dependent energy dissipation (qE); photoinhibition (qI); and state transition (qT)

The qE component of NPQ (which is induced after few seconds of high light exposure) requires  $\Delta\text{pH}$  (Krause *et al.* 1982). A lumen pH below 6 activates the enzyme violaxanthin epoxidase (VDE), which converts the xanthophyll violaxanthin (V) to antheraxanthin (A) and zeaxanthin (Z) in the so-called xanthophyll cycle, or V-cycle (Yamamoto *et al.* 2004), and leads to protonation of PsbS (Li *et al.* 2000; Li *et al.* 2002), a protein associated with PSII. Binding of Z to PSII and protonation of PsbS cause conformational changes in the antennae that induce the thermal dissipation (Holt *et al.* 2004). Several different hypotheses have been proposed to explain the mechanism of de-excitation of  $^1\text{Chl}^*$  molecules. One hypothesis is that Z, and to a lesser degree also A and lutein (L), may directly deactivate  $^1\text{Chl}^*$ . According to Frank *et al.* (1994), energy transfer can occur from  $^1\text{Chl}^*$  to Z since the lowest excited singlet state ( $S_1$ ) of xanthophylls is at lower energy than Chl singlet state. Recently, an electron transfer quenching mechanism has been proposed, in which a Chl-Z heterodimer could form *in vivo* and create a charge transfer (CT) state in the minor LHCs (Lhcb4, Lhcb5 and Lhcb6), leading to quenching of  $^1\text{Chl}^*$  by a complete transfer of an electron from Z to Chl which results in production of radical cations ( $Z^{+}$ ) (Dreuw *et al.* 2003; Avenson *et al.* 2008). In the third hypothesis Z functions indirectly as an allosteric effector of LHCs, leading to quenching via the formation of a Chl-Chl CT state (Miloslavina *et al.* 2008) or by energy transfer from  $^1\text{Chl}^*$  to L in LHCI (Ruban *et al.* 2007).

Photoinhibition (qI) is often observed after prolonged exposure of leaves to excessive light and is associated with reduction of the quantum yield of photosynthetic carbon fixation (Osmond 1994) due to the inactivation of the D1 protein in the PSII RC (Aro *et al.* 1993). The nature of qI is still

unclear, although Z seems to play a crucial function in its mechanism; it has been found that inactivation of PSII in response to high light and chilling temperatures (e.g. cold acclimated leaves of overwintering plants), is accompanied by the retention of Z under *in vivo* conditions (Adams *et al.* 1995; Jahns and Miescher 1995). Also, Nilkens *et al.* (2010) has proposed a new term qZ to describe the slowly inducible and reversible component of NPQ which requires Z. In the conventional definition with qE, qI and qT, qZ falls into part of qI.

The qT component of NPQ (state transition) consists in the phosphorylation of the peripheral LHCII and their subsequent migration from PSII to PSI. It occurs when the absorption of light in PSII is higher than in PSI and it balances the distribution of excitation energy between the two photosystems (Rochaix 2007). Recently it has been proposed that the state transition induces a switch from linear electron flow via PSII, PSI and cytochrome *b<sub>6</sub>f* complex, to cyclic electron transport around PSI, which generates  $\Delta pH$  and thus ATP without the accumulation of NADPH (Finazzi *et al.* 2002).

## 1.5 Carotenoids in photosynthesis

Carotenoids are a group of tetraterpenoid organic pigments that contain extended conjugated double-bound systems (Straub 1987). They are found in all photosynthetic organisms and are often responsible for the red, orange, and yellow colors of fruits, flowers, and tubers.

In plants, carotenoids are synthesized and accumulate in plastids where they serve essential functions for plant viability. In photosynthesis they augment light harvesting in the blue spectral region by transferring the absorbed light energy to Chl (see 1.2) and provide protection against photooxidative damage under excess light, such as regulation of thermal energy dissipation (see 1.4); furthermore they contribute to folding and stabilization of light harvesting antenna proteins (Demmig-Adams *et al.* 1996b; Yamamoto and Bassi 1996).

Four carotenoids are nearly ubiquitous amongst chloroplasts of higher plants: L,  $\beta$ -carotene ( $\beta$ -car), V and neoxanthin (N). In excess light conditions Z and A are also found (Young 1993). The leaf carotenoid composition has been conserved throughout evolution of higher plants which suggests distinct and indispensable functions of each of these pigments.

Two branches can be distinguished in the carotenoid biosynthetic pathway (Fig. 1.5.1; DellaPenna and Pogson 2006). After formation of lycopene, the activities of  $\beta$ - and  $\epsilon$ -cyclase split the pathway into two branches: the  $\beta$ -branch (with two  $\beta$ -ionone rings) and the  $\alpha$ -branch (with a  $\beta$ -ionone and an  $\epsilon$ -ionone ring). In the  $\beta$ -branch, the cyclization product of lycopene,  $\beta$ -car, either binds to photosystem core complexes or undergoes a series of reactions to produce the xanthophylls Z, A, V and N. Hydroxylation of  $\beta$ -car by  $\beta$ -ring hydroxylase gives rise to Z, followed by epoxidation to A and V by zeaxanthin epoxidase (ZEP) and further modification to N. The cyclization and hydroxylation reactions in the  $\alpha$ -branch, involving  $\epsilon$ -cyclase and  $\epsilon$ -ring hydroxylase in addition to the corresponding enzymes for  $\beta$ -ionone rings, produce L, the most abundant carotenoid in photosynthetic tissues (for reviews on carotenoid biosynthesis in plants, see Hirschberg 2001; DellaPenna and Pogson 2006).

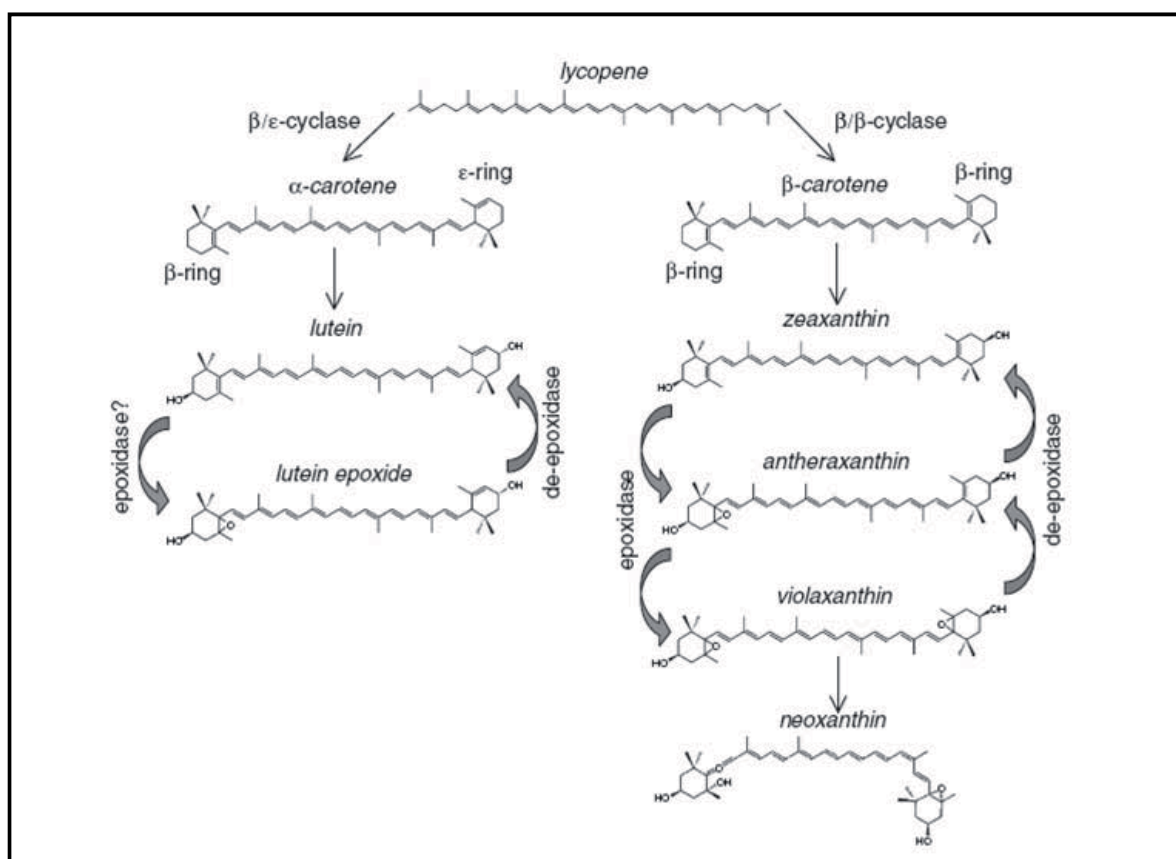


**Figure 1.5.1: Xanthophyll biosynthetic pathway.** Reactions of the lutein epoxide-cycle and the violaxanthin-cycle are indicated by arrows (adapted from Garía-Plazaola *et al.* 2007)

While  $\beta$ -car is the only carotenoid found in the RC of PSI and PSII, four xanthophyll binding sites have been identified in LHCII: L1, L2, N1 and V1 (Fig. 1.5.2; Bassi and Cafarri 2000). Lutein is the only ligand for the intrinsic L1 site, whose occupancy is essential for the stability of trimeric LHCII (Lokstein *et al.* 2002). Another intrinsic xanthophyll binding site, L2, also binds L although either V or Z can replace L in this site. The N1 site is specific for N and the peripheral V1 site is proposed to loosely bind V as available substrate for the enzyme VDE in the V cycle (Bassi and Cafarri 2000). In high-light conditions VDE converts V into A and Z, which plays an essential role in regulation of NPQ as above described; in the absence of excess light the enzyme ZEP restores the V pool through epoxidation of Z (Yamamoto *et al.* 1962).

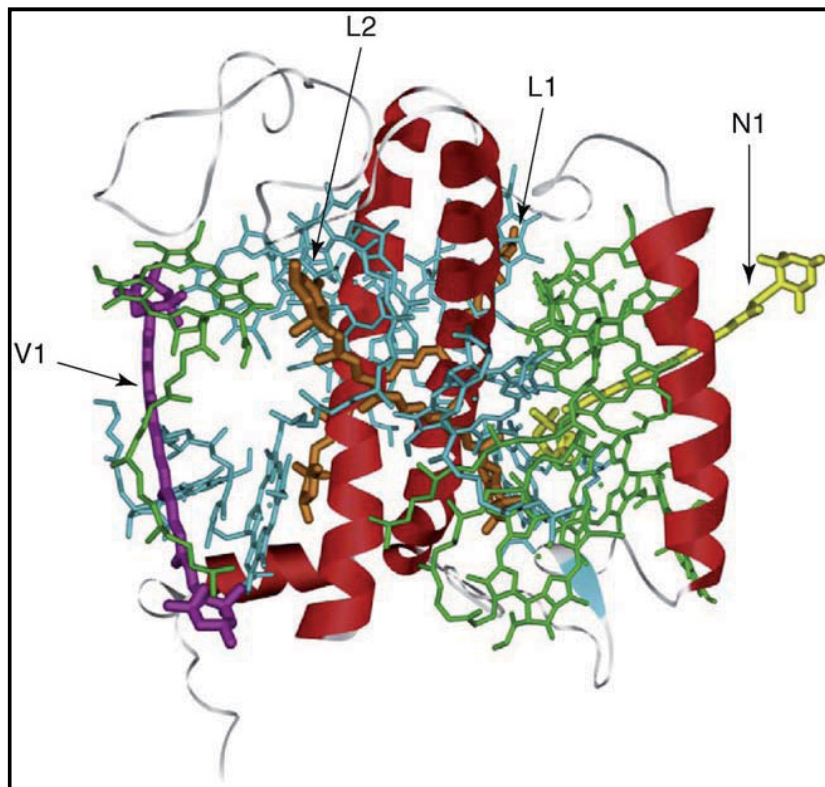


**Figure 1.5.2: Xanthophyll binding sites in the LHCII of green plants.** Each monomer of LHCII has three transmembrane  $\alpha$ -helices (indicated in red). Chlorophylls are in green or blue. Xanthophylls are indicated in the corresponding binding site: N (yellow) in N1, L (orange) in L1 and L2, V (purple) in V1 (adapted from Triantaphylidès *et al.* 2009).

Two additional carotenoids,  $\alpha$ -carotene ( $\alpha$ -car) and lutein epoxide (Lx), the precursor and epoxidation product of L, respectively (Fig 1.5.1), can accumulate in large amounts in leaves of certain taxa, especially in shade environments (García-Plazaola *et al.* 2007; Matsubara *et al.* 2009). When they occur,  $\alpha$ -car can replace  $\beta$ -car and Lx can replace L or the V-cycle pigments (V, A and Z) in pigment-protein complexes of PSII and PSI (Matsubara *et al.* 2007). Although little is known about the role of  $\alpha$ -car in the thylakoids, an adaptive advantage of having  $\alpha$ -car under low-light conditions has been proposed based on the predominant occurrence of this pigment in shade leaves (Krause *et al.* 2001; Matsubara *et al.* 2009).

## 1.6 Lutein epoxide cycle

Lx is synthesized in some higher plant species by epoxidation of the  $\beta$ -ring of L, presumably catalyzed by ZEP, in a reaction analogous to the epoxidation of Z to form A and V (Fig. 1.5.1). The product Lx usually accumulates in shade conditions, whereas light induces its de-epoxidation back to L, catalyzed by the enzyme VDE, giving rise to the Lx-cycle (García-Plazaola *et al.* 2007).

Originally discovered in green tomato fruits (Rabinowitch *et al.* 1975), the Lx-cycle has been found in a broad range of rather unrelated plant taxa (Matsubara *et al.* 2009). The highest contents of Lx have so far been found in sun-exposed photosynthetic stems of parasitic plant *Cuscuta reflexa* (Sydner *et al.* 2005), in leaves of the tropical tree species *Virola* (Matsubara *et al.* 2008) and in deeply shaded inner canopy leaves of tropical tree legume *Inga sapindoides* which is native to tropical central and southern America and is used as shade tree for coffee plantations (Matsubara *et al.* 2005). Due to high Lx levels in leaves, the genus *Inga* has been used in some studies to investigate the operation and the functions of the Lx-cycle (Matsubara *et al.* 2005, 2007, 2008).

Studies on *I. sapindoides* leaves revealed that the  $Lx \rightarrow L$  exchange occurs in the same binding sites as the  $V \rightarrow Z$  exchange: the V1 and L2 sites of the antenna complexes of PSII (Matsubara *et al.* 2007). The functions attributed to the Lx-cycle are associated with regulation of light harvesting and photoprotection. *In-vitro* reconstitution experiments with LHC proteins and purified pigments (Matsubara *et al.* 2007), which is supported by *in-vivo* studies on *I. marginata* plants (Matsubara *et al.* 2008), suggest that accumulation of Lx may facilitate efficient excitation energy transfer from LHCs to RC of PSII in shade leaves. On the other hand, the L formed from Lx in the light and retained in the subsequent darkness has been shown to enhance the  $\Delta pH$ -dependent qE component of NPQ in the absence of Z (Matsubara *et al.* 2008), playing therefore an important role, together with Z and A, in the mechanism of photoprotection.

Even though the V-cycle and the Lx-cycle occur in parallel and they are both regulated by light, the epoxidation reaction is slower in the Lx-cycle compared to the V-cycle. Two types of Lx-cycle have been described: a complete and a truncated one. Plants like *Amyema miquelii* and *Virola elongata*, with a complete Lx-cycle, show a full recovery of Lx pool overnight, although the recovery was slower than for V (Matsubara *et al.* 2001, 2009). As an example of the truncated Lx-cycle, the plant *Inga marginata* shows significant de-epoxidation when exposed to strong light, but substantial epoxidation of L back to Lx occurs only after several days in deep shade (Matsubara *et al.* 2008). The slower recovery of Lx compared to V suggests that the kinetics of the epoxidation reactions

differ significantly between the two substrates, L and Z. Two hypotheses have been proposed to explain this kind of behavior; either epoxidase enzyme (presumably a modified form of ZEP; Matsubara *et al.* 2003) has gained a certain but low affinity for L, or the access of the enzyme to L is restricted by its intra-protein binding in Lhcbs.

### 1.7 Zeaxanthin epoxidase

Although it has never been directly probed, an enzyme similar to ZEP is presumably responsible for the formation of Lx from L; in fact ZEP shows specificity for carotenoids with a 3-hydroxy- $\beta$ -cyclohexenyl ring (Hieber *et al.* 2000) in which it catalyzes epoxidation in position 5 and 6. As L has one  $\beta$ -ring, it could be a substrate for ZEP (Fig. 1.5.1). However, overaccumulation of L in transgenic Arabidopsis plants *lutOE* (Pogson and Rissler 2000) did not result in accumulation of Lx in this plant, demonstrating the inability of Arabidopsis ZEP to catalyse  $L \rightarrow Lx$  epoxidation even when L is abundantly available and accessible to the enzyme (Matsubara *et al.* 2003).

The enzyme ZEP has been the subject of numerous studies because its epoxidation reaction from Z to A and V occurs in the upstream of abscisic acid (ABA) biosynthetic pathway. The cDNA encoding ZEP was first isolated from *Nicotiana plumbaginifolia* (Marin *et al.* 1996) and this sequence was later used to isolate ZEP cDNA from *Capsicum annum* (Bouvier *et al.* 1996). The study of Bouvier *et al.* (1996) on *C. annum* ZEP is the only case where overexpression and purification of an active form of this enzyme has been reported.

The ZEP requires molecular oxygen as second substrate and NADPH and FAD as cofactors (Siefermann and Yamamoto 1975; Büch *et al.* 1995). Furthermore, according to Bouvier *et al.* (1996), ferredoxin, ferredoxin oxidoreductase and the thylakoid lipids mono- and digalactosyldiacylglycerol (MGDG and DGDG) are necessary for its activity.

Since NADPH cannot move through the thylakoid, ZEP has been associated with the stromal side of the membrane (Gilmore *et al.* 1994). This is also supported by the fact that the ZEP activity is optimal near pH 7.5 and that ZEP is active even during light-induced lumen acidification after inhibiting the enzyme VDE with dithiothreitol (Gilmore *et al.* 1994). Therefore the two enzymes responsible for the V-cycle, ZEP and VDE, are physically separated and localized on the opposite sides of the thylakoid membrane (Hieber *et al.* 1999).

The two enzymes VED and ZEP are the first lipocalin proteins identified in plants (Hieber *et al.* 1999). Lipocalins are a family of proteins that bind small hydrophobic molecules and share a conserved tertiary structure of eight-stranded anti-parallel  $\beta$ -strands forming a barrel configuration (Bugos *et al.* 1998) (Fig. 1.7.1a). Three conserved regions can be distinguished in the amino acid sequences of this family of proteins; the first motif is localized in the first  $\beta$ -strand, the second between the sixth and the seventh  $\beta$ -strand including the connecting loop, and the third conserved region in a portion of the eighth  $\beta$ -strand, including the loop and part of the C-terminal  $\alpha$ -helical structure (Fig. 1.7.1a). When compared to other lipocalin proteins, VED and ZEP share homology in the structurally conserved regions mainly in motif I, while homology in motifs II and III is much weaker, especially for ZEP (Fig. 1.7.1b). The main difference between ZEP and other lipocalin molecules consists in the number of amino acids between motif I and II; the distance between the two regions is longer in ZEP than in other lipocalin proteins, suggesting the presence of an extra  $\beta$ -strand or longer loop structures between the  $\beta$ -strands (Bugos *et al.* 1998).

In addition to the lipocalin motifs, other two conserved regions have been identified in the amino acidic sequences of ZEPs analyzed so far (Baroli *et al.* 2003; Wang *et al.* 2007): a flavoprotein associated domain, which contains the catalytic site of the enzyme, and a phosphopeptide binding domain. Both of these domains are supposed to be important for ZEP function.

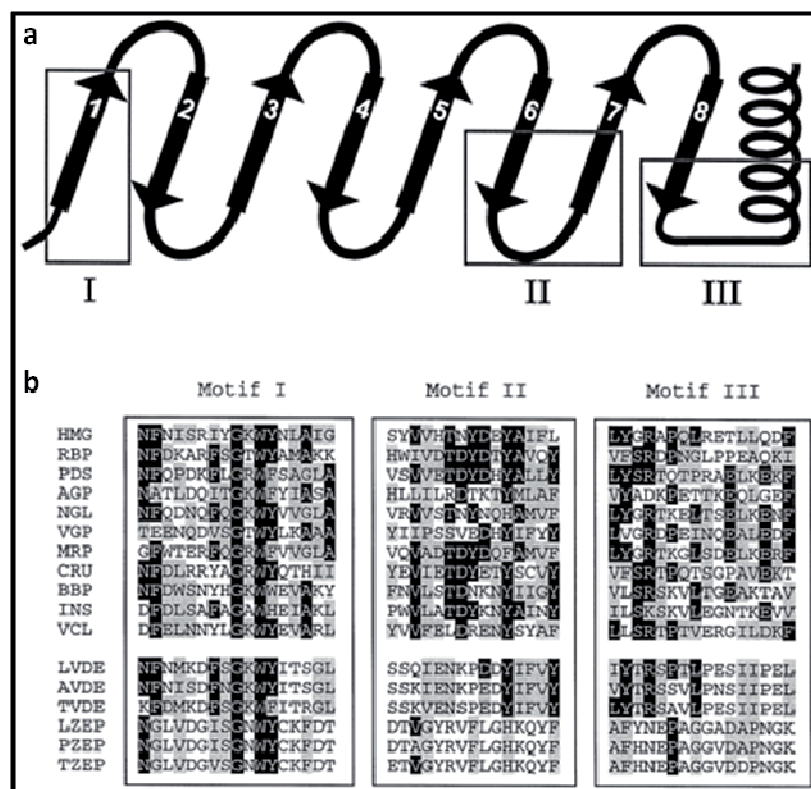


**Figure 1.7.1: Model of the lipocalin structure and sequence alignment of the three conserved motifs (adapted from Bugos *et al.* 1998).** (a) The eight  $\beta$ -strands, followed by a C-terminal  $\alpha$ -helix, are illustrated. The three conserved lipocalin motifs (I, II and III) are also shown. (b) Sequence alignment of the three conserved motifs belonging to lipocalin proteins from diverse species. *HMG*, human  $\alpha_1$ -microglobulin (P02760); *RBP*, human plasma retinol-binding protein (P02753); *PDS* human prostaglandin D synthase (M61900); *AGP*, human  $\alpha_1$ -acid glycoprotein-1 (P02763); *NGL*, human neutrophil gelatinase-associated lipocalin (P80188); *VGP*, rat von Ebner's gland protein 1 (P20289); *MRP*, rat  $\alpha_2$ -microglobulin-related protein (P30152); *CRU*, lobster crustacyanin A2 subunit (P80007); *BBP*, cabbage white butterfly bilinbinding protein (P09464); *INS*, tobacco hornworm insecticyanin (Q00630); *VCL*, *Vibrio cholerae* vlpA lipoprotein (AF025663); *LVDE*, lettuce violaxanthin de-epoxidase (U31462); *AVDE*, *Arabidopsis* violaxanthin de-epoxidase (U44133); *TVDE*, tobacco violaxanthin de-epoxidase (U34817); *LZEP*, tomato zeaxanthin epoxidase (Z83835); *PZEP*, pepper zeaxanthin epoxidase (X91491); and *TZEP*, tobacco zeaxanthin epoxidase (X95732).

## 1.8 Motivation

Since the Lx-cycle was reported in the parasitic angiosperm *C. reflexa* (Bungard *et al.* 1999), much effort has been made in studying the different manifestation of this cycle in terrestrial plants and its functions and relationship to the V-cycle (Matsubara *et al.* 2003; 2005; 2007; Esteban *et al.* 2008; 2010). However the reason why the Lx-cycle is present only in some plant species, whereas the V-cycle is universal, is still unclear. Thus, in the first part of this thesis I attempted to test the hypothesis that mutation to the enzyme ZEP may be responsible for the occurrence of the Lx cycle in a restricted number of species (Matsubara *et al.* 2003). In order to investigate *in-vivo* activity and substrate specificity of ZEP from species having the Lx-cycle, cDNAs encoding putative ZEP (ImZEP) were isolated from leaves of *I. marginata* and introduced in *A. thaliana npq2* mutants, lacking the functional native ZEP (AtZEP) (Niyogi *et al.* 1998).

In spite of many attempts in different laboratories, the work of Bouvier *et al.* (1996) showing the overexpression and isolation of active recombinant ZEP, could never be reproduced. Therefore, a novel expression system based on the bacterium *Rhodobacter capsulatus* (Katzke *et al.* 2009) was tested for overexpression of ZEP protein. Because of the formation of numerous intracytoplasmatic membrane systems under phototrophic growth conditions, *R. capsulatus* offers an expression system with extensive membrane surface, which is especially interesting for proteins associated with a membrane.

Operation of the Lx-cycle also raises the question as to the enigmatic role of L and all  $\alpha$ -branch carotenoids in photoprotection and photoacclimation in plants. Substitution of  $\beta$ -branch carotenoids by  $\alpha$ -car and Lx leads to a high  $\alpha$ -branch to  $\beta$ -branch ratio in shade leaves of a wide range of plant species, which generally decreases (i.e. shifts towards  $\beta$ -branch) in sun leaves (Matsubara *et al.* 2009). In order to gain an insight into physiological functions of  $\alpha$ - and  $\beta$ -branch carotenoids and the balance between them, I examined the phenotypic responses of four different Arabidopsis carotenoid mutants, *lut2*, *lut5*, *szl1npq1* and *npq1*, to photo-oxidative stress. Short and strong light pulses ('sunflecks') were applied in order to simulate photooxidative stress often found in shade environments. Sunflecks can expose shade-acclimated leaves to rapid and large increases in irradiance in highly variable natural light environments. While they deliver the major fraction of light energy available in shade environments and can improve carbon gain in some plants (Percy 1990), sunflecks also cause temporal excess of light and thus can become a source of photooxidative stress (Alter *et al.* submitted).

## 2 Materials and Methods

**Table 2.1** List of vectors

| Plasmid                                 | Size     | Characteristics   | Resistance                               | Application  | Reference                         |
|---|----------|---|--|--|-----------------------------------|
| pCR <sup>®</sup> II-TOPO <sup>®</sup>   | 4.0 Kb   | <i>LacZα</i> gene, Sp6 promoter, T7 promoter, pUC origin, f1 origin   | Kanamycin, ampicillin                    | cloning PCR products directly from a PCR reaction  | Invitrogen                        |
| pENTR <sup>™</sup> /D-TOPO <sup>®</sup> | 2.58 Kb  | <i>rrnB</i> T1 and T2 transcription termination sequences, <i>attL1</i> and <i>attL2</i> sites, directional TOPO <sup>®</sup> cloning site, T7 promoter, pUC origin | Kanamycin                                | Entry vector                                       | Invitrogen                        |
| pUC18                                   | 2.686 Kb | pMB1 replicon <i>rep</i> , <i>bla</i> gene, <i>Escherichia coli</i> operon <i>lac</i>   | Ampicillin                               | Entry vector                                       | Yanisch-Perron <i>et al.</i> 1985 |
| pRhotHi-2                               | 6.678 Kb | broad-host-range replicon REP, MOB site for conjugational transfer, T7 promoter, His <sub>6</sub> tag sequence  | Kanamycin, chloramphenicol spectinomycin | Expression vector in <i>Rhodobacter capsulatus</i> | Katzke <i>et al.</i> 2009         |
| pGWB2                                   | 17 Kb    | <i>attR1</i> -CmR- <i>ccdB</i> - <i>attR2</i> cassette, 35S promoter from cauliflower mosaic virus  | Kanamycin, hygromycin                    | Expression vector in plants                        | Nakagawa <i>et al.</i> 2007       |

Table 2.2 Primer List

| Name of the primer | Sequence   | Application  |
|--------------------|--|--|
| IsZep_1 fwd        | 5'-CCTGGTGGTGTGATGG-3'                             | Amplification of a partial cDNA sequence of <i>ImZep</i> isoform 1                                       |
| IsZep_1rev         | 5'-CCCATGTGAATATGGGTGT-3'                          |  |
| ZEP-multi- FWD2    | 5'-TGGTA(CT)TGCAAGTTTGAGAC-3'                      |  |
| IsZep_2fwd         | 5'-ACCTGGTGGCATGGATG-3'                            | Amplification of a partial cDNA sequence of <i>ImZep</i> isoform 2                                       |
| IsZep_2rev2        | 5'-ATGGGTTCCTAGTCATAAAT-3'                         |  |
| RACE_Iso1_fwd      | 5'-GTGGATGACGGAAGCAAGGTAACAGTAG-3'                 | RACE-PCR to isolate <i>ImZep1</i> cDNA sequence  |
| RACE_Iso1_rev3     | 5'-CTACTGTTACCTTGCTTCCGTCATCCAC-3'                 |  |
| ZepAraFwd1         | 5'-CATATG*AGTAAAGGCGGCGACGGCGTTAGTTG-3'            | Amplification of the <i>AtZep</i> cDNA sequence for heterologous overexpression in <i>R. capsulatus</i>  |
| AtZepExpRev1       | 5'-GTCGAC**TCAACTCTCATTCTTCCTCGTCGATTTTCG-3'       |  |
| AtZepExpREV        | 5'-GTCGAC**ACTCTCATTCTTCCTCGTCGATTTTCG-3'          |  |
| ZepIngalso1fwd1    | 5'-CATATG*AAGAACTGCTGCCGATTTAC-3'                  | Amplification of the <i>ImZep1</i> cDNA sequence for heterologous overexpression in <i>R. capsulatus</i> |
| ZepIngalso1Rev1    | 5'-CTCGAG*TCATCGTTCCAGTAAACCTTAGTTCC-3'            |  |
| ZepIngalso1Rev2    | 5'-CTCGAG*TCGTTCCAGTAAACCTTAGTTCCTTC-3'            |  |
| ImZepExpAtFWD1     | 5'-CACC <sup>+</sup> ACAATGGCTTCCACCTTGCTTACAGC-3' | Amplification of the <i>ImZep1</i> cDNA sequence for heterologous overexpression in <i>A. thaliana</i>   |
| ZepIngalso1Rev1    | 5'-CTCGAGTCATCGTTCCAGTAAACCTTAGTTCC-3'             |  |
| AthZEfwd           | 5'-CAGAGTGTTGAAACGACTAC-3'                         | Amplification of a short fragment of <i>AtZep</i> cDNA to check the insertion in the transformed plants  |
| AthZErev           | 5'-ATGTCGGACGATCTAAACC-3'                          |  |

| Name of the primer | Sequence                        | Application   |
|--------------------|---------------------------------|---|
| <i>aphII</i> -RTup | 5'-GAACTGTTCCGCCAGGCTCAA-3'     | Transcription and real-time-PCR analysis of the <i>aphII</i> gene as a control and for construction of a standard curve |
| <i>aphII</i> -RTdn | 5'-GAAAAGCGGCCATTTTCCAC-3'      |   |
| AH_409_RTln_up     | 5'-AGAGAGAGTACTGCGAGTTGCCATT-3' | Real-time-PCR analysis of the <i>ImZep1</i> gene  |
| AH_409_RTln_dn     | 5'-ATTACAAGCCTCCCTCCAACCTTC-3'  |   |
| AH_409_RTAt_up     | 5'-TCCAGGAAGAGTTGGTGGTAGATTC-3' | Real-time-PCR analysis of the <i>AtZep</i> gene   |
| AH_409_RTAt_dn     | 5'-GTCATCTTCAAACCACTCTCGAAGC-3' |   |
| SP6                | 5'- ATTTAGGTGACACTATAG – 3'     | Vector specific primers for colony PCR  |
| T7                 | 5'-TAATACGACTCACTATAGGG - 3'    |   |

\* Sequence recognized by the restriction enzyme *NdeI*; \*\* sequence recognized by the restriction enzyme *Sall*; \* part of the sequence necessary for directional cloning of the *ImZep1* gene in the pENTR<sup>TM</sup>/D-TOPO<sup>®</sup> vector. Stop codons are highlighted.

**Table 2.3 List of bacteria**

| Bacteria                                | Application  | Source  |
|---|--|---|
| <i>Escherichia coli</i> DH5- $\alpha$   | Cloning of all the vector used (Table 2.1)   | Invitrogen  |
| <i>Escherichia coli</i> BL21(DE3)       | Heterologous overexpression of <i>ImZep1</i> and <i>AtZep</i> inserted in pRhotHi-2 vector | T. Drepper, IMET, HHU Düsseldorf                                      |
| <i>Escherichia coli</i> S17.1           | Conjugation transfer of pRhotHi-2 vector to <i>R. capsulatus</i>                           | T. Drepper, IMET, HHU Düsseldorf                                      |
| <i>Rhodobacter capsulatus</i> B10S-T7   | Heterologous overexpression of <i>ImZep1</i> and <i>AtZep</i> inserted in pRhotHi-2 vector | T. Drepper, IMET, HHU Düsseldorf                                      |
| <i>Agrobacterium tumefaciens</i> GV3101 | Transformation of <i>A. thaliana</i> plants  | A. Wiese-Klinkenberg, IBG-2: Plant Sciences, Forschungszentrum Jülich |

**Table 2.4 List of plants**

All mutants of *Arabidopsis thaliana* (L.) Heynh. were kindly provided by Roberto Bassi (University of Verona, Italy). The *A. thaliana* ecotype Colombia-0 was used as wild type. Plants of *Inga marginata* Willd. were kindly provided by Klaus Winter (Smithsonian Tropical Research Institute, Panama).

| Plant                       | Reference                     |
|-----------------------------|-------------------------------|
| <i>I. marginata</i>         | Pennington and Fernandes 1998 |
| <i>A. thaliana npq2</i>     | Niyogi <i>et al.</i> 1998     |
| <i>A. thaliana szl1npq1</i> | Li <i>et al.</i> 2009         |
| <i>A. thaliana lut2</i>     | Pogson <i>et al.</i> 1996     |
| <i>A. thaliana lut5</i>     | Kim and DellaPenna 2006       |
| <i>A. thaliana npq1</i>     | Niyogi <i>et al.</i> 1998     |

## 2.1 Chemicals

Chemicals were purchased from Sigma-Aldrich and Fluka (Hamburg), Roth (Karlsruhe), Merck (Darmstadt), Roche (Mannheim) and Bio-rad (Munich).

## 2.2 Cultivation of biological material

### 2.2.1 Phototropic growth of *R. capsulatus* under high light condition (adapted from Klipp *et al.* 1987)



**Figure 2.2.1: *Rhodobacter capsulatus*** (a) *R. capsulatus* colonies grown on solid PY medium after 3 d of incubation. (b) *R. capsulatus* liquid cultures. (c) Experimental set up used to grow the bacterial culture phototrophically.

Cells of *R. capsulatus* strain B10S were grown at 30°C in anaerobic condition under light exposure both in solid medium and in liquid cultures.

For cultivation in solid medium (Fig. 2.2.1a) Petri dishes containing PY-agarose (15 g agarose, 10 g bacto peptone, 0.5 g yeast extract, 2 ml 1 M  $\text{MgCl}_2$ , 2 ml 1 M  $\text{CaCl}_2$ , 2.4 ml 0.5% (w/v)  $\text{FeSO}_4\cdot\text{HCl}$ , distilled water up to 1000 ml; 0.5% (w/v)  $\text{FeSO}_4\cdot\text{HCl}$  = 0.5%  $\text{FeSO}_4$ , 1 ml 32% HCl, distilled water up to 200 ml) (Klipp *et al.* 1987; Heck 2008) were used and inserted in a special anaerobic incubation jar provided with Gas-Pack Anaerobic-Systems (BD, New Jersey). For liquid cultures (Fig. 2.2.1b), bacteria were cultivated in RCV + N-minimal medium (40 ml 10% (w/v) DL-malate pH 6.8, 1 ml 20% (w/v)  $\text{MgSO}_4$ , 1 ml 7.5% (w/v)  $\text{CaCl}_2$ , 2 ml 1% (w/v)  $\text{Na}_2\text{-EDTA}$ , 2.4 ml 0.5% (w/v)  $\text{FeSO}_4\text{HCl}$ , 1 ml 0.1% (w/v) thiamin, 1 ml micronutrient solution, 9.6 ml 1 M phosphate buffer pH 6.8, 10 ml 10% (w/v)  $(\text{NH}_4)_2\text{SO}_4$ , distilled water up to 1000 ml) (Weaver *et al.* 1975, Heck 2008) inside capped airtight containers (up to 10 ml of culture volume) that were flushed with argon to create an oxygen-free atmosphere.

Under these growth conditions *R. capsulatus* was incubated for 3 d, illuminated with six light bulbs of 60 W (Osram, ca. 2500 lux) (Fig. 2.2.1c).

The cell density of the liquid cultures was determined by turbidity measurements by using a spectrophotometer (Thermo Scientific, Schwerte) at the wavelength of 660 nm ( $\text{O.D.}_{660} = 1$  corresponds ca. to  $3 \times 10^8$  cells per ml culture).

### 2.2.2 Cultivation of *E. coli* and *A. tumefaciens* strains

*Escherichia coli* DH- $\alpha$ , BL21 (DE3) and S17.1 strains (see table 2.3) were grown at 37°C in a incubator hood (Edmund Buehler, Hechingen) at 150-200 rpm in either LB-medium (10 g NaCl, 10 g tryptone, 5 g yeast extract, distilled water up to 1000 ml, pH 7.5) or SOC-medium (2% tryptone, 0.5% yeast extract, 10 mM NaCl, 2.5 mM KCl, 10 mM MgCl<sub>2</sub>, 10 mM MgSO<sub>4</sub>, 20 mM glucose). For cultivation in solid medium, standard nutrient agarose plates were prepared (10 g NaCl, 10 g tryptone, 5 g yeast extract, 20 g agarose, distilled water up to 1000 ml, pH 7.0). Cells of *A. tumefaciens* were also cultivated in the same growth media at 28°C.

Antibiotic (50 µg/ml) was added to the respective medium when bacterial growth under selective pressure was desired (e.g. to select transformed cells).

### 2.2.3 Plant material

Seedlings of *I. marginata* were brought back from the Smithsonian Tropical Research Institute (Panama) to the IBG-2: Plant Sciences; here seedlings were grown in 12 L pots (22.5 cm high) containing ED 73 Einheitserde® soil (Balster Einheitserdewerk, Fröndenberg) in a growth chamber with a 12-h/12-h (day/night) photoperiod under a constant relative air humidity of 75% and at 25°C/15°C air temperature.

Seeds of *A. thaliana* Columbia-0 (wt), carotenoid mutants and transgenic lines had been stratified in moist soil at 4°C in the dark for four to 5 d before they were transferred to a climate chamber. The conditions in the climate chamber were 23°C/18°C (day/night) air temperature, 60% constant relative air humidity and a 12-h/12-h photoperiod. Plants were grown in pots (7 x 7 x 8 cm, one plant per pot) containing soil (ED 73 Einheitserde; Balster Einheitserdewerk). For wt and mutants used for the sunfleck experiment (see 2.2.4.a) photosynthetically active photon flux density of approx. 60 µmol photons m<sup>-2</sup> s<sup>-1</sup> was provided by Osram Fluora Typ L36 W/77 fluorescent tubes during the day period. For leaf growth analysis of transgenic lines, seedlings were grown under an active photon flux density of approx. 150-180 µmol photons m<sup>-2</sup> s<sup>-1</sup> for three weeks after germination.

For analysis of root growth in the sunfleck experiment (see 2.2.4a), seeds were surface-sterilised with sodium hypochlorite solution (see 2.4.2) and sown on sterile 1% agarose (w/w) in Petri dishes (120 x 120 x 17 mm). The medium contained 1/3 modified Hoagland solution (stock solution: 1 M

KNO<sub>3</sub>, 1 M Ca(NO<sub>3</sub>)<sub>2</sub>, 1 M MgSO<sub>4</sub>, 1 M KH<sub>2</sub>PO<sub>4</sub>, trace elements). To examine the effect of osmotic stress on root system architecture, 100 mM sorbitol was added to the medium. The seeds were pushed slightly into the agarose through holes (diameter 2 mm, four holes for four seeds per Petri dish) on the upper side of the closed Petri dishes sealed with fabric tape (Micropore, 3M Health Care, Neuss) and placed vertically in a plastic box to avoid light exposure of roots. During germination, the holes were covered with a film (Parafilm, Pechiney Plastic Packaging, Menasha) to keep the seeds moist. In this way shoot could grow out of the Petri dish (and the plastic box) through the hole, while roots grew into the agarose in the dark (Nagel *et al.* 2006). Seeds had been stratified in the Petri dishes at 4°C in the dark for 5 d before they were placed vertically in the plastic box and transferred to the climate chamber condition described above. It should be noted that the number of replicates differed strongly between genotypes and treatments (11-13 for wt, 6-8 for *lut2*, 9-19 for *lut5*, 7-13 for *npq1* and 7-17 for *szl1npq1*) because of the susceptibility of sorbitol-containing agarose medium (used for osmotic stress experiment) to fungi contamination in the climate chamber.

## 2.2.4 Light treatments

### 2.2.4.a Sunfleck treatment

For sunfleck experiments with *A. thaliana* carotenoid mutants, after three or four weeks from germination, soil-grown plants of each genotype were divided into two populations (day 0): the first population ("control" plants) was kept in the growth light condition of ca. 60  $\mu\text{mol photons m}^{-2} \text{s}^{-1}$  (see 2.2.3) while the second population ("sunfleck" plants) was transferred to a fluctuating light condition where 20-s pulses of high light (ca. 1000  $\mu\text{mol photons m}^{-2} \text{s}^{-1}$ ) were applied every 6 min under the growth light condition during the day period. The sunfleck treatment was performed by using a setup described elsewhere (Alter *et al.* in preparation) with a minor modification. Three halogen lamps (Haloline; Osram) were automatically moved above the plants at a given velocity and frequency; the velocity and frequency of the movement were programmed such that each plant was under the halogen spotlight for 20 s and every 6 min.

For root growth analysis in the sunfleck experiment, Petri dishes containing growing *Arabidopsis* seedlings were kept for 12 d in the control conditions (see 2.2.3). After this period (day 0) half of the population was exposed for 5 d to the sunfleck treatment described above, while the other

half and plants growing in Petri dishes containing sorbitol (see osmotic stress treatment in 2.2.3) were kept in the control condition.

#### 2.2.4.b High-light treatment

For high-light treatment for *A. thaliana* transgenic lines, 4 to 5-weeks-old plants grown under a photosynthetically active photon flux density of approx. 50-95  $\mu\text{mol photons m}^{-2} \text{s}^{-1}$  were exposed to high light (600-700  $\mu\text{mol photons m}^{-2} \text{s}^{-1}$ ) for 30 min. After the high light exposure plants were transferred to dim light (10-20  $\mu\text{mol photons m}^{-2} \text{s}^{-1}$ ) to monitor dark recovery.

### 2.3 Molecular biological methods

#### 2.3.1 RNA isolation from leaves of *A. thaliana* and *I. marginata* plants

Leaves of *A. thaliana* and *I. marginata* were frozen in liquid nitrogen and ground thoroughly with a mortar and pestle. Total RNA was isolated from the frozen leaf material (70-100 mg for *A. thaliana* and 30-80 mg for *I. marginata*) by using the RNeasy® Plant Mini kit (Qiagen, Hilden) following the manufacturer's guidelines. In case of *I. marginata* plants the protocol was modified by the application of 250  $\mu\text{l}$  Na citrate/NaCl solution (1 M Na citrate, 1.2 M NaCl) twice to the RNeasy spin column before eluting the RNA. The isolated RNA was quantified by using the NanoDrop 1000 (Thermo Scientific).

#### 2.3.2 cDNA synthesis

Synthesis of cDNA was performed by using the iScript™ kit (Bio-Rad, Munich) following the manufacturer's guidelines. About 400 ng of total RNA isolated from *A. thaliana* and *I. marginata* leaves were used for each reaction of reverse transcription.

#### 2.3.3 Genomic DNA isolation from *A. thaliana* transformed plants

A single leaf of each transformed plant was ground in 400  $\mu\text{l}$  extraction buffer (200 mM Tris HCl pH 7.5, 250 mM NaCl, 25 mM EDTA, 0.5% (w/v) SDS). The ground material was transferred to a

2ml Eppendorf tube and 150  $\mu$ l of potassium acetate (3 M, pH 6) were added. The mixture was centrifuged for 2 min at 13000 rpm and room temperature (RT) (Centrifuge 5415 D Eppendorf, Hamburg) and the supernatant was mixed with 500  $\mu$ l isopropanol. After 2-min incubation at RT, the sample was centrifuged again for 2 min at 13000 rpm and RT. The supernatant was discarded and the pellet was washed in 1 ml 80% ethanol. The pellet was then dried for 1 h under continuous ventilation in a fume hood and then dissolved in 80  $\mu$ l water.

#### 2.3.4 PCR (Polymerase Chain Reaction)

PCR conditions described in Table 2.5 were used to amplify DNA fragments. A 50  $\mu$ L reaction mixture consisted of 1  $\mu$ M primer (for each forward and reverse primer), 2 mM  $MgCl_2$ , 0.2 mM dNTP mix, 10-100 ng cDNA or genomic DNA (or 1 ng plasmidic DNA), 1x appropriate buffer, 1.25 units *Taq* polymerase (Fermentas, ST. Leon-Rot) and sterile water. The PCR reaction was performed using a My Cycler thermal cycler (Bio-Rad).

For PCR amplification of the full-length cDNA of *A. thaliana Zep* gene, 2.5 units of the HotStar HiFidelity DNA Polymerase enzyme (Qiagen) was used instead of the *Taq* polymerase.

*Pfu* DNA polymerase (Fermentas) was used for amplification of the putative fulllength cDNA of *I. marginata Zep* gene (1.25 units, for PCR condition see Table 2.5).

**Table 2.5 PCR program**

|                  |            |      |          |
|------------------|------------|------|----------|
| Denaturation     | 3 min      | 95°C | } 30-40x |
| Denaturation     | 15 s-1 min | 95°C |          |
| Annealing        | 1 min      | *    |          |
| Elongation       | 1 min      | 72°C |          |
| Final Elongation | 10 min     | 72°C |          |

\* See each individual primer pair in Table 2.6

**Table 2.6 Primer pairs**

| Probe                          | 5' primer       | 3' primer       | Annealing temperature | PCR product (bp) |
|--------------------------------|-----------------|-----------------|-----------------------|------------------|
| <i>ImZep1</i> partial sequence | IsZep_1 fwd     | IsZep_1rev      | 53°C                  | 155 bp           |
| <i>ImZep1</i> partial sequence | ZEP-multi-FWD2  | IsZep_1rev      | 53°C                  | 587 bp           |
| <i>ImZep2</i> partial sequence | IsZep_2 fwd     | IsZep_2rev2     | 53°C                  | 145 bp           |
| <i>AtZep</i> gene              | ZepAraFwd1      | AtZepExpRev1    | 68°C                  | 1804 bp          |
| <i>AtZep</i> gene              | ZepAraFwd1      | AtZepExpRev     | 68°C                  | 1801 bp          |
| <i>ImZep1</i> gene             | ZepIngalso1fwd1 | ZepIngalso1Rev1 | 63°C                  | 1868 bp          |
| <i>ImZep1</i> gene             | ZepIngalso1fwd1 | ZepIngalso1Rev2 | 63°C                  | 1865 bp          |
| <i>ImZep1</i> gene             | ImZepExpAtFWD1  | ZepIngalso1Rev1 | 66°C                  | 1991 bp          |
| <i>AtZep</i> short fragment    | AthZEfwd        | AtZErev         | 53°C                  | 500 bp           |
| Vector insertion               | SP6             | T7              | 53°C                  | variable         |

### 2.3.5 RACE-PCR (Rapid Amplification of cDNA Ends)

In order to obtain the full-length sequence of putative *ImZep1* gene, RACE-PCR was carried out with *I. marginata* RNA (ca. 1 µg) using the SMART<sup>TM</sup> RACE cDNA Amplification kit and the Advantage<sup>®</sup> 2 Polymerase Mix (Clontech, Saint-Germain-en-Laye) following the manufacturer's guidelines. The specific primers for *ImZep1* were used to perform the 5'-(RACE\_Iso1\_rev3; see Table 2.2) and 3'-(RACE\_Iso1\_fwd; see Table 2.2) RACE-PCR reactions.

### 2.3.6 DNA extraction from agarose gel

The PCR products were separated on 1.2-2.5% agarose gel (depending on the length of the PCR product) in 1x TAE buffer (40 mM Tris, 18 mM acetic acid, 1 mM EDTA) (Ausubel *et al.* 2002), GeneRuler<sup>TM</sup> DNA ladders (Fermentas) allowed size comparison. After staining with ethidium bromide (100 µl ethidium bromide, 500 ml distilled water) and destaining with water, the bands containing PCR products were excised from the gel under UV light and DNA was extracted from the gel piece using QIAquick<sup>®</sup> gel extraction kits (Qiagen) according to manufacturer's guidelines.

### 2.3.7 Purification of PCR products

When the DNA extraction from agarose gel had to be avoided because it caused problems for the subsequent cloning step, PCR products were purified from primers and unincorporated dNTPs directly after the PCR reaction. The Montage® PCR centrifugal filter (Millipore, Schwalbach) was used following manufacturer's guidelines.

### 2.3.8 Cloning of PCR products

#### 2.3.8.a TOPO TA cloning system

For cloning PCR products in pCR® II-TOPO® and pENTR™/D-TOPO® vectors (Invitrogen, Darmstadt; see Table 2.1) the manufacturer's guidelines were followed.

#### 2.3.8.b Cloning into pGWB2 vector via Gateway sites

To transfer fragments from the entry clone pENTR™/D-TOPO® in the pGWB2 vector, an LR reaction was performed using the Gateway® LR clonase II (Invitrogen) according to the manufacturer's instructions.

#### 2.3.8.c Cloning into pUC18 vector

For cloning into pUC18, the vector was first cut with the restriction enzyme *Sma*I (Fermentas) following manufacturer's guidelines. For the ligation ca. 180 ng purified PCR product were mixed with 50 ng vector, 1x appropriate buffer, 1 unit T4 DNA ligase (Fermentas) and sterile water. The mixture was incubated for 1 h at 30°C.

#### 2.3.8.d Cloning into pRhotHi-2 vector

Inserts were excised from the pUC18 vector by using the restriction enzymes *Nde*I and *Sal*I (Fermentas) for *A. thaliana* Zep and *Nde*I and *Xho*I (Fermentas) for *I. marginata* Zep following manufacturer's guidelines. The excised fragments and the linearized pRhotHi-2 vectors (cut with the same restriction enzymes used to excise the fragments from pUC18) were separated on 0.8% agarose gel and extracted (see 2.3.6). A ligation mixture was prepared by mixing the DNA-

fragment and the vector at a 3:1 molar ratio and adding 1 unit T4 DNA ligase, 1x appropriate buffer and sterile water. The mixture was incubated for 1 h at 30°C.

#### **2.3.8.e Transformation of *E. coli* DH5- $\alpha$**

Transformation of the ligated plasmids was carried out using One Shot® DH5- $\alpha$ -T1 competent bacterial cells (Invitrogen). Competent cells (50  $\mu$ l) were incubated on ice with 2  $\mu$ l of the ligation mixture for 10 min. In order to enable the transformation, a heat shock was then applied for 40 s at 42°C. After that the reaction mixture was directly transferred onto ice and 250  $\mu$ l SOC-medium (see 2.2.2) was added. The transformed bacteria were cultivated for 1 h at 37°C under constant agitation at 150 rpm. Aliquots of 50  $\mu$ l and 500  $\mu$ l transformation culture were plated out onto standard nutrient agarose plates containing antibiotics (see 2.2.2) and plates were incubated at 37°C overnight.

In case of transformation with pCR® II-TOPO® and pUC18 vectors (see Table 2.1), 100  $\mu$ l IPTG (100 mM) and 25  $\mu$ l X-gal (50 mg/ml in DMF) were spread on the surface of the plates before plating the transformation mixture. In this way it was possible to distinguish colonies that were transformed with the recombinant plasmid (white colonies) from non-recombinant ones (blue colonies).

#### **2.3.8.f Transformation of *E. coli* strain S17-1 and BL21 (DE3) cells**

For transformation of *E. coli* S17-1 or BL21 (DE3), 200  $\mu$ l of competent cells (kindly provided by Thomas Drepper, Institute of Molecular Enzyme Technology, Heinrich-Heine-Universität Düsseldorf) were mixed with ca. 100 ng of plasmidic DNA and incubated on ice for 45 min. A heat-shock was then applied by keeping the mixture for 2 min at 42°C. Then, 700  $\mu$ l of LB medium (see 2.2.2) was added and the cells were cultivated at 37°C for 2 h. Subsequently, 50  $\mu$ l of this culture were plated on kanamycin selective LB-agarose plates. The remaining mixture was centrifuged (Hettich, Tuttlingen) for 3 min at 1600 x g and RT, the pellet was resuspended in 50  $\mu$ l of LB medium and also plated on selective agarose plates.

### 2.3.8.g Induced gene expression in *E. coli* BL21 (DE3)

For expression of *Zep* genes cloned in pRhotHi-2 plasmid into *E. coli* BL21 (DE3), cells were incubated at 37°C and 120 rpm in LB-glucose medium (10 g tryptone, 10 g NaCl, 5 g yeast extract, 4 g glucose, distilled water up to 1000 ml) containing kanamycin (50 µg/ml) until the logarithmic growth phase was reached ( $O.D_{580} = 0.5$ ). Gene expression was then induced by adding IPTG to a final concentration of 1 mM and incubating the cells overnight under the same conditions.

### 2.3.8.h Conjugation transfer of plasmidic DNA from *E. coli* to *R. capsulatus* (Elhai and Wolk 1988)

In total 6-8 colonies of transformed *E. coli* S17-1 were picked from a fresh solid culture and resuspended in 1 ml of PY-medium (without agarose, see 2.2.1); 500 µL of this cell suspension was mixed with *R. capsulatus* cells suspended in 1 ml RCV + N-minimal medium (see 2.2.1). The mixture was centrifuged for 10 min at 16000 x g and RT in order to pellet the bacterial cells. Then 1200 µl of supernatant was discarded and the pellet was resuspended in the remaining medium. The cell suspension was incubated on a nitrocellulose filter (Schleicher und Schüll, pore diameter 0.2 µm) placed on a PY-agarose plate at 30°C overnight. After the incubation the filter was inserted in a 2 ml Eppendorf tube together with 1 ml of RCV + N-minimal medium and vigorously shaken (with a Vortex) in order to resuspend the bacterial cells in the medium. The filter was then removed and the cell suspension was centrifuged for 5 min at 16000 x g and RT. The supernatant was almost completely discarded and the pellet was resuspended in the remaining medium before plating on streptomycin + kanamycin selective PY-agarose plates (25 µg/ml kanamycin, 200 µg/ml streptomycin). Plates were incubated phototrophically for 3 d at 30°C.

### 2.3.8.i Transformation of *A. tumefaciens* GV3101

For transformation of *A. tumefaciens*, 50 µl of competent cells (kindly provided by Anika Wiese-Klinkenberg, IBG-2: Plant Sciences, Forschungszentrum Jülich) were incubated on ice with ca. 1 µg pGWB2 recombinant plasmidic DNA for 10 min. Then the mixture was frozen in liquid nitrogen for 5 min and thawed on ice for 10 min. Subsequently, 1 ml of LB-medium was added and the cells were cultivated overnight at 28°C. The following day the transformation mix was plated out onto standard nutrient selective agarose plates containing kanamycin and hygromycin and incubated for 2 d at 28°C.

### 2.3.8.j Colony PCR

The presence of the ligated plasmid in the transformed *E. coli* cells was checked by colony PCR analysis. Using a sterile toothpick a single colony was picked from a growing culture and transferred to a sterile PCR tube to which standard PCR reaction mix was added. A reaction mix (50 µl) contained 1 µM primer (each T7 and SP6 or insert specific primers; see Table 2.2), 0.2 mM dNTP mix, 2 mM MgCl<sub>2</sub>, 1x appropriate buffer, 1.25 units *Taq* polymerase (Fermentas) and distilled water. PCR was carried out with the programs in Table 2.5.

The presence of the expression vectors in transformed cells of *A. tumefaciens* was checked by performing a PCR reaction on plasmidic DNA instead of making a colony PCR.

### 2.3.8.k Plasmid mini preparation

Plasmidic DNA was isolated from bacterial cultures by using QIAprep® Spin Miniprep kits (Qiagen) according to the manufacturer's instructions. Plasmidic DNA was eluted from the column with 50 µl sterile water.

### 2.3.8.l Sequence analysis of nucleotides

Sequencing of the cDNA fragments amplified and cloned was performed by Eurofins MWG Operon (Ebersberg). Analysis of the nucleotide sequences was carried out using DNAMAN software (Version 4.15, Lynnon BioSoft, Quebec) and BLAST (Basic Local Alignment Search Tool) from National Center for Biotechnology Information (NCBI; <http://blast.ncbi.nlm.nih.gov/Blast.cgi>).

### 2.3.9 Northern Blotting

The RNA samples were separated by electrophoresis on 1.3% agarose gel, containing 18% formaldehyde as a denaturing agent, in 1x MOPS buffer (40 mM morpholino-3-propanesulphonic acid, 10 mM sodium acetate, 1 mM EDTA, pH 7). Each RNA loading sample contained 1x MOPS, 18% formaldehyde, 50% formamide, 5 µg RNA and sterile water. Samples were denatured for 15 min at 65°C to melt secondary structures before mixing with a loading buffer to the final concentration of 5% (v/v) glycerol, 100 µM EDTA, 0.003% (w/v) bromophenol blue and 0.003%

(w/v) xylene cyanol. Then the samples were loaded on the gel described above and electrophoresis was carried out at 60-80 V for ca. 4 h.

After the gel electrophoresis the RNA was transferred overnight from the gel onto a positively charged nylon membrane (Roche) by capillary force with 10x SSC buffer (Eppendorf) (1.5 M NaCl, 0.15 M sodium citrate, pH 7). The RNA was then fixed to the membrane using UV-light (Stratalinker® 1800, Stratagene, Heidelberg).

The membrane was stained with methylene blue (0.03% methylene blue in 0.3 M sodium acetate, pH 5.2; Herrin and Schmidt 1988) before pre-hybridization to confirm equal sample loading.

The pre-hybridization (1 h) and hybridization (overnight) steps were performed at 50°C in a rolling oven, using DIG Easy Hyb and DIG Wash and Block Buffer Set according to manufacturer's guidelines (Roche). For hybridization, DIG-labeled probes (see 2.3.10) were denatured for 10 min at 95°C before being added to the hybridization buffer (40 ng probe/ml hybridization solution).

For the post-hybridization step, the membrane was washed twice with 2x SSC, 0.1% SDS solution for 5 min and then washed twice with 0.5x SSC, 0.1% SDS solution for 15 min at 50°C. The following steps were all performed at RT. The membrane was first washed with 1x washing buffer (Roche) and then incubated for 30 min in 1x blocking solution. This was followed by 30 min incubation with alkaline phosphatase-conjugated antibody (Anti-DIG-AP, Roche) diluted to 1:10000 in 1x blocking solution. After that the membrane was washed twice with 1x washing buffer to remove unbound antibody and equilibrated in 1x detection buffer for 5 min. The chemiluminescent alkaline phosphatase substrate, CDP-star (Roche), was diluted to 1:100 in 1x detection buffer and applied to the membrane for 5 min. The chemoluminescence signal from the CDP-Star was detected by a luminescent imager (Fluorescence Imaging System LAS 3000, FUJIFILM Europe, Düsseldorf). Data analysis and interpretation were assisted by AIDA software, version 3.27 (Raytest, Strubenhardt).

### 2.3.10 DIG (Digoxigenin) labeling of probes

Labeled probes were generated with the PCR DIG synthesis kit (Roche). The PCR conditions used are described in Table 2.5. A 50 µl reaction mixture consisted of 1 µM primer (IsZep\_1 fwd and IsZep\_1rev for *ImZep1* probe; IsZep\_2fwd and IsZep\_2rev2 for *ImZep2* probe; see Table 2.2), ca. 1

ng plasmid DNA template, DIG-mix (containing DIG labeled dUTPs), 1x appropriate buffer, enzyme mix and sterile water.

After the PCR reaction, primers and unincorporated dNTPs were removed from the DIG-labeled probes using the Montage® PCR centrifugal filter device (Millipore) according to manufacturer's guidelines. The PCR product was then checked by separation of an aliquot on 1.5% agarose gel in 1X TAE buffer. For estimation of the size and quantity of the PCR product, MassRuler™ low range ladder (Fermentas) was also loaded on the same gel.

### **2.3.11 Real-time-PCR analysis of *R. capsulatus* transformed cells**

#### **2.3.11.a RNA extraction from *R. capsulatus***

Liquid cultures of *R. capsulatus* were grown phototrophically until an O.D.<sub>660</sub> of 0.8 was reached, cells were separated, resuspended in 50 µL TE buffer (10 mM Tris, 1 mM EDTA, pH 8) containing lysozyme (400 µg/ml), and frozen in liquid nitrogen. After re-thawing at RT, another 50 µL of TE + lysozyme buffer was added. The total RNA was extracted by using the RNasy Mini Kit (Quiagen) according to the manufacturer's instructions, followed by a DNAase digestion with RQ1 RNase-free DNase kit (Promega, Mannheim). The isolated DNA-free RNA was stored at -80°C until use.

The concentration of RNA was determined photometrically by using the Bio Photometers (Eppendorf) and a Hellma TrayCell cuvette.

#### **2.3.11.b Reverse transcription from extracted RNA and real-time PCR**

Starting from the total RNA extracted from *R. capsulatus* cells, *Zep* cDNA was synthesized by reverse transcriptase and quantified by real-time PCR. For this experiment QuantiTect SYBR Green PCR One step Kit (Quiagen) was used according to the manufacturer's guidelines. For reverse transcription of RNA samples and for real-time PCR reactions with the reverse transcribed cDNA samples, primers were designed by using the Primer3 software (<http://frodo.wi.mit.edu>). The primers used were AH\_409\_RTIn\_up and AH\_409\_RTIn\_dn for *ImZep1* insertion and AH\_409\_RTAt\_up and AH\_409\_RTAt\_dn for *AtZep* insertion (see Table 2.2). A standard curve was constructed by using different dilutions of the control plasmid and the *aph* gene (gene for kanamycin resistance) as a control. The primers for *aph* were aphII-RTup and aphII-RTdn (see table

2.2). As internal standard, the *rpoD* gene, encoding for the sigma factor of *R. capsulatus* RNA polymerase, was used.

Real-time PCR reactions were performed by using Mastercycler ep gradient S realplex<sup>4</sup> (Eppendorf) by using the following program (Table 2.8).

**Table 2.8 Program for real-time PCR**

|                  |   |         |       |
|------------------|---|---------|-------|
| Denaturation     | 15 min  | 95°C    |       |
| Denaturation     | 15 s  | 95°C    | } 35x |
| Annealing        | 15 s  | 60°C    |       |
| Elongation       | 20 s<br>fluorescence<br>detection                 | 68°C    |       |
| Final Elongation | 10 min  | 68°C    |       |
| Melting curve    | 20 min<br>continuous<br>fluorescence<br>detection | 60-95°C |       |

## 2.4 Transformation of *A. thaliana*

### 2.4.1 Floral dipping transformation

Cells of *A. tumefaciens* carrying *Zep* insertions were cultivated overnight at 28°C in 5 ml LB-medium containing rifampicin, kanamycin and gentamicin for binary vector selection. From these bacterial cells a fresh overnight culture was subsequently prepared in 250 ml LB-medium (see 2.2.2) containing antibiotics. When the bacterial growth reached the stationary phase ( $O.D._{600} = 0.8$ ) the culture was centrifuged at 2500 x g for 20 min at 4°C (Allegra™ 25R centrifuge, Beckman Coulter, Krefeld). The supernatant was discarded and *A. tumefaciens* cells were resuspended in 20 ml 5% sucrose. The cell suspension was transferred to a glass container and surfactant Silwet L-77 (Lehle Seeds, Round Rock) was added to a concentration of 0.05% (v/v).

While flowering, above-ground parts of *A. thaliana npq2* and *szl1npq1* plants were dipped into the bacterial solution for ca. 10 s with gentle agitation. Dipped plants (T0 generation) were then covered with a wet plastic cover to maintain high humidity and kept in the dark for 16-24 h. Plants were well watered on the following day and grown for about 1 month until seeds became mature. At that point watering was stopped and dry seeds (T1 generation) were harvested using a sieve when siliques turned brown.

### 2.4.2 Seed sterilization

Seeds were collected in 1.5 ml Eppendorf tubes and incubated with 0.5 ml 70% ethanol for 3 min. Ethanol was removed and 0.5 ml sodium hypochlorite solution (0.5% (w/v) NaOCl, one drop of Tween 20, sterile water up to 10 ml) was added. After 10 min, the seeds were washed three times with sterile water. After the last wash they were kept in 0.5 ml sterile water.

### 2.4.3 Seeds germination on selective agarose plates

Sterilized seeds were placed on selective plant agarose medium containing 0.5 g/l 2-(*N*-morpholino)ethanesulfonic acid, 0.8% (w/v) agarose, 2.2 g/l Murashige & Skoog medium (Sigma), 200 µg/ml cefatoxime, 50 µg/ml kanamycin and sterile water (pH 5.8). The plates were kept for 5 d at 4°C to allow stratification and were then transferred to a climate chamber at 22°C air

temperature, 150-180  $\mu\text{mol photons m}^{-2} \text{ s}^{-1}$  with 12-h/12-h photoperiod and 60% constant relative air humidity. Due to the presence of antibiotics only the transformed plants survived on the selective agarose medium. Surviving seedlings (T1 generation) were transferred to soil (ED 73 Einheitserde) and let grow until they produced new seeds (T2 generation).

Segregation analysis was carried out to check approx. number of the insertion and homozygosity by growing the T2 and T3 seeds on the selection agarose plates.

## 2.5 Biochemical methods

### 2.5.1 Western blot of *R. capsulatus* proteins

#### 2.5.1.a Protein isolation from *R. capsulatus* (Katzke *et al.* 2009)

*Rhodobacter capsulatus* cells were grown phototrophically in 10 ml of RCV + N-minimal medium (see 2.2.1) containing kanamycin (25  $\mu\text{g/ml}$ ) until the logarithmic growth phase was reached. The cell density was determined by turbidity measurements at 660 nm and a new liquid culture was prepared by diluting the first one in order to have an O.D. of 0.02. Then, 8 mM fructose was added to the culture to induce the ZEP expression. After 48 h of incubation, cell density was again measured and the bacterial cells were harvested by centrifugation for 10 min at 16000 x g and RT. The supernatant was discarded and the pellet was resuspended in 1 ml of 1x SDS-stacking gel buffer (4x SDS-stacking gel buffer: 1.5 M Tris-HCl in distilled water, pH 6.8). The cells were again pelleted by centrifugation for 5 min at 16000 x g and RT, the supernatant was removed and the pellet was suspended in 75  $\mu\text{l}$  of SDS-sample buffer (50 mM Tris, 10% (v/v) glycerol, 4% (w/v) SDS, 2% (v/v)  $\beta$ -mercaptoethanol, 0.03% (w/v) bromophenol blue, pH 6.8). The resuspended protein sample was denatured for 10 min at 99°C in agitation (Eppendorf thermomixer) and then centrifuged at 16000 x g and RT for 10 min. The supernatant (which contained the extracted proteins) was collected in a new Eppendorf tube.

#### 2.5.1.b SDS polyacrylamid gelelectrophoresis (SDS-PAGE) (method modified from Laemmli *et al.* 1970)

The extracted proteins were separated under denaturing conditions in a discontinuous gel system composed of a stacking gel (0.715 ml 40% (w/v) acrylamid:bisacrylamid 37.5:1, 1.25 ml 4x SDS-

stacking gel buffer, 0.05 ml 10% (w/v) SDS, 0.05 ml 10% (w/v) APS, 0.0035 ml TEMED, 3.15 ml distilled water) cast over a separation gel (3.75 ml 40% (w/v) acrylamide:bisacrylamide 37.5:1, 2.5 ml 1.5 M Tris-HCl, pH 8.8, 3.15 ml 87% (v/v) glycerol, 0.1 ml 10% (w/v) SDS, 0.075 ml 10% (w/v) APS, 0.015 ml TEMED), in which the proteins were separated according to their apparent molecular size. A protein amount corresponding to a cell density of O.D. = 3 was loaded on the gel for each sample, together with a SDS-PAGE molecular weight standard (Precision Plus Protein™ Dual Color standard 161-0734, Bio-Rad) to enable size comparison. The electrophoresis was performed in a gel cell mini-PROTEAN II (Bio-Rad) in a running buffer (2.5 mM Tris-HCl, 19.2 mM glycine, 0.01% SDS) at 120 V for 15 min (while the samples were in the stacking gel) and then at 200 V (when the proteins reached the resolving gel) at RT until the bromophenol blue front had just left the gel.

#### **2.5.1.c Coomassie blue staining (Merril 1990)**

To visualize the protein bands the gel was transferred to Coomassie blue staining dye containing 25% (v/v) methanol, 10% (v/v) acetic acid and 0.2% (w/v) Coomassie brilliant blue (Bio-Rad). The gel was stained at RT in a water bath with gentle shaking for 30 min, then the staining solution was replaced with a destaining solution (5% (v/v) methanol, 7% (v/v) acetic acid) which was repeatedly changed until the background color had been removed. Destained gel was placed in water until digital documentation occurred.

#### **2.5.1.d Protein transfer to polyvinylidene difluoride (PVDF) membrane (Dunn 1986; Wilsom and Juan 1989)**

After the SDS-PAGE the separated proteins were transferred to a PVDF membrane by using a mini-blot transfer Electrophoretic Transfer cell (Bio-Rad). First the PVDF membrane was incubated in methanol for 1 min, then transferred to distilled water for 10 min before 2-min equilibration in a carbonate blot buffer (1 mM NaHCO<sub>3</sub> and 0.3 mM Na<sub>2</sub>CO<sub>3</sub>, pH 9.9, in 2% methanol). Also the gel was equilibrated for 10 min in the same carbonate blot buffer. The transfer of the proteins was performed in carbonate blot buffer at 150 mA for 15 min followed by 20 min at 300 mA.

#### **2.5.1.e Immunodetection of proteins**

After being transferred to a PVDF membrane, the proteins were detected immunologically. The membrane was first saturated with TBST buffer (1.25 mM Tris-HCl, 7.5 mM NaCl, 0.15 mM KCl,

0.2% (v/v) Tween 20, pH 8.0) + 3% (w/v) milk powder at 30°C for 1 h in order to block the free binding sites. Subsequently, the membrane was washed with TBST buffer at 30°C for 15 min and then incubated with the  $\alpha$ -histidine antibody ( $\alpha$ -His, diluted to 1:15000; Invitrogen) for 1 h at 30°C under agitation. After that the membrane was washed twice for 25 min in TBST buffer in order to remove the unbound antibody. The  $\alpha$ -His antibody is coupled with horseradish peroxidase, so that the protein bound to the antibody could be detected by using Enhanced-chemo-luminescence Western blotting detection system (Amersham/GE Healthcare Europe, Glattburgg) according to manufacturer's instructions, followed by a photographic documentation. The resulting image was analyzed with STELLA- and AIDA- software (Raytest, Straubenhardt).

#### **2.5.1.f Staining of PVDF membrane**

After the immunodetection the membrane was washed in TBST buffer for 15 min, incubated with an amido black solution (0.1% (w/v) amido black; 45% (v/v) methanol; 10% (v/v) acetic acid) for 30 min and dried overnight, so that the proteins linked to the membrane could be stained.

### **2.5.2 Western blot of *A. thaliana* proteins**

#### **2.5.2.a Protein isolation from *A. thaliana* leaves**

Leaf discs (2.0 cm<sup>2</sup>) were ground in 100  $\mu$ l extraction buffer (50 mM Tris-HCl pH 7.6, 7 M urea, 5% SDS, sterile water). Once the leaf material was totally ground, the mixture was centrifuged at 13000 rpm for 10 min at 4°C (centrifuge 5417R, Eppendorf). The supernatant (containing the extracted proteins) was transferred to a new 1.5 ml Eppendorf tube and the chlorophyll concentration was determined (see 2.6).

#### **2.5.2.b SDS PAGE**

Protein samples corresponding to 2  $\mu$ g total Chl were mixed with 1x SDS-sample buffer (see 2.5.1.a), heated at 95°C for 15 min and loaded together with a SDS-PAGE molecular weight standard (Precision Plus Protein™ Dual Color Standards, Bio-Rad) on Mini-PROTEAN® TGX™ Precast-gels (Bio-Rad). The electrophoresis was performed in a running buffer (as described in 2.5.1.b) at 100 V.

### 2.5.2.c Protein transfer to a nitrocellulose membrane

After the SDS-PAGE a first gel was stained with Coomassie blue dye (as described in 2.5.1.c) and a second gel was used to transfer the proteins onto a nitrocellulose membrane (Bio-Rad). The blotting was performed in a blotting buffer (25 mM Tris, 0.19 M glycine, 800 ml sterile water, 200 ml methanol) in a mini-blot transfer Electrophoretic Transfer cell (Bio-Rad) at 100 V for 1 h.

### 2.5.2.d Immunodetection of the proteins

After the blotting the membrane was washed 10 min with TBS buffer (20 mM Tris-HCl, 134 mM NaCl, sterile water) and then saturated for 1 h in the blocking buffer (TBS buffer + 8% milk powder). Incubation with  $\alpha$ -PsbS or  $\alpha$ -Zep antibody (kindly provided by Roberto Bassi, University of Verona) diluted to 1:1500 in blocking buffer was performed at RT overnight. The following day the membrane was washed twice with both TBS and TBST buffer (1x TBS buffer, 0.05% Tween 20) and incubated 1 h with alkaline phosphatase-conjugated secondary antibody (Sigma-Aldrich) diluted to 1:5000 in blocking buffer. After two washing steps with TBS and TBST the protein was detected by addition of 7.5  $\mu$ l nitro blue tetrazolium (75 mg/ml in 70 % dimethylformamide; Loewe Biochemica, Sauerlach) and 45  $\mu$ l 5-bromo-4-chloro-3-indolyl phosphate (50 mg/ml in 100% dimethylformamide; Loewe Biochemica,) solutions diluted in 15 ml alkaline-phosphatase buffer (0.1 M Tris, 0.1 M NaCl, 5 mM  $MgCl_2$ , sterile water).

## 2.6 Photometric determination of total chlorophyll (Porra *et al.* 1989)

Pigments were extracted by grinding frozen leaf discs (0.5 cm<sup>2</sup>) in 1 ml 80% acetone; the homogenate was transferred to a 1.5 ml Eppendorf tube and centrifuged at 13000 rpm for 5 min at 4°C. The supernatant was collected in a new 1.5 ml Eppendorf tube and absorbance was measured at two different wavelengths:  $\lambda = 663$  nm and  $\lambda = 646$  nm, by using the photometer LKB Biochrom Ultraspek II (American Laboratory Trading, East Lyme). For calculation of Chl *a* and Chl *b* amount the method by Porra *et al.* (1989) was used.

## 2.7 HPLC (High Performance Liquid Chromatography) analysis

For pigment analysis leaf discs ( $1.0\text{ cm}^2$ ) were ground in a small amount of liquid nitrogen by using a mortar and pestle. Pigments were extracted twice in chilled acetone and the final volume of the extract was adjusted to 1 ml. Then the extracts were centrifuged at 13000 rpm for 5 min and syringe-filtered (Chromafil®; Macherey-Nagel, Düren) prior to the HPLC analysis.

Photosynthetic pigments were separated by an Allsphere ODS-1 column (5- $\mu\text{m}$  particle size, 250 mm x 4.6 mm; Alltech Associates Inc., Deerfield) by using the solvents and protocols modified from Gilmore & Yamamoto (1991). Two solvents were used as the mobile phase: solvent A, acetonitrile: methanol: Tris HCl (0.1 M, pH 8) (80:12:8.5) and solvent B, hexane: methanol (1:4). 100% solvent A was run from 0 to 24 min followed by a 2-min linear gradient to 100% solvent B. From 26 to 31.5 min solvent B was run isocratically. A linear gradient back to 100% solvent A occurred in the following 2 min. 100% solvent A was then run from 33.5 to 42 min to equilibrate the column before the next sample injection. The flow rate was  $1\text{ ml min}^{-1}$  and the sample injection volume was 20  $\mu\text{l}$ .

Pigments were identified by retention times and absorption spectra monitored by a Waters 996 photodiode array detector (Waters Corporation, Milford). Peak area was integrated in chromatograms detected at 440 nm and data were analysed with Waters Empower software. The HPLC system was calibrated for quantitative analysis of carotenoids and chlorophylls by using pure standards.

## 2.8 Plant physiological methods

### 2.8.1 Chlorophyll *a* fluorescence analysis

Chlorophyll *a* fluorescence measurements were performed by using a portable Chl fluorometer (PAM-2100; Walz, Effeltrich) and the saturation pulse method (Schreiber 2004). Fluorescence nomenclature is according to van Kooten and Snel (1990).

In the sunfleck experiments with *A. thaliana* carotenoid mutants (see 2.2.4), the maximal photosystem II efficiency,  $F_v/F_m = (F_m - F_o)/F_m$ , was measured in leaves of dark-adapted plants at the end of the night period. Immediately after the  $F_v/F_m$  measurement, leaves were exposed to actinic light of 600-800  $\mu\text{mol photons m}^{-2} \text{s}^{-1}$  for 5 min followed by 2 min of darkness. The actinic light intensity slowly increased from about 600 to 800  $\mu\text{mol photons m}^{-2} \text{s}^{-1}$  during the experiment on each day. Non-photochemical fluorescence quenching,  $\text{NPQ} = (F_m - F_m')/F_m'$ , was determined by applying a train of saturation pulses every 30 s throughout the actinic light illumination and subsequent dark relaxation. The  $F_m$  values of the  $F_v/F_m$  measurements were used for calculation of NPQ for each plant.

In the high-light treatment on transgenic *A. thaliana* plants (see 2.2.4), after determining  $F_v/F_m$  on dark-adapted leaves,  $\phi_{\text{PSII}} = (F_m' - F_t)/F_m'$  and NPQ were measured at the end of the 30-min high-light exposure and at several time points during the subsequent dark recovery.

### 2.8.2 Analysis of leaf growth with GROWSCREEN FLUORO (Jansen *et al.* 2009)

Rosette area growth was analysed by using the GROWSCREEN FLUORO method described in Jansen *et al.* (2009). The leaf growth measurements in the sunfleck experiment were started about three weeks after germination. The total projected leaf area was measured at around the same time (13:00) every other day from day 0 to day 12; at this time of day, leaves of *Arabidopsis* plants were positioned almost horizontally above the soil. The data of the total projected leaf area were fitted to an exponential growth curve  $A_x = A_0 \cdot \exp^{(b \cdot x)}$ , where  $A_x$  and  $A_0$  are the total projected leaf area on day  $x$  and day 0, respectively, and  $b$  the growth factor. Relative growth rate (RGR, %  $\text{d}^{-1}$ ) of leaves was obtained by multiplying  $b$  by 100.

### 2.8.3 Analysis of root growth with GROWSCREEN-ROOT (Nagel *et al.* 2009)

Root system architecture was analysed by using GROWSCREEN-ROOT (Nagel *et al.* 2009). On day 0 and day 5 of the sunfleck experiment (see 2.2.4), all Petri dishes were placed in an automated carousel device and images of the root systems were taken for individual Petri dishes via a high-resolution CCD-camera (IPX-6M3-TVM, Imperx Inc., Boca Raton) under infra-red illumination. Images of the root systems were then analysed by using the GROWSCREEN-ROOT method (for technical details, see Mühlich *et al.* 2008; Nagel *et al.* 2009). Length of the primary root and number of lateral roots were determined for each plant. The RGR of primary root was then calculated as:  $\text{Root RGR } [\% \text{ d}^{-1}] = 1/t * \ln (PRL_5/PRL_0)$ , where  $t$  denotes the time interval between two measurement points (i.e. 5 d) and  $PRL_0$  and  $PRL_5$  the primary root length on day 0 and day 5. Likewise, the increase in the number of lateral roots was calculated as:  $\text{Increase in the number of lateral roots } [\% \text{ d}^{-1}] = 1/t * \ln (LRN_5/LRN_0)$ , where  $LRN_0$  and  $LRN_5$  stand for the number of lateral roots on day 0 and day 5.

### 2.8.4 Determination of leaf dry mass

On the last day of the leaf growth analysis in the sunfleck experiment, the aboveground part of plants were harvested for each genotype and treatment ( $n=12$  for wt and  $n=6$  for all mutants). Samples were dried in an oven at 70°C until a constant mass was reached. The dry weight was measured by using an analytical balance (Explorer; Ohaus Europe, Nänikon). Leaf mass per area ( $\text{g m}^{-2}$ ) was calculated from the dry weight and the total projected leaf area (see 2.8.2) determined for each plant.

### 2.8.5 Seed harvesting from sunfleck treated plants

Following the experiments of leaf growth analysis in the sunfleck experiment, some plants were left under the control and sunfleck conditions. After bolting, inflorescence stems were covered with white paper bags so that only rosette leaves were directly exposed to strong light of the sunflecks, but not inflorescence and cauline leaves. Following about 20 more weeks to complete flowering and senescence under the corresponding light conditions, plants were moved to a low-light condition (ca.  $20 \mu\text{mol photons m}^{-2} \text{ s}^{-1}$ ) in the same climate chamber and watering was stopped. When they were completely dried, seeds were harvested for each plant separately and weighed with an analytical balance (Explorer, Ohaus). The number of plants used for seed harvesting was 6 and 5 (control and sunfleck, respectively) for wt, 6 and 3 for *lut2*, 10 and 4 for

*lut5*, 7 and 7 for *szl1npq1* and 7 and 7 for *npq1*. Some plants of *lut2* and *lut5* prematurely died under the sunfleck condition so that fewer plants were available for seed harvesting.

## 2.9 Statistical data analysis

All data were statistically tested by using SigmaStat (SYSTAT Software GmbH, Erkrath, Germany). Analysis of variance (ANOVA) was used for comparing data. In the high light experiment, data related to the different genotypes were compared with one-way ANOVA; for all pairwise multiple comparisons the Tukey test was used. In the sunfleck experiment, in which the different genotypes as well as the two different treatments (control and sunfleck) were compared at the same time, the Tukey test of two-way ANOVA was performed.

## 3 Results

### 3.1 Investigation of the role of *I. marginata* ZEP (ImZEP) in the Lx-cycle and its regulation in the V-cycle

High amounts of Lx have been found in shade leaves of the plant *I. marginata* (mostly above 20 mmol mol<sup>-1</sup> Chl), presumably synthesized from L by the enzyme ZEP (Matsubara *et al.* 2008); the fact that no Lx is detectable in leaves of *A. thaliana* raises the question of whether ImZEP has a higher affinity for L than AtZEP.

In order to clarify the role of ImZEP in the Lx-cycle and to study its activity *in vivo* and *in vitro*, putative *Zep* genes were isolated from *I. marginata* and the gene products have been heterologously expressed in both bacterial and plant expression systems.

#### 3.1.1 Isolation of the Zep isoform 1 (ImZep1) cDNA from *I. marginata* leaves

According to a previous study with *I. spectabilis*, two isoforms of *Zep* (termed *Zep1* and *Zep2*) may be present in the genus *Inga* (Seltmann 2006). In the study by Seltmann, partial DNA sequences in the middle of *Zep* genes were amplified by PCR by using degenerate primers that recognize conserved sequence motifs found in many known *Zep* sequences of other plant species.

In order to isolate the two *Zep* isoforms from *I. marginata* the total RNA was extracted from leaves of this plant and cDNA was synthesized. Based on the known short regions of *Zep1* and *Zep2* found in *I. spectabilis*, specific primers were designed to amplify separately the partial cDNA sequences relative to the two isoforms in *I. marginata* (primers for *Zep1*: ZEP-multi-FWD2; IsZep\_1rev. Primers for *Zep2*: IsZep\_2fwd; IsZep\_2rev2. For nucleotide sequences of the primers, see Table 2.2). After PCR, the amplification products (587 bp long for isoform1 and 145 bp long for isoform2) were purified from agarose gel, cloned into the pCR®II-TOPO® vector and sent to the company “Eurofins MWG operon” for sequencing.

Two different cDNA sequences corresponding to *Zep1* and *Zep2* found in *I. spectabilis* were obtained; a sequence comparison made by using the BLAST program of NCBI confirmed that the amplified sequences belonged to *Zep* genes.

Figure 3.1.1a shows the deduced amino acid sequence alignment between the *I. marginata* partial *Zep* isoform 1 and 2 and partial *Zep* sequences of other species taken from databases. The phylogenetic tree based on the multiple alignment shows the distance between the two *ImZep* isoforms (Fig. 3.1.1b); isoform 1 is closer to the *Zep* of *Vigna unguiculata* (85.7% of identity) which also belongs to the family Fabaceae and contains small amounts of Lx ( $< 5 \text{ mmol mol}^{-1} \text{ Chl}$ ) (Seltmann 2006), while isoform 2 has similarity (58.73 % of identity) to *Cucumis sativus* (Cucurbitales) *Zep*, in which high amounts of Lx have been found ( $> 20 \text{ mmol mol}^{-1} \text{ Chl}$ ) in leaves and cotyledons (Esteban *et al.* 2009).

Starting from this short region it was possible to design specific primers to perform a RACE-PCR experiment on RNA extracted from *I. marginata* leaves. The RACE-PCR allowed the isolation of the full length cDNA sequence of the *ImZep* isoform 1 gene. The gene consists of a 1992 bp open reading frame, encoding a 663-residue polypeptide. The deduced amino acidic sequence of the cDNA showed that it encoded a polypeptide of approximately 73 kDa.

A multiple sequence alignment of the deduced *ImZEP* protein with several known plant ZEP revealed a high degree of identity (Fig. 3.1.2). The predicted protein contains a less conserved, N-terminal extension that likely functions as chloroplast transit peptide (Baroli *et al.* 2003) and four regions of strong sequence homology that were previously defined: the two typical domains of the lipocalin family proteins, the flavoprotein monooxygenase domain that contains the catalytic site of the enzyme and confirms the requirement of FAD for its activity, and the phosphopeptide-binding domain (forkhead associate domain or FHA domain) which is thought to be involved in protein-protein interactions (Durocher and Jackson 2002; Baroli *et al.* 2003; Wang *et al.* 2008).

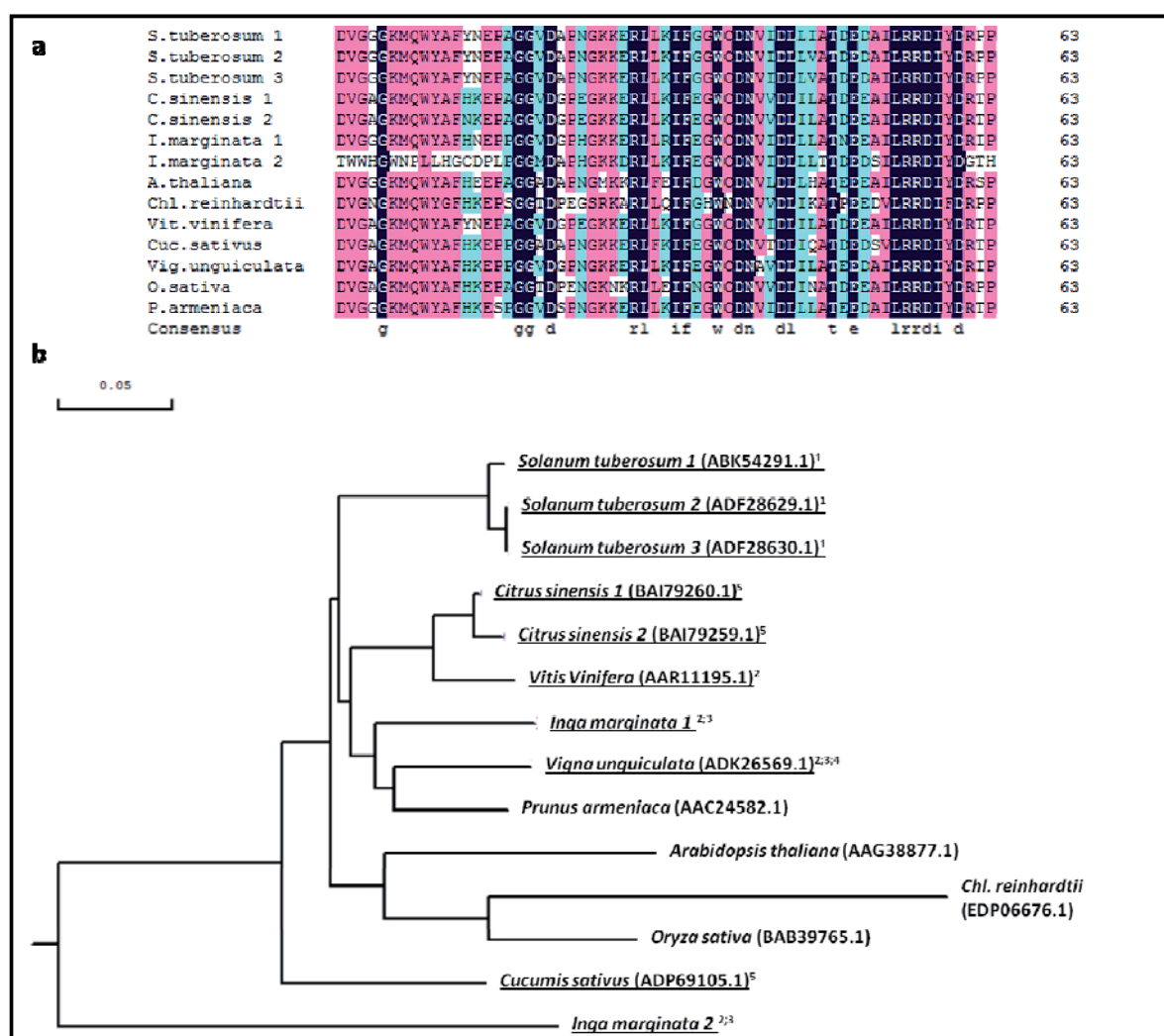


**Figure 3.1.1: Bioinformatical analysis of the partial amino acid sequence of ImZEP1 and ImZEP2.**

(a) Deduced amino acid alignment of partial ImZEP1 and ImZEP2 and partial ZEP from nine plant species. Only the small regions corresponding to the sequences isolated from *I. marginata* Zep isoforms were analyzed. Amino acid with homology = 100% are shaded in black, with homology  $\geq 75\%$  in pink and with homology  $\geq 50\%$  in blue. (b) Phylogenetic tree based on the multiple alignment. The accession numbers of ZEP protein sequences in GeneBank are indicated for each plant species. Species belonging to a family where Lx has been found are underlined: <sup>1</sup>Rabinowitch *et al.* 1975; <sup>2</sup>Matsubara *et al.* 2009; <sup>3</sup>Matsubara *et al.* 2008; <sup>4</sup>Seltmann 2006; <sup>5</sup>Esteban *et al.* 2009

|                 |   |     |
|-----------------|---|-----|
| Vit.vinifera    | ...MASAVFYSVQV...SI...FSRTHIPIS...KDSFEEFHS...INRYHYFRSNPC.GQKRVAVKATLAEATPAPSAPSLPSKRV...R1...L  | 80  |
| Vig.unguiculata | ...M.LVKGAVVEAPPVSPSSQGGSGAASKQLRV...L  | 33  |
| Sol.tuberosum   | ...MYSTLYSSSLNP...LSPKQLPLLSIDFFETLYHSLPCRSLENGHIKKVGK...VKATIAEAPVPTPEKSDSGVNGDLKVPQKKLKV...L  | 89  |
| Prun.armeniaca  | ...MASTLYFNYSNL...SAVFSRTHFPINIDFFLEFSPC...IHTDYHLASRTSRGQKKCLTEVRAIVASPTVEPSAPASTQPKKL...R1...L  | 84  |
| Or.sativa       | ...MALLSATAPAKTRFSLFSHEEAQHPEHALSACCGGGAAGRRQARARVAAMRPAADAAS.VAQAAFPGGGEGTRFRV...L   | 81  |
| In.marginatal   | ...MASTLYSSSLNP...SITTSFRTNFSIPTCYFSLDIPPP...GSRTIKHKMKLL.PITAARVAEAPPASPSPTQLTENHENRTPRKKI...R1...L  | 85  |
| Gen.lutea       | ...MASAVFYNSLNPSTSL.VSFAHVPLISLLEYLQFHQQKSFNGKKNRNFNKITK...AKAATTELVSFGAIESDNKPT...QKMRD...L  | 81  |
| Cit.sinensis    | ...MVSSMYNSVNL...STAVFSRTHFPVYVYHSCIEFSRYDHCINYK...FRITGSGQSKNPTQMKAAVAESPNNNSDENKKL...R1...L   | 85  |
| Cuc.sativus     | ...MALTRFHNPNFL...SSSLSRCTCFVPFATREYLVESPC...QRICNFGGKSGACGRKKLTQVKAATVEAPPAAGAEISRLSPKTVRI...L   | 88  |
| Ar.thaliana     | MGSTPFCYSINPSPSKLDFTRTHVFSVPKQFYLDLSSFSKGP...GGVSGFRSRRALLGVKAATLVEKEEKREAVTEKKKSRV...L   | 84  |
| Consensus       |   | 1   |
| Vit.vinifera    | VAGGGIGGLVLAALAKRGEVVFPRDLASRGEQYRGPIQIQSNALAAALDMDVAEENRAGCVTGRINGLVDGSGGWWKFDFTTFAERGL  | 180 |
| Vig.unguiculata | VAGGGIGGLVLAALAKRGEVVFPRDLASRGEQYRGPIQIQSNALAAALDMDVAEENRAGCVTGRINGLVDGSGGWWKFDFTTFAERGL  | 133 |
| Sol.tuberosum   | VAGGGIGGLVLAALAKRGEVVFPRDLASRGEQYRGPIQIQSNALAAALDMDVAEENRAGCVTGRINGLVDGSGGWWKFDFTTFAERGL  | 189 |
| Prun.armeniaca  | VAGGGIGGLVLAALAKRGEVVFPRDLASRGEQYRGPIQIQSNALAAALDMDVAEENRAGCVTGRINGLVDGSGGWWKFDFTTFAERGL  | 184 |
| Or.sativa       | VAGGGIGGLVLAALAKRGEVVFPRDLASRGEQYRGPIQIQSNALAAALDMDVAEENRAGCVTGRINGLVDGSGGWWKFDFTTFAERGL  | 181 |
| In.marginatal   | VAGGGIGGLVLAALAKRGEVVFPRDLASRGEQYRGPIQIQSNALAAALDMDVAEENRAGCVTGRINGLVDGSGGWWKFDFTTFAERGL  | 185 |
| Gen.lutea       | VAGGGIGGLVLAALAKRGEVVFPRDLASRGEQYRGPIQIQSNALAAALDMDVAEENRAGCVTGRINGLVDGSGGWWKFDFTTFAERGL  | 185 |
| Cit.sinensis    | VAGGGIGGLVLAALAKRGEVVFPRDLASRGEQYRGPIQIQSNALAAALDMDVAEENRAGCVTGRINGLVDGSGGWWKFDFTTFAERGL  | 181 |
| Cuc.sativus     | VAGGGIGGLVLAALAKRGEVVFPRDLASRGEQYRGPIQIQSNALAAALDMDVAEENRAGCVTGRINGLVDGSGGWWKFDFTTFAERGL  | 188 |
| Ar.thaliana     | VAGGGIGGLVLAALAKRGEVVFPRDLASRGEQYRGPIQIQSNALAAALDMDVAEENRAGCVTGRINGLVDGSGGWWKFDFTTFAERGL  | 184 |
| Consensus       | vagggigglv alaa kg v vfe d sa rgeg rgiqiqsnalaa l a d va m gc tg ringlvdg sg wy kfdftpa gl  |     |
| Vit.vinifera    | FVTRVSRMLQIILAVGDEIINSSNVVIFEDGKVVILELGGQHYEGDILGADGITSKVRNLFQSGEATYSYCTCYTIADFPADIDIVGYR   | 280 |
| Vig.unguiculata | FVTRVSRMLQIILAVGDEIINSSNVVIFEDGKVVILELGGQHYEGDILGADGITSKVRNLFQSGEATYSYCTCYTIADFPADIDIVGYR   | 233 |
| Sol.tuberosum   | FVTRVSRMLQIILAVGDEIINSSNVVIFEDGKVVILELGGQHYEGDILGADGITSKVRNLFQSGEATYSYCTCYTIADFPADIDIVGYR   | 289 |
| Prun.armeniaca  | FVTRVSRMLQIILAVGDEIINSSNVVIFEDGKVVILELGGQHYEGDILGADGITSKVRNLFQSGEATYSYCTCYTIADFPADIDIVGYR   | 284 |
| Or.sativa       | FVTRVSRMLQIILAVGDEIINSSNVVIFEDGKVVILELGGQHYEGDILGADGITSKVRNLFQSGEATYSYCTCYTIADFPADIDIVGYR   | 281 |
| In.marginatal   | FVTRVSRMLQIILAVGDEIINSSNVVIFEDGKVVILELGGQHYEGDILGADGITSKVRNLFQSGEATYSYCTCYTIADFPADIDIVGYR   | 285 |
| Gen.lutea       | FVTRVSRMLQIILAVGDEIINSSNVVIFEDGKVVILELGGQHYEGDILGADGITSKVRNLFQSGEATYSYCTCYTIADFPADIDIVGYR   | 285 |
| Cit.sinensis    | FVTRVSRMLQIILAVGDEIINSSNVVIFEDGKVVILELGGQHYEGDILGADGITSKVRNLFQSGEATYSYCTCYTIADFPADIDIVGYR   | 281 |
| Cuc.sativus     | FVTRVSRMLQIILAVGDEIINSSNVVIFEDGKVVILELGGQHYEGDILGADGITSKVRNLFQSGEATYSYCTCYTIADFPADIDIVGYR   | 288 |
| Ar.thaliana     | FVTRVSRMLQIILAVGDEIINSSNVVIFEDGKVVILELGGQHYEGDILGADGITSKVRNLFQSGEATYSYCTCYTIADFPADIDIVGYR   | 284 |
| Consensus       | pvtrv sr lq ila avg i n s v f d g kv le g gd l gadgi skvr fg e ys yctcytiadf p di vgyr  |     |
| Vit.vinifera    | VFLGHKQYFVSSDVGGKMQWYAHFEPAGGDSPEGKERRILIRFEGWCNDVOLLATDEAIIIRDIYDRPHETWGRVITLLGDSHAMQPNQG  | 380 |
| Vig.unguiculata | VFLGHKQYFVSSDVGGKMQWYAHFEPAGGDSPEGKERRILIRFEGWCNDVOLLATDEAIIIRDIYDRPHETWGRVITLLGDSHAMQPNQG  | 333 |
| Sol.tuberosum   | VFLGHKQYFVSSDVGGKMQWYAHFEPAGGDSPEGKERRILIRFEGWCNDVOLLATDEAIIIRDIYDRPHETWGRVITLLGDSHAMQPNQG  | 389 |
| Prun.armeniaca  | VFLGHKQYFVSSDVGGKMQWYAHFEPAGGDSPEGKERRILIRFEGWCNDVOLLATDEAIIIRDIYDRPHETWGRVITLLGDSHAMQPNQG  | 384 |
| Or.sativa       | VFLGHKQYFVSSDVGGKMQWYAHFEPAGGDSPEGKERRILIRFEGWCNDVOLLATDEAIIIRDIYDRPHETWGRVITLLGDSHAMQPNQG  | 381 |
| In.marginatal   | VFLGHKQYFVSSDVGGKMQWYAHFEPAGGDSPEGKERRILIRFEGWCNDVOLLATDEAIIIRDIYDRPHETWGRVITLLGDSHAMQPNQG  | 385 |
| Gen.lutea       | VFLGHKQYFVSSDVGGKMQWYAHFEPAGGDSPEGKERRILIRFEGWCNDVOLLATDEAIIIRDIYDRPHETWGRVITLLGDSHAMQPNQG  | 385 |
| Cit.sinensis    | VFLGHKQYFVSSDVGGKMQWYAHFEPAGGDSPEGKERRILIRFEGWCNDVOLLATDEAIIIRDIYDRPHETWGRVITLLGDSHAMQPNQG  | 381 |
| Cuc.sativus     | VFLGHKQYFVSSDVGGKMQWYAHFEPAGGDSPEGKERRILIRFEGWCNDVOLLATDEAIIIRDIYDRPHETWGRVITLLGDSHAMQPNQG  | 388 |
| Ar.thaliana     | VFLGHKQYFVSSDVGGKMQWYAHFEPAGGDSPEGKERRILIRFEGWCNDVOLLATDEAIIIRDIYDRPHETWGRVITLLGDSHAMQPNQG  | 384 |
| Consensus       | vflghkqyfvsdvvg gkmqwya f e p g g d s p e g k e r r i l i r f e g w c n d l a t e a i i r d i y d r p h e t w g r v i t l l g d s h a m q p n g q |     |
| Vit.vinifera    | GGCMAIEDGQLAEFLDKAWNESKSGSEHDICSLRSYERARIRVAVIHGUARAAAMMASTYKYLGVGLPLSFLTRPHFPGRVGGRFVIDIDMP  | 480 |
| Vig.unguiculata | GGCMAIEDGQLAEFLDKAWNESKSGSEHDICSLRSYERARIRVAVIHGUARAAAMMASTYKYLGVGLPLSFLTRPHFPGRVGGRFVIDIDMP  | 433 |
| Sol.tuberosum   | GGCMAIEDGQLAEFLDKAWNESKSGSEHDICSLRSYERARIRVAVIHGUARAAAMMASTYKYLGVGLPLSFLTRPHFPGRVGGRFVIDIDMP  | 489 |
| Prun.armeniaca  | GGCMAIEDGQLAEFLDKAWNESKSGSEHDICSLRSYERARIRVAVIHGUARAAAMMASTYKYLGVGLPLSFLTRPHFPGRVGGRFVIDIDMP  | 484 |
| Or.sativa       | GGCMAIEDGQLAEFLDKAWNESKSGSEHDICSLRSYERARIRVAVIHGUARAAAMMASTYKYLGVGLPLSFLTRPHFPGRVGGRFVIDIDMP  | 481 |
| In.marginatal   | GGCMAIEDGQLAEFLDKAWNESKSGSEHDICSLRSYERARIRVAVIHGUARAAAMMASTYKYLGVGLPLSFLTRPHFPGRVGGRFVIDIDMP  | 485 |
| Gen.lutea       | GGCMAIEDGQLAEFLDKAWNESKSGSEHDICSLRSYERARIRVAVIHGUARAAAMMASTYKYLGVGLPLSFLTRPHFPGRVGGRFVIDIDMP  | 485 |
| Cit.sinensis    | GGCMAIEDGQLAEFLDKAWNESKSGSEHDICSLRSYERARIRVAVIHGUARAAAMMASTYKYLGVGLPLSFLTRPHFPGRVGGRFVIDIDMP  | 481 |
| Cuc.sativus     | GGCMAIEDGQLAEFLDKAWNESKSGSEHDICSLRSYERARIRVAVIHGUARAAAMMASTYKYLGVGLPLSFLTRPHFPGRVGGRFVIDIDMP  | 488 |
| Ar.thaliana     | GGCMAIEDGQLAEFLDKAWNESKSGSEHDICSLRSYERARIRVAVIHGUARAAAMMASTYKYLGVGLPLSFLTRPHFPGRVGGRFVIDIDMP  | 484 |
| Consensus       | ggcmaied qla el e p d e l ye r rv ih ar aa na ty ylgvgl pl flt r phpg ggr mp  |     |
| Vit.vinifera    | MLLWVLGGNSRLRGPPLSCRLSRKANDQIRWFEEDDAIRAIINGWMLPBGD.SGL.Q.FICLSKD.ENKFCIIGSVSHSTDFPGISTVIPSFK   | 573 |
| Vig.unguiculata | MLLWVLGGNSRLRGPPLSCRLSRKANDQIRWFEEDDAIRAIINGWMLPBGD.GTS.LSRPIVLSRN.EMKPFIIIGSAPADHPHTSVTIPSFK   | 528 |
| Sol.tuberosum   | MLLWVLGGNSRLRGPPLSCRLSRKANDQIRWFEEDDAIRAIINGWMLPBGD.GTS.LSRPIVLSRN.EMKPFIIIGSAPADHPHTSVTIPSFK   | 584 |
| Prun.armeniaca  | MLLWVLGGNSRLRGPPLSCRLSRKANDQIRWFEEDDAIRAIINGWMLPBGD.DND.ASQCILCNRD.EKNECTIGSAPHGDSVGSISIAIPKPK  | 579 |
| Or.sativa       | MLLWVLGGNSRLRGPPLSCRLSRKANDQIRWFEEDDAIRAIINGWMLPBGD.DND.ASQCILCNRD.EKNECTIGSAPHGDSVGSISIAIPKPK  | 576 |
| In.marginatal   | MLLWVLGGNSRLRGPPLSCRLSRKANDQIRWFEEDDAIRAIINGWMLPBGD.EAG.LLKFLISLQD.ENKFCIIGSTQCEHLSRISVIPSFK  | 580 |
| Gen.lutea       | MLLWVLGGNSRLRGPPLSCRLSRKANDQIRWFEEDDAIRAIINGWMLPBGD.EAG.LLKFLISLQD.ENKFCIIGSTQCEHLSRISVIPSFK  | 575 |
| Cit.sinensis    | MLLWVLGGNSRLRGPPLSCRLSRKANDQIRWFEEDDAIRAIINGWMLPBGD.EAG.LLKFLISLQD.ENKFCIIGSTQCEHLSRISVIPSFK  | 577 |
| Cuc.sativus     | MLLWVLGGNSRLRGPPLSCRLSRKANDQIRWFEEDDAIRAIINGWMLPBGD.EAS.VSQFICLAKD.ENKFCIIGSVEKEVDSGLVATLBPQ  | 583 |
| Ar.thaliana     | MLLWVLGGNSRLRGPPLSCRLSRKANDQIRWFEEDDAIRAIINGWMLPBGD.DCCVSETLICLTKDEDQPCVIGSEFDQDFPGMRIVIPS.....Q  | 579 |
| Consensus       | ml wvlgn kl ka d l wf dd e w l p  |     |
| Vit.vinifera    | VSKMHARISQCDCAFFLIDLSEHGTYWTDNECRRYRVFENPFRFHSSEVIDFGSD.KAS.FRVKVVRTFPDAAKDEESKLFQAV.....   | 658 |
| Vig.unguiculata | VSKMHARISQCDCAFFLIDLSEHGTYWTDNECRRYRVFENPFRFHSSEVIDFGSD.KAS.FRVKVVRTFPDAAKDEESKLFQAV.....   | 612 |
| Sol.tuberosum   | VSKMHARISQCDCAFFLIDLSEHGTYWTDNECRRYRVFENPFRFHSSEVIDFGSD.KAS.FRVKVVRTFPDAAKDEESKLFQAV.....   | 670 |
| Prun.armeniaca  | VSKMHARISQCDCAFFLIDLSEHGTYWTDNECRRYRVFENPFRFHSSEVIDFGSD.KAS.FRVKVVRTFPDAAKDEESKLFQAV.....   | 661 |
| Or.sativa       | VSKMHARISQCDCAFFLIDLSEHGTYWTDNECRRYRVFENPFRFHSSEVIDFGSD.KAS.FRVKVVRTFPDAAKDEESKLFQAV.....   | 626 |
| In.marginatal   | VSKMHARISQCDCAFFLIDLSEHGTYWTDNECRRYRVFENPFRFHSSEVIDFGSD.KAS.FRVKVVRTFPDAAKDEESKLFQAV.....   | 663 |
| Gen.lutea       | VSKMHARISQCDCAFFLIDLSEHGTYWTDNECRRYRVFENPFRFHSSEVIDFGSD.KAS.FRVKVVRTFPDAAKDEESKLFQAV.....   | 663 |
| Cit.sinensis    | VSKMHARISQCDCAFFLIDLSEHGTYWTDNECRRYRVFENPFRFHSSEVIDFGSD.KAS.FRVKVVRTFPDAAKDEESKLFQAV.....   | 664 |
| Cuc.sativus     | VSKMHARISQCDCAFFLIDLSEHGTYWTDNECRRYRVFENPFRFHSSEVIDFGSD.KAS.FRVKVVRTFPDAAKDEESKLFQAV.....   | 665 |
| Ar.thaliana     | VSKMHARISQCDCAFFLIDLSEHGTYWTDNECRRYRVFENPFRFHSSEVIDFGSD.KAS.FRVKVVRTFPDAAKDEESKLFQAV.....   | 667 |
| Consensus       | k af d s gt d g r p s   |     |
| Vit.vinifera    | .....   | 658 |
| Vig.unguiculata | .....   | 612 |
| Sol.tuberosum   | .....   | 670 |
| Prun.armeniaca  | .....   | 661 |
| Or.sativa       | .....   | 626 |
| In.marginatal   | .....   | 663 |
| Gen.lutea       | .....   | 663 |
| Cit.sinensis    | .....   | 664 |
| Cuc.sativus     | .....   | 665 |
| Ar.thaliana     | .....   | 667 |
| Consensus       | .....   |     |

**Figure 3.1.2: Deduced amino acid sequence alignment of Zep from several plant species.** Conserved domains are indicated below the alignment: lipocalin motifs are indicated by the red underline; the flavoprotein monooxygenase domain by the black underline and the FHA domain by the green underline. Amino acid with homology = 100% are shaded in black, with homology  $\geq 75\%$  in pink and with homology  $\geq 50\%$  in blue. Dashes indicate gaps introduced to optimize alignment. The accession numbers of ZEP protein sequences in GeneBank are indicated in figure 3.1.1 except for *Gentiana Lutea* ZEP (ACF21781).

The isolation of *ImZep2* by RACE-PCR was unsuccessful, probably due to a low expression level of this isoform in the leaf material used for the experiment. In fact a northern blot analysis carried out on the total RNA extracted from *I. marginata* leaves did not show any signal against a probe generated from a short sequence of *ImZep2*; on the contrary, a clear band was observed for *ImZep1* (Fig. 3.1.3).

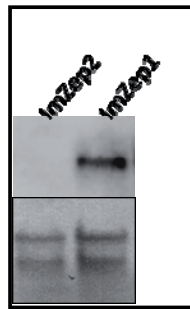


**Figure 3.1.3: Gene expression level of *ImZep1* and *ImZep2* in *I. marginata* leaves.** Equal amounts of the total RNA (5  $\mu$ g) were separated by agarose gel electrophoresis in the presence of formaldehyde and transferred onto nitrocellulose membranes. Specific probes were used to differentially detect the two isoforms. Two bands of rRNA visualised by the methylen blue staining of the membrane are shown as a control for loading.

### 3.1.2 Isolation of *ImZep1* splice variant (*ImZep1\_splice*) from *I. marginata* leaves

When specific primers (ImZepExpAtFWD1; ZepIngalso1Rev1; for nucleotide sequences of the primers, see Table 2.2) were used to isolate by PCR the *ImZep1* sequence from the total cDNA samples of *I. marginata* leaves, two different kinds of DNA sequences were obtained. As shown in Fig. 3.1.4, the deduced amino acid sequences of the two PCR products were identical except that one was missing 72 amino acids near the C-terminal end. The missing part of the shorter version contains the entire FHA domain. It seems that ImZEP1 has two splice variants, as is also the case for AtZEP; in the truncated variant the conserved FHA domain, presumably having an important regulatory function, is missing.

|           |  |     |
|-----------|--|-----|
| 537       | MASTLSYSSLNPSTTSFRTNFSIPTCKYFSLDIPPPGSRITIKHMKLLPITAABAEAPPSASPSTQTLTENHENRTPRKKIRILVAGGGIGGLVFAALAA   | 100 |
| 539       | MASTLSYSSLNPSTTSFRTNFSIPTCKYFSLDIPPPGSRITIKHMKLLPITAABAEAPPSASPSTQTLTENHENRTPRKKIRILVAGGGIGGLVFAALAA   | 100 |
| Consen    | mastlsysslnpsttsftrtnfsiptckyfsldippggsrtikhmkkllpitaabaeappsaspstqtltenhenrtprkkirilvagggigglvfaalaa  |     |
| 537       | KRKGFVFLVFEKDLSAIRGEGQYRGPIQIQSNALAALAEADPEVADEVMRVGCITGDRINGLVDGVSGSWYVKFDFTTPAVERGLPVTRVISRMTLQEIIL  | 200 |
| 539       | KRKGFVFLVFEKDLSAIRGEGQYRGPIQIQSNALAALAEADPEVADEVMRVGCITGDRINGLVDGVSGSWYVKFDFTTPAVERGLPVTRVISRMTLQEIIL  | 200 |
| Consen    | krkgfvlvfekdlsaairgegqyrgpiqiqsnalaaleaidpevadevmrvgcitgdringlvdgvsgswyvkfdfttpaverglpvtrvisrmtlqeil   |     |
| 537       | ACAVGEDSIMNSSNVNFVDDGSKVTVELENGEKYDGLLVGADGIWSKVRKNLFGPTEAVYSGYTCYTGIADFVPADIESVGYRVFLGHKQYFVSSDVG     | 300 |
| 539       | ACAVGEDSIMNSSNVNFVDDGSKVTVELENGEKYDGLLVGADGIWSKVRKNLFGPTEAVYSGYTCYTGIADFVPADIESVGYRVFLGHKQYFVSSDVG     | 300 |
| Consen    | acavgedsimssnvnvfvddgskvtvelengekydgdllvgadgiwskvrknlfpgpteavysgytcyctgiadfpadiesvggyrvflghkqyfvssdvg  |     |
| 537       | GGKMQWYAFHNEPPGGVDGPHGKKERLLRIFEGWCDNVIDLLLATNEEAAILRRDIYDRIPIFTWGKGRVTLGLDGSVHAMQPNLGQGGCMAIEDSYQLAWE | 400 |
| 539       | GGKMQWYAFHNEPPGGVDGPHGKKERLLRIFEGWCDNVIDLLLATNEEAAILRRDIYDRIPIFTWGKGRVTLGLDGSVHAMQPNLGQGGCMAIEDSYQLAWE | 400 |
| Consen    | ggkmgwyafhneppggvddgphgkkerllrifegwcdnvidlllatneeaailrrdiydripiftwgkgrvtllgdsvhamqpnlgqggcmaiedsyqlawe |     |
| 537       | LDNAWERSIKSGSPIDIDSSLSRYERERVLRAIIHGLARMAALMASTYKAYLGVGLGLEFLTKFRIPHGRVGGRLVIDKVMPLMLTUVLGGNSFKLE      | 500 |
| 539       | LDNAWERSIKSGSPIDIDSSLSRYERERVLRAIIHGLARMAALMASTYKAYLGVGLGLEFLTKFRIPHGRVGGRLVIDKVMPLMLTUVLGGNSFKLE      | 500 |
| Consen    | ldnawersiksgspididsslsryerervlrvaiahglarmaalmastykaylgvlgglefltkfriphgrvgrlvidkvmpmltuvwlggnsfkile     |     |
| 537       | GRPACCRSLDKANDQLPKWFQDDDALERAINGEWTLPCGDEAGLLKPIISLSDENKPCIIGSTQQEDHLSRSIVIPSPQVSQTHARINYLKDGAFFLTDL   | 600 |
| 539       | GRPACCRSLDKANDQLPKWFQDDDALERAINGEWTLPCGDEAGLLKPIISLSDENKPCIIGSTQQEDHLSRSIVIPSPQVSQTHARINYLKDGAFFLTDL   | 592 |
| Consen    | grpaccrslsdkandqlpkwfqdddaleraingewtlpcgdeagllkpiislsqdenkpciigstqqedhlrsrsivipspqvsqthari             |     |
| 537       | RSQHGWTISDNEGRYRVPPNYPTRVHPSDCIEFGSDKAAFRVKVTRSAAPRYSEEGTKVLLLE  | 662 |
| 539       | .....  | 592 |
| Consensus |  |     |

Figure 3.1.4: Alignment of the deduced amino acid sequence of *ImZep1* (upper sequence) and *ImZep1\_splice* (lower sequence).

### 3.1.3 Heterologous Expression of *I. marginata* and *A. thaliana* Zep in *R. capsulatus* and *E. coli*

In order to study *in vitro* the activity of *I. marginata* Zep1 gene product and its substrate specificity, heterologous expression was carried out in bacterial expression systems.

Due to the localization of its substrate and the proposed requirement of the membrane lipids I MGDG and DGDG for its activity (Bouvier *et al.* 1996), ZEP has been often reported as a membrane protein. Furthermore, Siefermann and Yamamoto (1975) also suggested membrane binding of the enzyme based on the fact that washing isolated chloroplasts in several different media did not diminish epoxidation activity. As a first attempt for the heterologous expression of *I. marginata*

*Zep*, a novel expression system based on the gram-negative bacterium *R. capsulatus* (Katzke *et al* 2010) has been chosen.

*Rhodobacter capsulatus* is a photosynthetic, non-sulfur, purple  $\alpha$ -proteobacterium that displays a versatile metabolic lifestyle. It is capable of growing phototrophically, i.e. anaerobically in the light by generating energy via anoxygenic photosynthesis, or chemoheterotrophically, i.e. aerobically in the dark by performing aerobic respiration to acquire energy. When grown in phototrophic conditions, *R. capsulatus* starts to synthesize a continuous system of intra-cytoplasmic membranes (ICM) in which the protein complexes of its photosystems are integrated in high amounts. Taking advantage of this property, an expression system based on *R. capsulatus* was proposed to synthesize heterologously high levels of membrane proteins (Katzke *et al.* 2010).

The *ImZep1* and *A. thaliana Zep* (*AtZep*: AT5G67030.1 ordered from Gateway) cDNAs were cloned into the expression vector pRhotHi-2 (see Table 2.1), containing the T7 promoter for the control of the gene expression (Katzke *et al.* 2009).

Two plasmids were generated for *ImZep1* and two for *AtZep*. For each plant species, the *Zep* sequence in one of the two clones was fused with a sequence coding a C-terminal 6-residue histidine tag (His-tag). The obtained plasmids were used to transform *E. coli* S17-1, and then subsequently the *R. capsulatus* B10S-T7 strain by bi-parental conjugation.

The transformed cells were grown phototrophically in order to promote formation of ICM. Since the *R. capsulatus* B10S-T7 strain contains the T7 RNA polymerase gene that is under the control of a fructose-inducible promoter, fructose was added to induce protein expression.

Quantitative real-time PCR revealed the presence of *ImZep1* and *AtZep* transcripts in the transformed *R. capsulatus* cells (Fig. 3.1.5a). However, western blot analysis carried out on the total protein extract with both  $\alpha$ -His-tag antibody and  $\alpha$ -ZEP antibody did not show any band, indicating no accumulation of ZEP protein with or without His-tag (Fig. 3.1.5b). Thus, there seemed to be a problem at the translational and/or post-translational level.

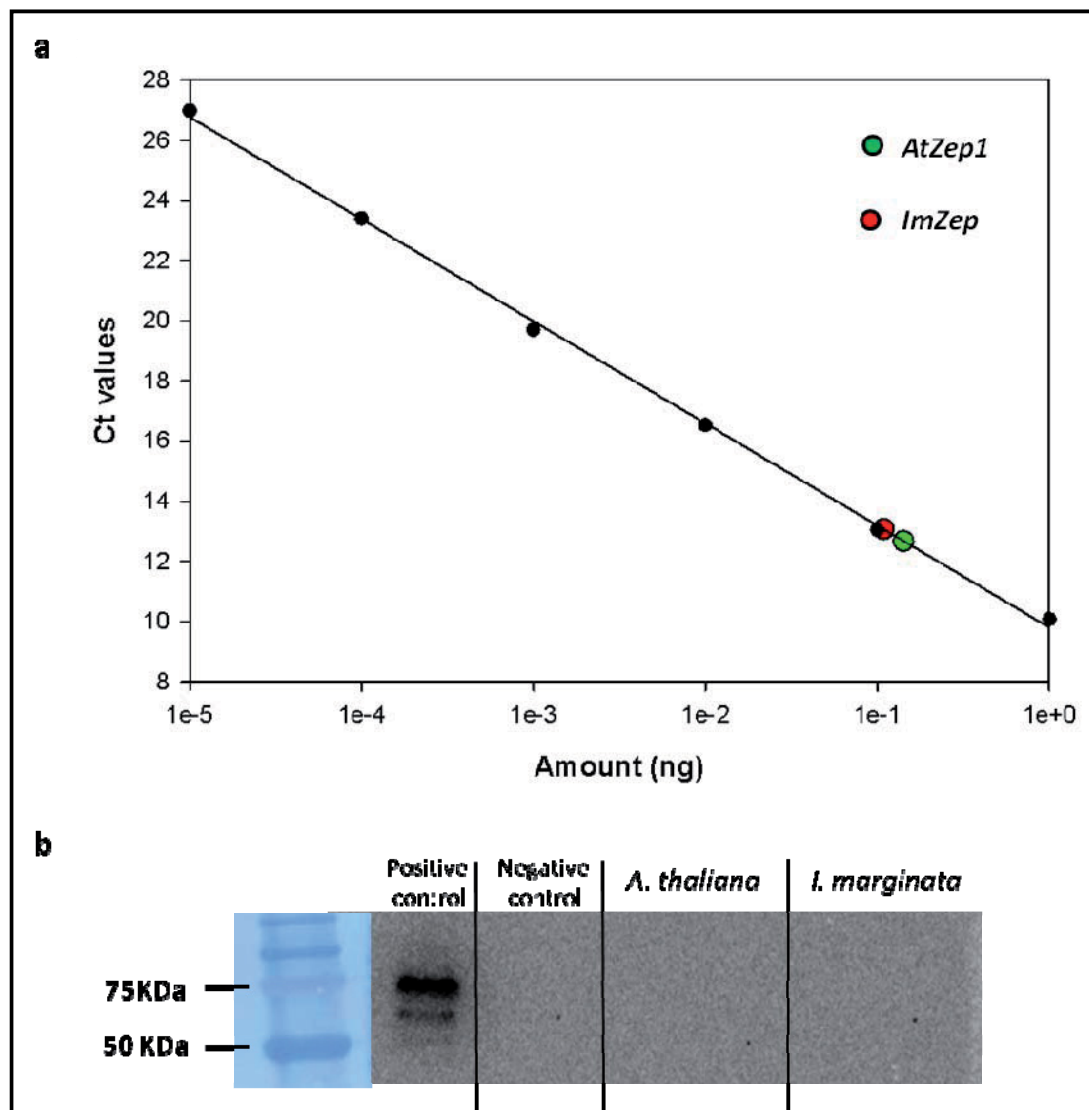


**Figure 3.1.5: Real-time-PCR and western blot analysis of transformed *R. capsulatus*.** (a) Graphical representation of the real-time-PCR results of *ImZep1* and *AtZep* transcripts with His-tag, inserted in *R. capsulatus*. The amount of the synthesized PCR products is indicated as a function of Ct values. Ct values (cycle threshold) indicate the number of cycles required for the fluorescent signal (SYBR Green dye) to exceed the background noise. A standard curve was constructed by using a sample of known concentrations ( $R^2=0.9995$ ). Because of DNA contaminations it was not possible to make a quantitative analysis of the transcripts. (b) Western blot analysis of protein extracts from *R. capsulatus* transformed with *AtZep* and *ImZep1*. Protein samples were resolved by SDS-PAGE and then electrophoretically transferred onto a PVDF membrane before immunoblotting using an  $\alpha$ -His-tag antibody. The membrane was then stained with an amido black solution (see Materials and Methods for details).

Due to the difficulty to express *Zep* in *R. capsulatus*, a second expression system based on *E. coli* was chosen to check the functionality of the vector constructs. The same plasmids constructed for *R. capsulatus* transformation (pRhotHI-2*ImZep1*; pRhotHI-2*AtZep* with and without His-tag) were used to transform the *E. coli* BL21 (DE3) strain; in this case the T7 polymerase-dependent expression was induced by IPTG.

When the protein extracts derived from the transformed *E. coli* cells were analyzed by SDS-PAGE and western blot, a prominent band corresponding approx. to the molecular mass of ZEP was observed in the sample transformed with His-tagged *ImZep1* after IPTG induction (Fig. 3.1.6). Yet, the ZEP protein accumulation was not found in the sample transformed with *A. thaliana* ortholog (*AtZep*) with or without His-tag.

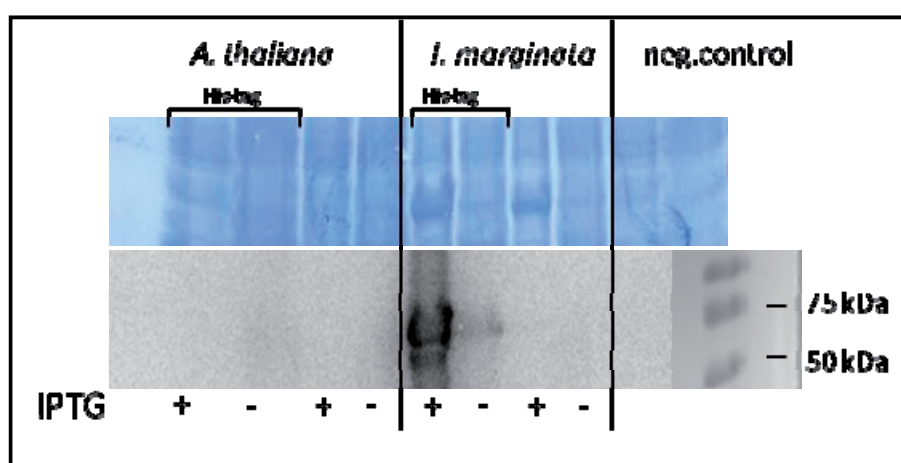


**Figure 3.1.6: Western blot analysis of protein extracts from the transformed *E. coli* BL21(DE3).** Same amounts of protein samples extracted from the *E. coli* cells transformed with *AtZep* and *ImZep1* with and without His-tag were loaded. In some of the bacterial cultures (indicated by +) the protein expression was induced by adding IPTG.

The attempt to express ZEP protein of *I. marginata* was therefore successful in *E. coli*, but not in *R. capsulatus*. Since ZEP from *A. thaliana* expressed in the same *E. coli* strain has been shown to be inactive (Niczyporuk 2009), purification of the protein from the *E. coli* strain for *in vitro* activity assay was not attempted in the present study. Instead, heterologous expression was performed in *A. thaliana* mutants in order to study the enzyme activity *in vivo*.

### 3.1.4 *ImZep1* heterologous expression in *A. thaliana npq2* mutants

*ImZep1*, *ImZep1\_splice* and *AtZep* genes were cloned into the expression vector pGWB2 (see Table 2.1), which contains the NPTII gene for kanamycin selection and the cauliflower mosaic virus 35S promoter. The constructed plasmids were introduced in *A. tumefaciens* strain GV3101 to transform *A. thaliana npq2* mutants by floral-dip method. The *npq2* plants lack functional ZEP, and thus they accumulate high levels of Z and no detectable A, V or N in leaves, all of which are derived after epoxidation of Z by ZEP (Niyogi *et al.* 1998).

The successful transformation was monitored in the T<sub>0</sub> progeny by selecting kanamycin-resistant seedlings and by making a PCR on genomic DNA of the surviving plants (T<sub>1</sub>). A segregation analysis was made on the T<sub>1</sub> progeny to select individuals with a single T-DNA insertion. Seeds from the T<sub>1</sub> plants were sowed on selective agarose medium (containing kanamycin) and the number of surviving or dead seedlings was counted; only those plants, which gave a segregation ratio of 1:3, were kept for further analysis. The third generation plants (T<sub>3</sub>) were obtained for the chosen transformants, and the progeny of this generation was also analyzed by segregation in order to select homozygous individuals. The T<sub>3</sub> plants, which gave only kanamycin-resistant seedlings, were used for subsequent experiments.

Two transgenic lines with *ImZep1* insertion (line 20.72 and line 24.75) and one with *AtZep* insertion (line 34.25) were chosen for phenotyping experiments. The transformation with *ImZep1\_splice* was not successful.

The morphology of the selected transformants is shown in Fig. 3.1.7. While *npq2* plants are much smaller than wt, the wt phenotype was recovered in the plants after the transformation with *ImZep* or *AtZep*, demonstrating clearly the similar activity of these enzymes *in vivo*.

A RT-PCR experiment was conducted on the T<sub>3</sub> plants of the selected lines to confirm the presence of *Zep* transcripts (Fig. 3.1.8). For plants 20.72 and 24.75 it was possible to amplify the inserted *I. marginata Zep1* by using the specific *ImZep* primers (*ImZepExpAtFWD1*; *ZepIngalso1Rev1*; for primer sequences, see Table 2.1) separately from the native *A. thaliana Zep* transcript. In 34.25 line the inserted *AtZep* and the native *AtZep* were probably both amplified by RT-PCR because the amplification products were also found in wt plants and the *npq2* mutants with the same primers (*AthZEFwd*; *AthZEREv*; for primer sequences, see Table 2.1).

Although the pGWB2 plasmids contained the 35S promoter upstream of the cloning site for these *Zep* genes, no ZEP protein overexpression has been observed in any of the transgenic lines. The western blot analysis with an  $\alpha$ -AtZEP antibody (kindly provided by R. Bassi) showed a single dominant band with equal intensity in all plants (Fig. 3.1.9). Obviously, the expressed ZEP protein did not accumulate to more-than-wt levels, which contrasts the successful overexpression of His-tagged *AtZep* in *A. thaliana* plants in a previous study (Niczyporuk 2009). Presumably, the presence or absence of a C-terminal His-tag affects the accumulation of *Zep* gene products in *A. thaliana*. A minor band was found just beneath the major ZEP band in the wt (Fig. 3.1.9), as has been documented by Niczyporuk (2009). Notably, this minor band of small MW was missing in *npq2* mutants as well as all the transgenic lines with the *npq2* background.



**Figure 3.1.7: Morphology of *A. thaliana* wt (Col-0), *npq2* mutants and the transgenic lines 20.72, 24.75 and 34.25.** Plants were grown in low light ( $50\text{--}95\ \mu\text{mol photons m}^{-2}\ \text{s}^{-1}$ ) with a 12-h/12-h day/night photoperiod and photographed four weeks after sowing. In 20.72 and 24.75 *ImZep1* gene was inserted in the *npq2* background, while 34.25 was transformed with *AtZep* gene (also in the *npq2* background). Plants of the T3 generation are shown.

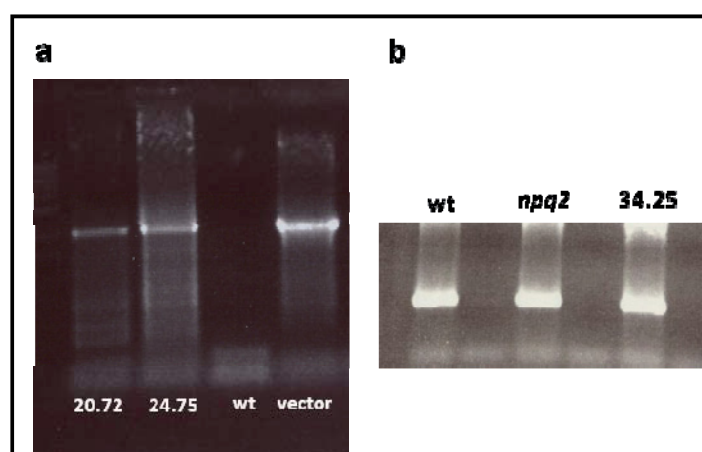


**Figure 3.1.8: RT-PCR of *ImZep1* and *AtZep* transcripts in the transgenic lines.** The total RNA samples extracted from leaves of the T3 plants, as well as wt and *npq2* plants, were subjected to reverse transcription, followed by 30 cycles of PCR amplification. (a) Specific primers for *ImZep* were used for 20.72 and 24.75 lines; the plasmid pGWB2-*ImZep1* was used as a positive control. (b) Specific primers for *AtZep* were used for wt, *npq2* and 34.25 plants.

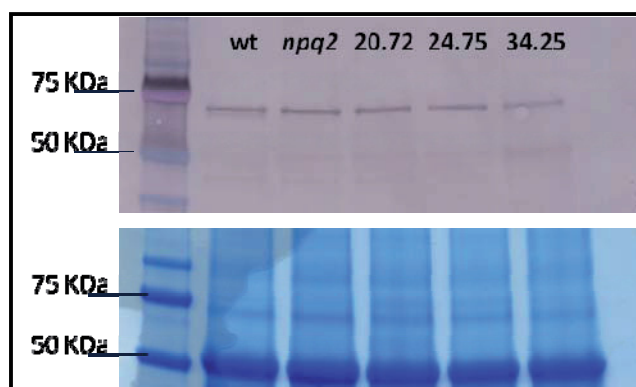


**Figure 3.1.9: Western blot analysis of ZEP protein.** Proteins were extracted from leaves of wt and *npq2* plants as well as T3 transgenic plants of 20.72, 24.75 and 34.25 lines. Samples corresponding to 2  $\mu$ g total chlorophyll were loaded and separated by SDS-PAGE before transfer onto a nitrocellulose membrane. ImZEP1 and AtZEP proteins were detected using an  $\alpha$ -AtZEP antibody (kind gift from R. Bassi).

In addition to the observation of morphological rescuing (Fig. 3.1.7), the functionality of the expressed ImZEP and AtZEP enzymes were also examined by checking the carotenoid composition in dark-adapted leaves of the T3 plants (Fig. 3.1.10). The homologous expression of *AtZep* in 34.25 allowed the complete recovery of the wt carotenoid composition; both N and V accumulated to wt-levels in 34.25. Although ZEP from another plant species (*I. marginata*) was introduced in lines 20.72 and 24.75, the enzyme turned out to be functional in *A. thaliana* (Fig. 1.4.4). Nevertheless, different activities of ImZEP1 were observed in the two lines, as indicated by the presence of A

and Z in dark-adapted samples of 20.72, but not 24.75. It seems that the ZEP activity is somehow lower in 20.72 than in wt and the other transgenic lines. Interestingly, the level of V was more strongly affected by the low ZEP activity in 20.72 than the level of N (Fig. 3.1.10), even though N is the downstream product of V.

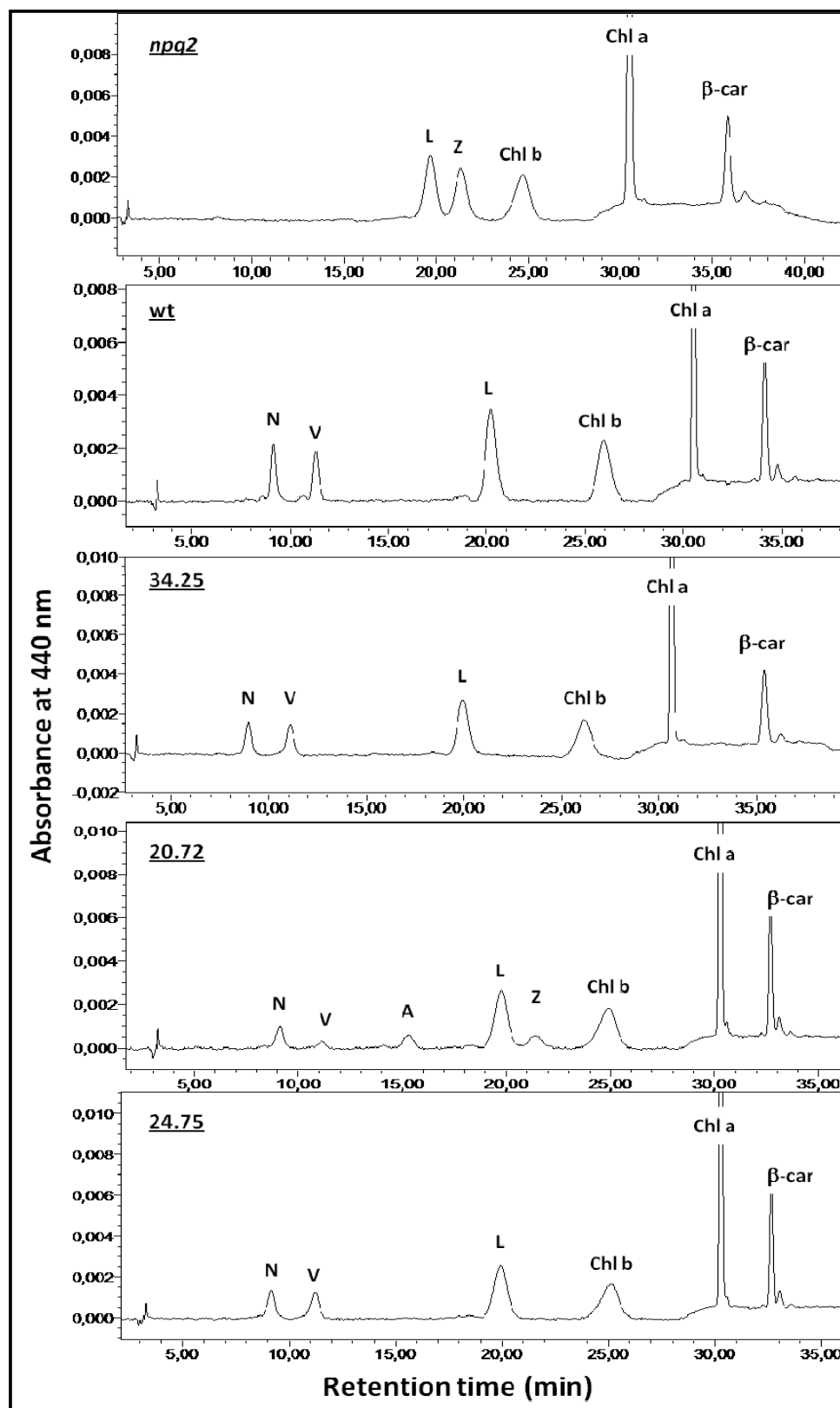


**Figure 3.1.10: HPLC chromatograms of leaf pigment extract from wt, *npq* and transformed plants.** Predawn T3 plants were used for pigment extraction. N, neoxanthin; V, violaxanthin; A, antheraxanthin; L, lutein; Z, zeaxanthin; Chl *b*, chlorophyll *b*; Chl *a*, chlorophyll *a*;  $\beta$ -car,  $\beta$ -carotene.

No Lx has been found in the *npq2* plants transformed with *ImZep1*, suggesting that ImZEP1 may not be able to catalyze the formation of Lx from L. The reason for this inability could be the substrate affinity of ImZEP1 or inaccessibility of the substrate L to allow its epoxidation by ImZEP1.

In order to test the second possibility of the substrate (L) availability, *A. thaliana szl1npq1* mutants, which lack Z (the main substrate of ZEP) and over-accumulate L (Li *et al.* 2009), were also transformed with *ImZep1*.

### 3.1.5 *ImZep1* heterologous expression in *A. thaliana szl1npq1* mutants

*A. thaliana szl1npq1* mutants lack Z due to the *npq1* mutation that results in defective VDE; the plants accumulate an extremely large amount of L at the expense of N and V because of a point mutation in the lycopene  $\beta$ -cyclase gene (Li *et al.* 2009). In the *szl1npq1* mutants, the excess L molecules replace some of the xanthophylls in the peripheral V (and Z) binding sites, from which these xanthophyll molecules can be released to the lipid membrane phase to become accessible to VDE and ZEP. Thus, at least a pool of L molecules must become accessible to ZEP in the *szl1npq1* plants. If the *ImZep1* gene product is able to epoxidise L to Lx, transformation of *szl1npq1* mutants with *ImZep1* should result in Lx accumulation.

The construct pGWB2-*ImZep1* was used to transform *szl1npq1* plants. The line 565.02 was selected in the T1 generation and analyzed by RT-PCR. Figure 3.1.11 shows that the *ImZep1* gene was inserted and transcribed in this line. In the same plants the leaf carotenoid composition was determined by HPLC analysis (Fig. 3.1.12). No Lx was detected in the *szl1npq1* transformants, even though L was accumulating excessively. These results indicate that ImZEP1 may not be able to use L as substrate for its epoxidation reaction, in much the same way as the native AtZEP in *szl1npq1* plants does not epoxidise L to Lx.

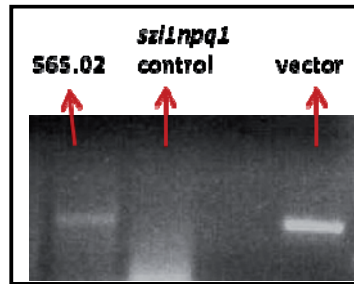


**Figure 3.1.11: RT-PCR of *lmZep1* transcript.** Total RNA was extracted from leaves of 565.02 and *szl1npq1* plants, and subjected to reverse transcription. Specific primers for *lmZep1* were used for its amplification. The pGWB2-*lmZep1* vector was used as a positive control.

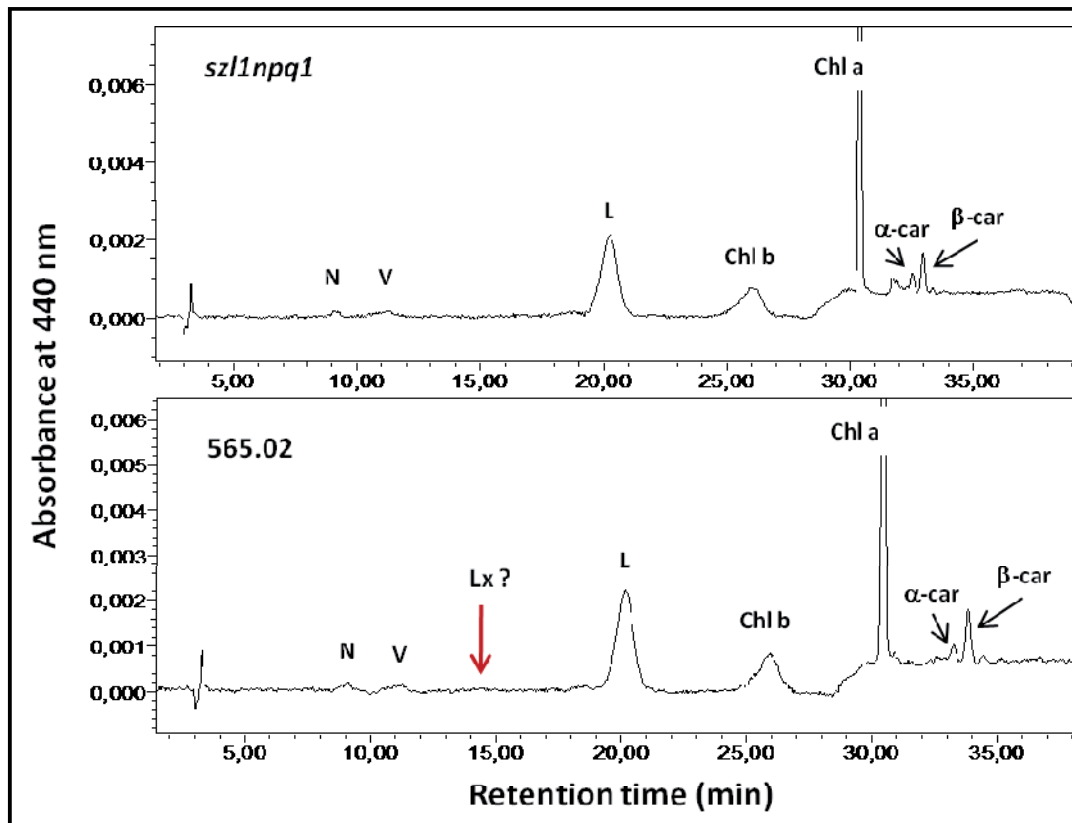


**Figure 3.1.12: HPLC chromatograms of leaf pigment extracts from *szl1npq1* and 565.02 transgenic line (T1).** Predawn leaf samples were used for pigment extraction. N, neoxanthin; V, violaxanthin; Lx, lutein epoxide; L, lutein; Chl *b*, chlorophyll *b*; Chl *a*, chlorophyll *a*; α-car, α-carotene; β-car, β-carotene.

### 3.1.6 Investigation *in vivo* of ImZEP1 activity in the transgenic lines 20.72 and 24.75

In order to analyze the activity of ZEP in the V-cycle, a high-light treatment was applied to the transgenic lines expressing *ImZep1* and *AtZep*, together with wt and *npq2* plants. Dark-adapted plants, which had been grown for four or five weeks under a low-light condition ( $50\text{--}95\ \mu\text{mol photons m}^{-2}\ \text{s}^{-1}$ ), were exposed to strong light ( $600\text{--}700\ \mu\text{mol photons m}^{-2}\ \text{s}^{-1}$ ) for 30 min. Subsequently, the plants were transferred to dim light ( $10\text{--}20\ \mu\text{mol photons m}^{-2}\ \text{s}^{-1}$ ) to monitor recovery for 5 min, 15 min, 30 min, 1 hour and 3 hours after the treatment.

The carotenoid composition was analyzed in leaves of these genotypes taken at different times during the treatment. The data of this experiment confirm the impaired activity of ImZEP1 in the line 20.72 compared with wt and the other transgenic lines; almost 20 mmol of each Z and A per mol Chl were found in dark-adapted leaves of this line (BHL, before high light), concomitant with much less amounts of V and N compared to the other genotypes (Fig. 3.1.13). Despite high variability of A and Z levels in 20.72, the tendency to retain A and Z (especially Z) was persistent in this line throughout the experiment (Fig. 3.1.13c, d). The behavior of the other two transgenic lines, 24.75 and 34.25, was practically identical to wt, indicating that the heterologously expressed ImZEP1 can be fully functional in *A. thaliana* leaves and can replace the role of AtZEP in the V-cycle.

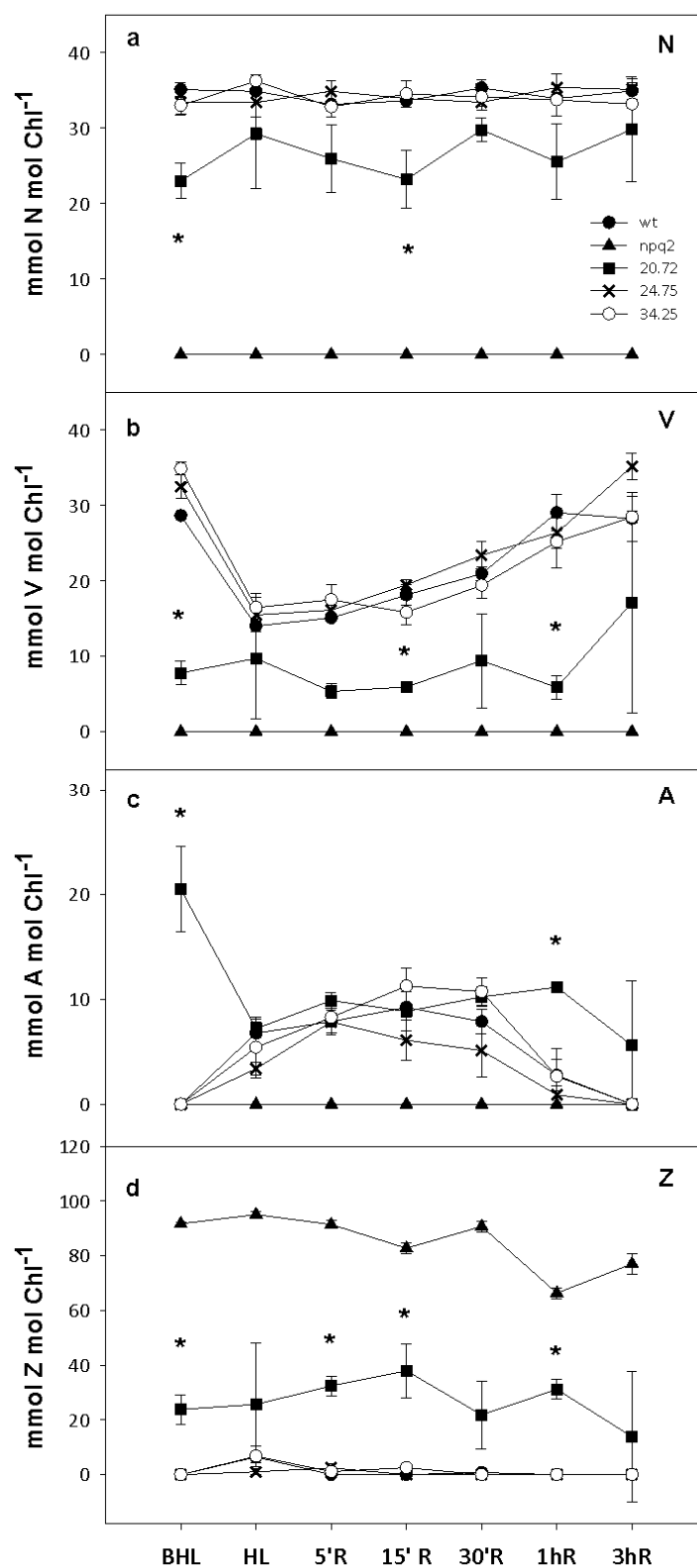


**Figure 3.1.13: Levels of N and the V-cycle pigments (V,A and Z) during the high-light treatment and subsequent recovery.** Samples were harvested from dark-adapted plants before the high-light treatment (BHL), after 30 min exposure to 600-700  $\mu\text{mol photons m}^{-2} \text{s}^{-1}$  (HL) and 5 min (5'R), 15 min (15'R), 30 min (30'R), 1 hour (1hR), and 3 hours (3hR) recovery under dim light (10-20  $\mu\text{mol photons m}^{-2} \text{s}^{-1}$ ) after the high-light treatment. (a) Neoxanthin (b) Violaxanthin (c) Antheraxanthin (d) Zeaxanthin. Pigment contents are given on a Chl basis ( $\text{mmol mol Chl}^{-1}$ ). Data are means  $\pm$  S.E. (n=4 for the line 20.72 and n=3 for the other genotypes). Significant differences (Tukey test of the One-Way ANOVA) between 20.72 and all the other genotypes are marked with “\*” ( $P \leq 0.05$ ).

The photochemical efficiency of PSII ( $\phi_{\text{PSII}}$ ) during the experiment showed that the retention of Z reduced  $\phi_{\text{PSII}}$  (Fig. 3.1.14). This was evident in *npq2* mutants which always contained a large amount of Z and no A, V and N (Fig. 3.1.13). Also in the line 20.72 the quantum yield of PSII tended to recover more slowly than in wt and other transgenic lines after the high-light exposure. Unlike in *npq2*, however, the difference in  $\phi_{\text{PSII}}$  between 20.72 and wt became detectable only after the high-light treatment; the  $\phi_{\text{PSII}}$  values before the high-light treatment (i.e. Fv/Fm) were comparable in 20.72 and wt (Fig. 3.1.14).

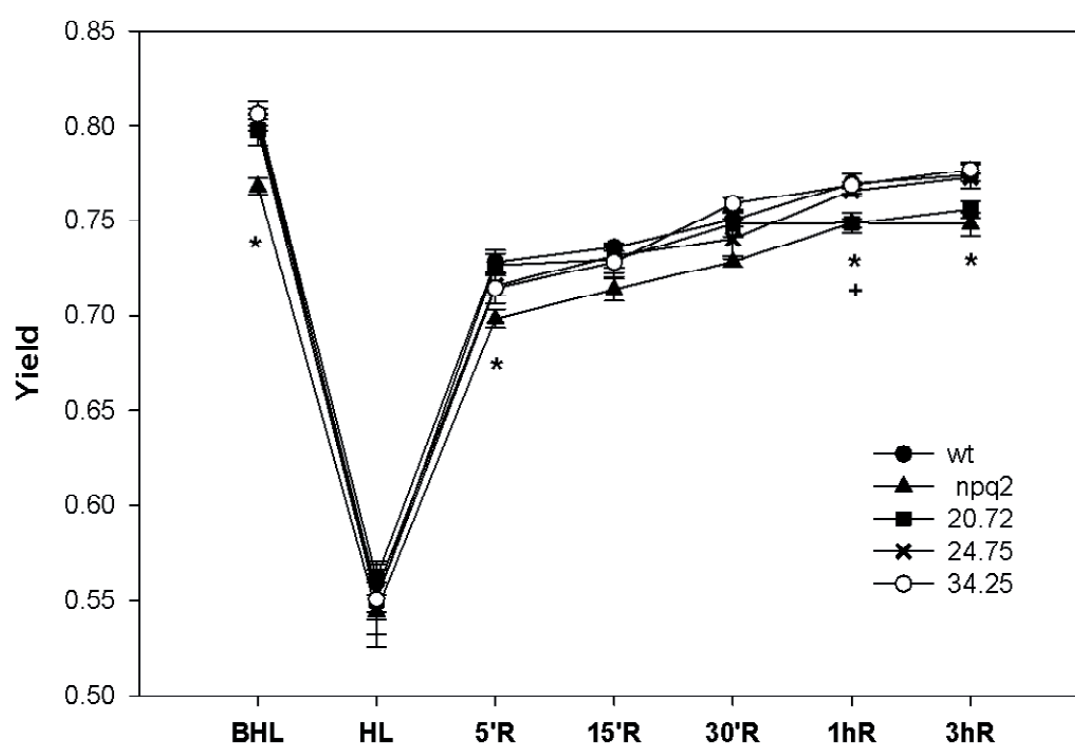


**Figure 3.1.14: Quantum yield of PSII photochemistry in wt and *npq2* plants as well as the transgenic lines during the high-light treatment and subsequent recovery.** Measurements were made on dark-adapted leaves before the high-light treatment (BHL; Fv/Fm), after 30-min exposure to 600-700  $\mu\text{mol photons m}^{-2} \text{s}^{-1}$  (HL) and at different time points during the subsequent recovery in dim light (5 min, 15 min, 30 min, 1 h and 3 h after the high-light treatment). Data are means  $\pm$  S.E. (n=3). Significant differences (Tukey test of the One-Way ANOVA) compared with wt plants are marked with “\*” for *npq2* plants and with “+” for line 20.72 ( $P \leq 0.05$ ).

The differences between the genotypes were less evident for NPQ (Fig 3.1.15). Except for the lower values of *npq2* mutants having the constitutive Fm quenching, no significant difference in NPQ with respect to wt was found in any of the transgenic lines.

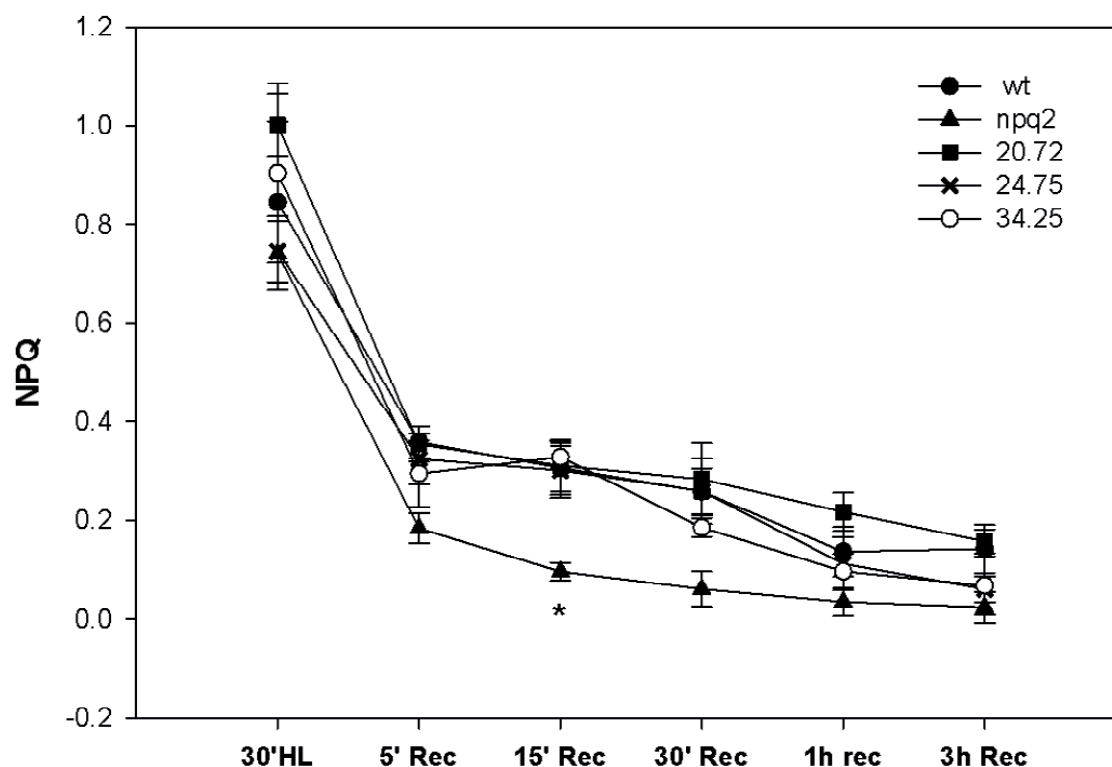


**Figure 3.1.15: Changes in NPQ in wt and *npq2* plants as well as the transgenic lines.** NPQ was measured after 30-min high-light treatment (HL) and during the subsequent recovery in dim light (5 min, 15 min, 30 min, 1 h and 3 h after the high-light treatment). Data are means  $\pm$  S.E. ( $n=3$ ). Significant differences (Tukey test of the One-Way ANOVA) compared with wt are marked with “\*” ( $P \leq 0.05$ ).

The partial retention of A and Z in leaves had no influence on leaf area growth of the line 20.72 (Fig. 3.1.16). The projected leaf area of the different genotypes was measured for 12 days during exponential growth and fitted to an exponential function to calculate the relative growth rate (RGR, %  $d^{-1}$ ). No significant difference was detected for the mean RGR values between wt and the transgenic lines. Interestingly, the RGR value of *npq2* mutants was not substantially lower than the others, although *npq2* plants looked much smaller (Fig. 3.1.7).

In order to check whether the insertion of *Zep* gene influenced ABA metabolism and/or ABA-related stress responses, leaf growth was analyzed also under drought stress condition. No

difference was found between the genotypes in response to drought and subsequent re-watering; the extent of the decrease in leaf RGR (ca. -11%) during the drought treatment and the recovery upon re-watering were similar in all plants, except for *npq2* mutants which showed a higher RGR decrease under the drought conditions (ca. -21%) (data not shown).

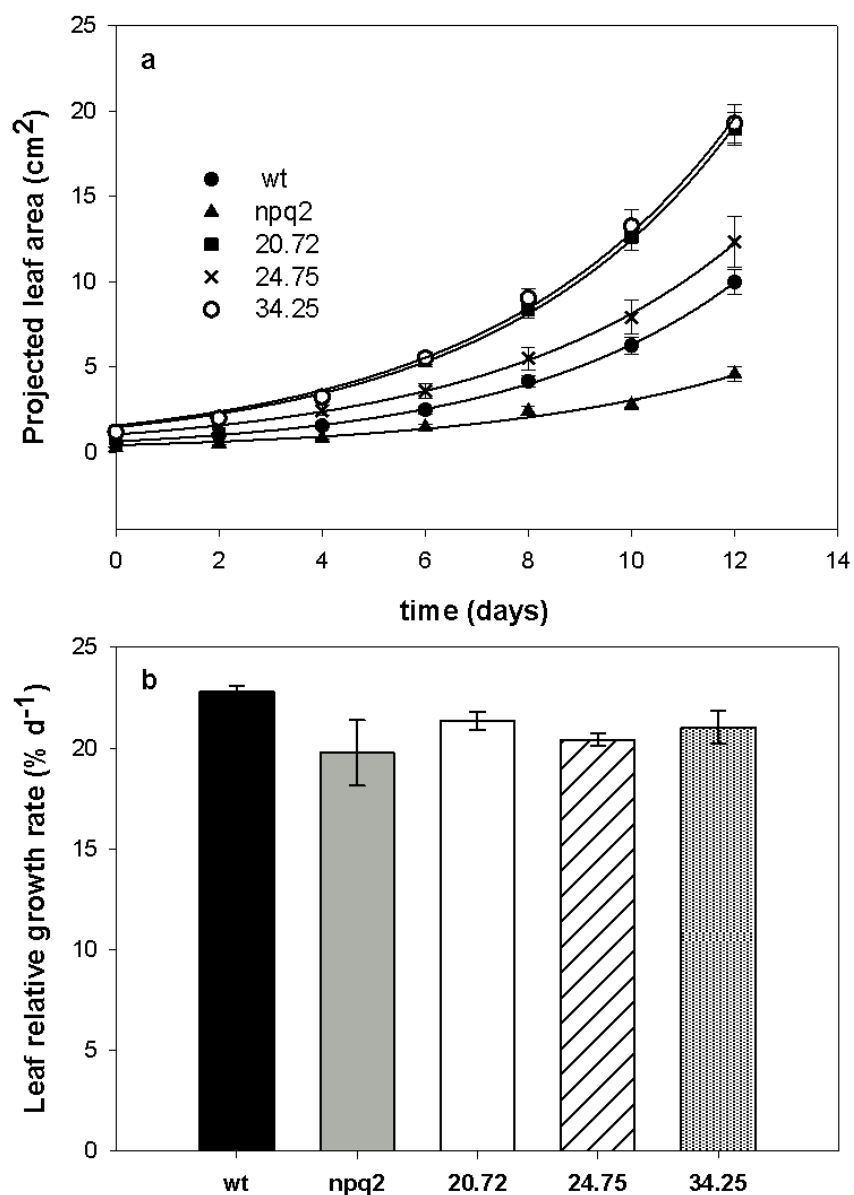


**Figure 3.1.16: Leaf growth of wt and *npq2* plants as well as the transgenic lines.** (a) Increase of the projected leaf area during 12 days of the experiment. Data were collected every two days under 150-180  $\mu\text{mol photons m}^{-2}\text{s}^{-1}$  and were fitted to an exponential growth curve. See Materials and Methods for description of leaf RGR analysis. (b) Leaf relative growth rate (RGR) derived from the growth curve of each genotype. Data are expressed as means  $\pm$  S.E. (n=12-17). There was no statistically significant difference between the genotypes.

### 3.2 Roles of $\alpha$ -branch carotenoids in photoprotection and photoacclimation under fluctuating light

Beside Lx,  $\alpha$ -car can also accumulate in large amounts in leaves of certain taxa, especially in shade environments (García-Plazaola *et al.* 2007; Matsubara *et al.* 2009). Together with L, Lx and  $\alpha$ -car are synthesized in the  $\alpha$ -branch of the carotenoid biosynthetic pathway (Fig. 1.5.1). While the photoprotective roles of  $\beta$ -branch carotenoids have been established (Demmig-Adams and Adams 1996a; Müller *et al.* 2001), the reason why some higher plants accumulate large amounts of  $\alpha$ -carotenoids, in addition to the ubiquitous L, is still not clear.

In order to study the impact of altered  $\alpha$ - and  $\beta$ -branch carotenoid composition on photoprotection and photoacclimation, *Arabidopsis* mutants *lut2*, *lut5*, *npq1* and *szl1npq1* were examined under photooxidative stress induced by simulated short “sunflecks”. *Lut2* plants lack the  $\epsilon$ -cyclase activity, thus having no L but increased amounts of  $\beta$ -carotenoids (Pogson *et al.* 1996). *Lut5* plants lack one of the  $\beta$ -hydroxylases, which leads to the accumulation of  $\alpha$ -car at the expense of  $\beta$ -car and all xanthophylls (Fiore *et al.* 2006; Kim and DellaPenna 2006). The mutant *npq1* cannot synthesize Z from V because of the mutation to VDE (Niyogi *et al.* 1998) and *szl1npq1* is a double mutant with an additional point mutation to  $\beta$ -cyclase in the *npq1* background, which is characterized by low levels of all  $\beta$ -carotenoids and remarkably high accumulation of L along with the presence of  $\alpha$ -car (Li *et al.* 2009; Fig. 3.1.11).

Photooxidative stress was applied by exposing the plants grown under low light (ca. 60  $\mu\text{mol photons m}^{-2} \text{s}^{-1}$ ) to repetitive short sunflecks (ca. 1000  $\mu\text{mol photons m}^{-2} \text{s}^{-1}$ , lasting ca. 20 s) during the daytime. Unlike continuously high irradiance which is used in many studies on photooxidative stress, this treatment, simulating a fluctuating light condition, does not allow *Arabidopsis* plants to increase the capacities for photosynthesis, carbohydrate accumulation or growth (Alter *et al.* submitted). Instead, during several days of treatment with short sunflecks, the most pronounced response observed in *Arabidopsis* plants is mainly the upregulation of photoprotection. Furthermore, 20-s sunflecks are too short to induce substantial de-epoxidation of the V-cycle pigments in the  $\beta$ -branch pathway. Therefore, the short-sunfleck treatment was used to investigate photoprotective roles of  $\alpha$ -branch carotenoids.

### 3.2.1 Effect of sunfleck treatment on the pigment composition of wt, *lut2*, *lut5*, *npq1* and *szl1npq1* mutants

The carotenoid content (relative to Chl) in leaves of wt, *lut2*, *lut5*, *szl1npq1* and *npq1* plants taken at the end of the night period after 7 d of the control or sunfleck treatment is shown in Figure 3.2.1. The pigment profiles previously described for these mutants were confirmed in the control plants: lack of L together with a decreased level of N and increased levels of  $\beta$ -car and V+A+Z in *lut2* (Pogson *et al.* 1996), pronounced accumulation of  $\alpha$ -car at the expense of all xanthophylls and  $\beta$ -car (with more than twice as much  $\alpha$ -car as  $\beta$ -car, Fig. 3.2.1b) in *lut5* (Fiore *et al.* 2006; Kim and DellaPenna 2006) and over-accumulation of L accompanied by appearance of  $\alpha$ -car and strong reduction of all  $\beta$ -carotenoids in *szl1npq1* (Li *et al.* 2009). Under the control condition, the carotenoid composition of *npq1* was very similar to that of wt except for a slightly lower amount of N (Fig. 3.2.1c). Only *lut2* leaves contained A in the control condition even after 12 h of dark period, as indicated by the de-epoxidation state of the V-cycle pigments (0.2, Fig. 3.2.1d).

The sunfleck treatment did not significantly alter the carotenoid composition in leaves of wt and *lut2* plants; only the extent of dark-sustained de-epoxidation in *lut2* increased from 0.2 to 0.3 (Fig. 3.2.1d), which was attributable to A and not Z. In all other mutants (*lut5*, *szl1npq1* and *npq1*) levels of L significantly increased under the sunfleck condition (Fig. 3.2.1a). This increase in L was accompanied by an increase in N, although the changes in *npq1* were not statistically significant (Fig. 3.2.1c). Generally, carotenes changed little in response to the sunfleck treatment (Fig. 3.2.1b). An increase in the V-cycle pigments (V+A+Z) was found in *npq1* (+35%) while the content of V+A+Z decreased in *lut5* (-37%) under the same condition (Fig. 3.2.1d). Following 7 h of sunfleck exposure, a trace of Z and somewhat increased amounts of A were detected in leaves of the *lut2* mutants (de-epoxidation state ca. 0.5, data not shown), indicating operation of the V-cycle in these plants under the sunfleck condition. De-epoxidation was not detected in other plants after 7-h sunfleck exposure.

The Chl *a* and Chl *b* contents per unit leaf area uniformly declined in the five genotypes during the sunfleck treatment (Fig. 3.2.2); the sunfleck-induced decrease was statistically significant for both Chl *a* and Chl *b* in all plants except for *lut2* which always had lower Chl contents than wt even under the control condition. Following the 7-d sunfleck treatment, the largest reduction in the total Chl content was observed in *lut5* and *szl1npq1* mutants; Chl *a* declined by nearly 25% and Chl *b* by 30 to 35% compared with the levels found in the corresponding plants under the control

condition. The reduction in the Chl content did not significantly alter the ratio of Chl *a* to Chl *b* (Chl *a/b*) in any of the plants examined, although the values tended to increase in the mutants under the sunfleck condition. The Chl *a/b* values measured on day 7 were 4.3 ( $\pm 0.2$ ), 3.9 ( $\pm 0.4$ ), 4.3 ( $\pm 0.2$ ), 4.5 ( $\pm 0.2$ ) and 4.5 ( $\pm 0.3$ ) for the control plants and 4.0 ( $\pm 0.1$ ), 4.2 ( $\pm 0.4$ ), 4.6 ( $\pm 0.2$ ), 5.3 ( $\pm 0.5$ ) and 4.9 ( $\pm 0.2$ ) for the sunfleck plants of wt, *lut2*, *lut5*, *szl1npq1* and *npq1*, respectively.

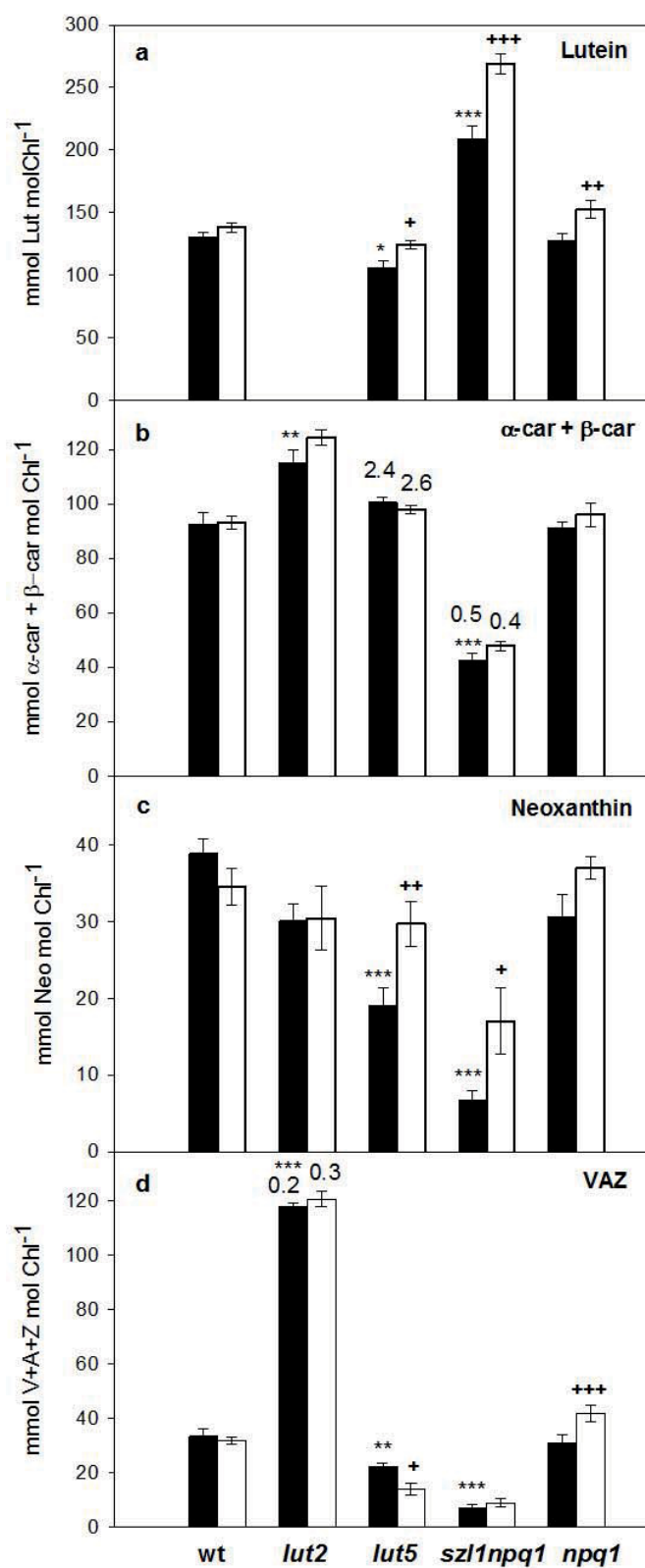


**Figure 3.2.1: Carotenoid composition in dark-adapted leaves of wild type, *lut2*, *lut5*, *szl1npq1* and *npq1* plants.** Samples were harvested at the end of the night period after seven days of exposure to the growth light environment (control; ca. 60  $\mu\text{mol photons m}^{-2} \text{ s}^{-1}$ ; closed bars) or the growth light with high-light pulses (sunfleck; ca. 1000  $\mu\text{mol photons m}^{-2} \text{ s}^{-1}$  for 20 s every 6 min; open bars). (a) Lutein. (b) Sum of  $\alpha$ -car and  $\beta$ -car. Only *lut5* and *szl1npq1* plants accumulated  $\alpha$ -car in leaves. The numbers above the bars of *lut5* and *szl1npq1* indicate the ratio of  $\alpha$ -car to  $\beta$ -car. (c) Neoxanthin. (d) Sum of the V-cycle pigments (V + A + Z). None of the samples contained Z. Antheraxanthin was detected only in *lut2* plants, signifying sustained de-epoxidation of the V-cycle pigments; the numbers above the bars of *lut2* show the de-epoxidation state calculated as  $A/(V+A)$  for these plants. Carotenoid contents are given on a Chl basis ( $\text{mmol mol Chl}^{-1}$ ). Data are means  $\pm$  S.E. (n=5 for wild type and n=4 for mutants). Significant differences (Tukey test of the Two-Way ANOVA) between the control and sunfleck treatments are marked with "+" for each plant; significant differences between wild type and mutants under the control condition are marked with "\*" (\* and +,  $P \leq 0.05$ ; \*\* and ++,  $P \leq 0.01$ ; \*\*\* and +++,  $P \leq 0.001$ ).

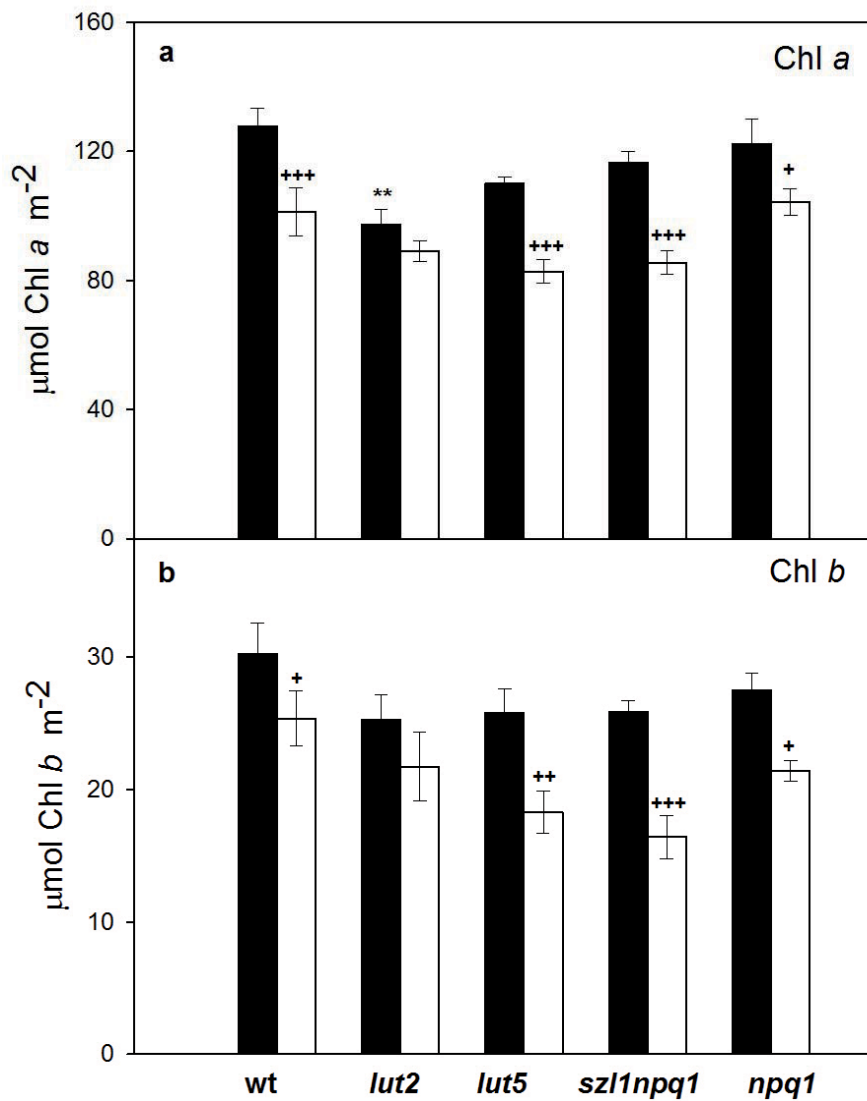


**Figure 3.2.2: Chlorophyll content of dark-adapted leaves of wild type and mutant plants harvested on day 7.** Closed bars, control; open bars, sunfleck. For descriptions of the treatments, see legend to Fig. 3.2.1. (a) Chlorophyll *a*. (b) Chlorophyll *b*. Chlorophyll concentrations are expressed on a leaf area basis ( $\mu\text{mol m}^{-2}$ ). Data are means  $\pm$  S.E. ( $n=5$  for wild type and  $n=4$  for mutants). Significant differences (Tukey test of the Two-Way ANOVA) between the two treatments are marked with "+" for each plant; significant differences between wild type and mutants under the control condition are marked with "\*" (+,  $P \leq 0.05$ ; \*\* and ++,  $P \leq 0.01$ ; +++,  $P \leq 0.001$ ).

### 3.2.2 PSII activity and PsbS protein level under sunfleck condition

The maximal PSII efficiency ( $F_v/F_m$ ) was measured in leaves of wt and the mutants at the end of the night period during the 7-d experiment (Fig. 3.2.3). None of the plants exhibited a significant decline in  $F_v/F_m$  in response to the sunfleck treatment; the values remained almost unchanged under both conditions. The *szl1npq1* mutants always had lower values of around 0.72, indicating constitutively reduced PSII efficiency in these plants.

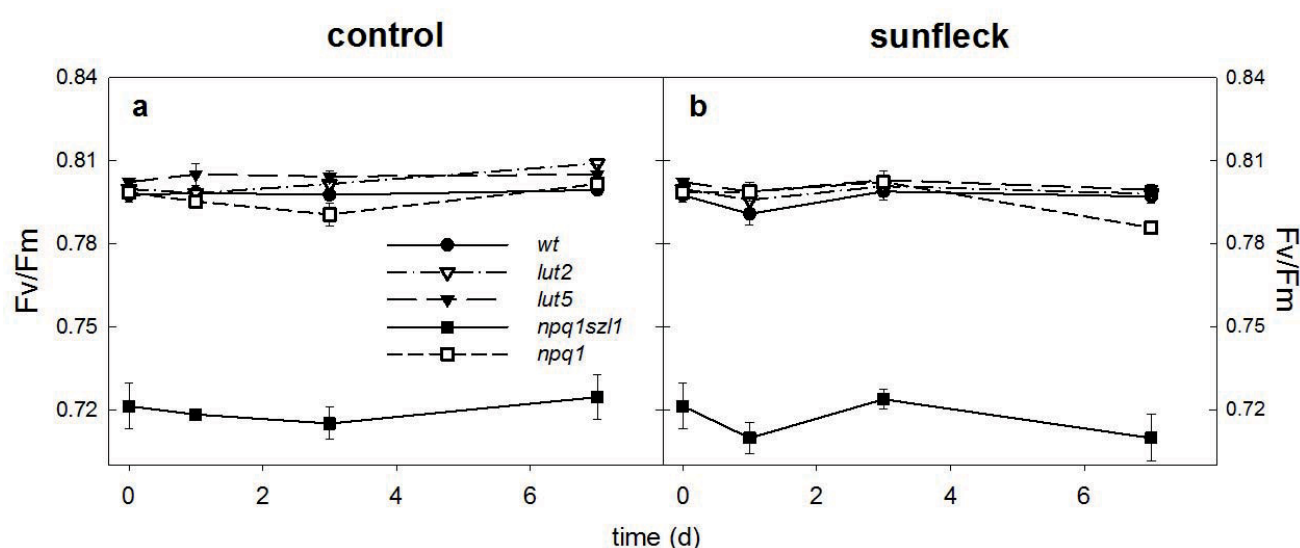


**Figure 3.2.3: Maximal photosystem II efficiency ( $F_v/F_m$ ) of dark-adapted leaves of wild type and mutant plants during 7-day exposure to the control (a) or sunfleck (b) condition.** Measurements were performed at the end of the night period on days 0, 1, 3 and 7. Data are means  $\pm$  S.E. ( $n=8$  for wild type and  $n=4$  for mutants).

Following the  $F_v/F_m$  measurements, light induction and dark relaxation of NPQ were analysed in the same leaf spots. In the control plants of wt, NPQ rapidly developed to reach 0.6–0.8 in the first 30 s of high-light illumination and the maximum of 1.2–1.5 was achieved within 5 min (Fig. 3.2.4a). Subsequently, darkening quickly diminished NPQ to about 0.6 in 30 s, which was followed by a slower decrease to 0.4 over 2 min. The NPQ induction in the control plants of the four mutants (Figs. 3.2.4b–e) was comparable with the report in the previous studies. The plants of *lut2* exhibited slower induction of NPQ (Pogson *et al.* 1998) despite retention of a large amount of A (Fig. 3.2.4d), reaching no more than 0.2–0.5 in the first 30 s of illumination (Fig. 3.2.4b). Likewise, low initial NPQ values were measured in *lut5* which also attained much lower maximal NPQ levels than in wt (-50%, Fig. 4c; Dall'Osto *et al.* 2007b). In contrast, the NPQ induction of *szl1npq1* was characterised by a fast rise (Li *et al.* 2009) to ca. 0.8 within 30 s (Fig. 3.2.4d); thereafter NPQ did

not increase in *szl1npq1*, or even decreased down to 0.4-0.6, during the illumination. The NPQ values of about 0.5 were found in *npq1* in which this level remained also in the subsequent dark period (Fig. 3.2.4e, Niyogi *et al.* 1998). Apart from *npq1*, the control plants of *lut5* and *szl1npq1* retained the highest and the lowest NPQ, respectively, at the end of the measurements.

During the 7-d sunfleck treatment, the maximal NPQ capacity increased progressively in the wt plants (Fig. 3.2.4f). The enhanced NPQ in the sunfleck plants was rapidly reversible upon darkening. The maximal NPQ levels of *lut2* varied considerably from day to day under both conditions (Fig. 3.2.4g) so that effects of the sunfleck treatment on NPQ could not be inferred in these plants. The sunfleck plants of *lut5* strongly upregulated the NPQ capacity already on day 1, followed by a continuous increase until day 7 (Fig. 3.2.4h). As with the increasing NPQ capacity, the levels of sustained NPQ measured in *lut5* after the 2-min dark adaptation decreased from day 0 to day 7. No or only minor increase in NPQ, respectively, was detected in the sunfleck plants of *npq1* (Fig. 3.2.4j) and *szl1npq1* (Fig. 3.2.4i) even though significantly increased levels of L were found in these plants under the sunfleck condition (Fig. 3.2.1a).

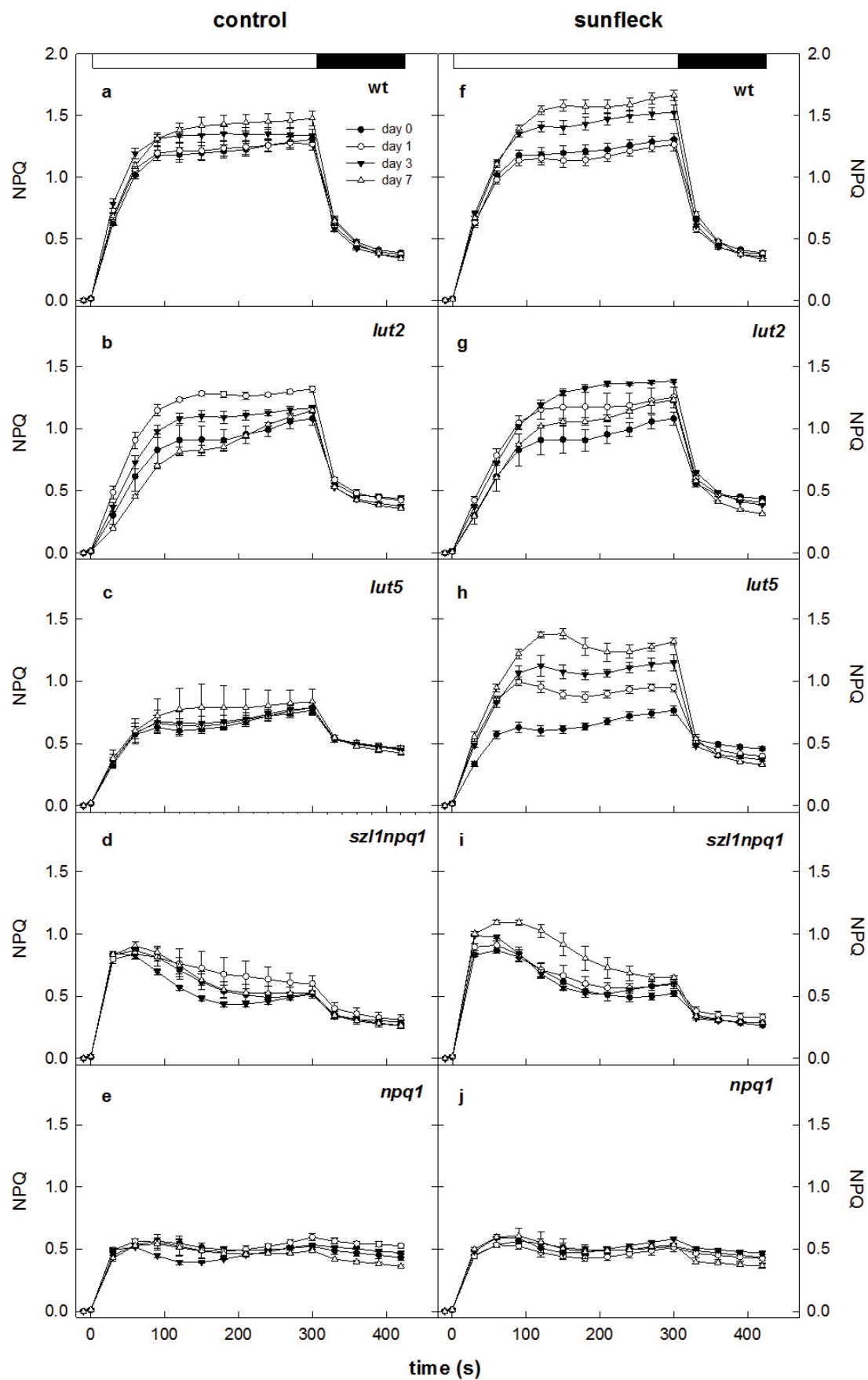


**Figure 3.2.4: Light induction and dark relaxation of non-photochemical quenching (NPQ) in wild type (a and f), *lut2* (b and g), *lut5* (c and h), *szl1npq1* (d and i) and *npq1* (e and j) plants during 7-day exposure to the control (a-e) or sunfleck (f-j) condition.** Light-induction measurements were started immediately after the Fv/Fm measurements shown in Fig. 2.2.1. NPQ was measured during 5-min illumination at  $600\text{--}800\ \mu\text{mol photons m}^{-2}\text{ s}^{-1}$  (indicated by white bars at the top of the panels a and f) followed by 2-min dark relaxation (indicated by black bars). Data are means  $\pm$  S.E. (n=8 for wild type and n=4 for mutants).

The levels of PsbS protein, which is essential for the light-inducible and rapidly reversible component of NPQ in higher plants (Li *et al.* 2000), were also analysed in leaves of wt and different mutants after 7 d of the control or sunfleck treatment (Fig. 3.2.5). Except in *lut2* which exhibited large variations between the individual plants, an increase of PsbS (relative to Chl) was observed in all plants under the sunfleck condition; the increase was statistically significant in wt and *npq1* plants (+40%).

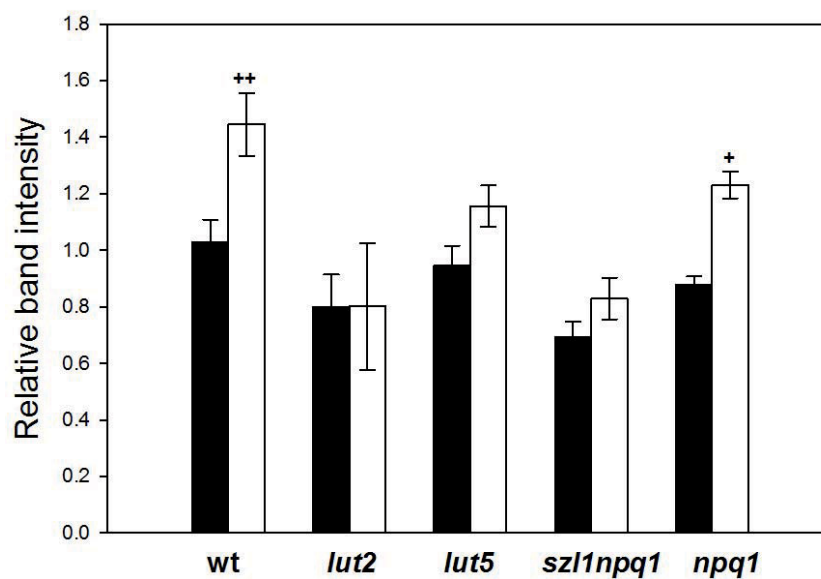


**Figure 3.2.5: Levels of PsbS protein in leaves of wild type and mutant plants.** Leaves were collected after 7-d exposure to the control (closed bars) or sunfleck (open bars) condition. Protein samples corresponding to 2µg total chlorophyll were loaded and separated by SDS-PAGE. PsbS content was determined by western blot analysis and the band intensity of each sample was normalized to a reference sample. Data are means  $\pm$  S.E. (n=3). Significant differences (Tukey test of the Two-Way ANOVA) between the two treatments are marked with "+" for each plant (+,  $P \leq 0.05$ ; ++,  $P \leq 0.01$ ). The minor differences between wild type and mutants under the control condition are not statistically significant.

### 3.2.3 Growth analysis of wt and carotenoid mutants under fluctuating light

Leaf and root growth was analysed in wt and the mutants during 10 d (leaf growth) or 5 d (root growth) of the control or sunfleck treatment (Figs. 3.2.6 and 3.2.7). The RGR calculated from the total projected leaf area was similar in all plants under both conditions, ranging between 19 and 22%  $d^{-1}$  (Fig. 3.2.6a). A slight decrease of leaf RGR observed in wt and *lut2* plants during the sunfleck treatment, or a minor increase in *szl1npq1*, was statistically not significant. The plants had different leaf dry mass per area (LMA) under the control condition, with the largest LMA found in

wt and the lowest in *szl1npq1* and *npq1* (Fig.3.2.6b). While this parameter remained unchanged in the latter two, it decreased in the sunfleck plants of wt and *lut5*. Only *lut2* exhibited a significant increase in LMA under the sunfleck condition.

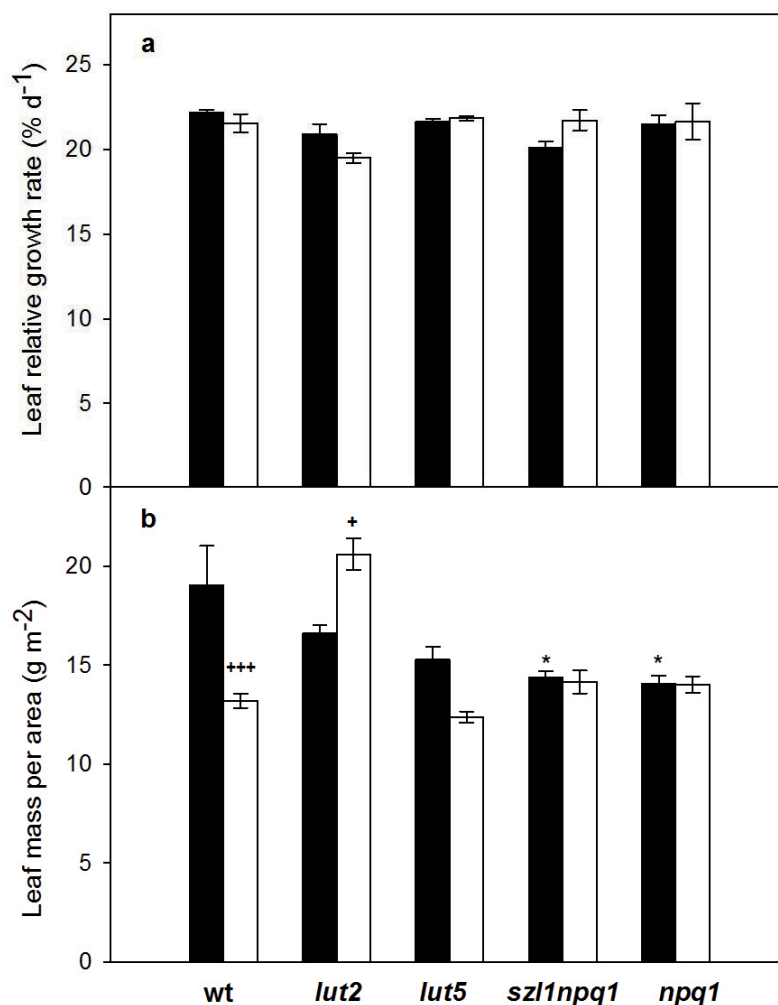


**Figure 3.2.6: Leaf relative growth rate (RGR) and leaf mass per area (LMA) of wild type and mutant plants during 10 days under the control (closed bars) or sunfleck (open bars) condition.** (a) Leaf relative growth rate. (b) Leaf mass per area. LMA was calculated from the leaf dry weight and the total projected leaf area measured for each sample on day 10. Values are means  $\pm$  S.E. ( $n=15-37$  for leaf RGR analysis and  $n=6-12$  for dry weight measurements). There was no significant difference between the two treatments or genotypes for leaf RGR. For LMA, significant differences (Tukey test of the Two-Way ANOVA) between the control and sunfleck treatments are marked with "+" for each plant; significant differences between wild type and mutants under the control condition are marked with "\*\*\*" (\* and +,  $P \leq 0.05$ ; +++,  $P \leq 0.001$ ).

For root growth analysis, plants were grown in Petri dishes filled with agarose. The experiment was stopped after 5 d due to the susceptibility of this cultivation system to fungi attack in non-sterile conditions. The control plants showed similar rates of lateral root formation (Fig. 3.2.7b) whereas the RGR of the primary root was somewhat lower in the *lut2* and *lut5* plants (Fig. 3.2.7a). The sunfleck treatment resulted in a significant decrease in the primary root growth of wt and especially *npq1*, while it reduced lateral root formation in *lut2*, *lut5* and *szl1npq1*.

In order to check if the observed root growth responses are similar to the responses to drought or osmotic stress, an additional treatment with 100 mM sorbit was included in the root growth experiment. The osmotic stress suppressed both primary and lateral root growth in all plants (Fig. 3.2.7) although the primary root of *npq1* and lateral roots of *szl1npq1* were much less affected by the high sorbit concentration. Overall, the patterns of root growth responses to the osmotic stress were different from the patterns found in the sunfleck plants, demonstrating distinct effects of the two treatments.

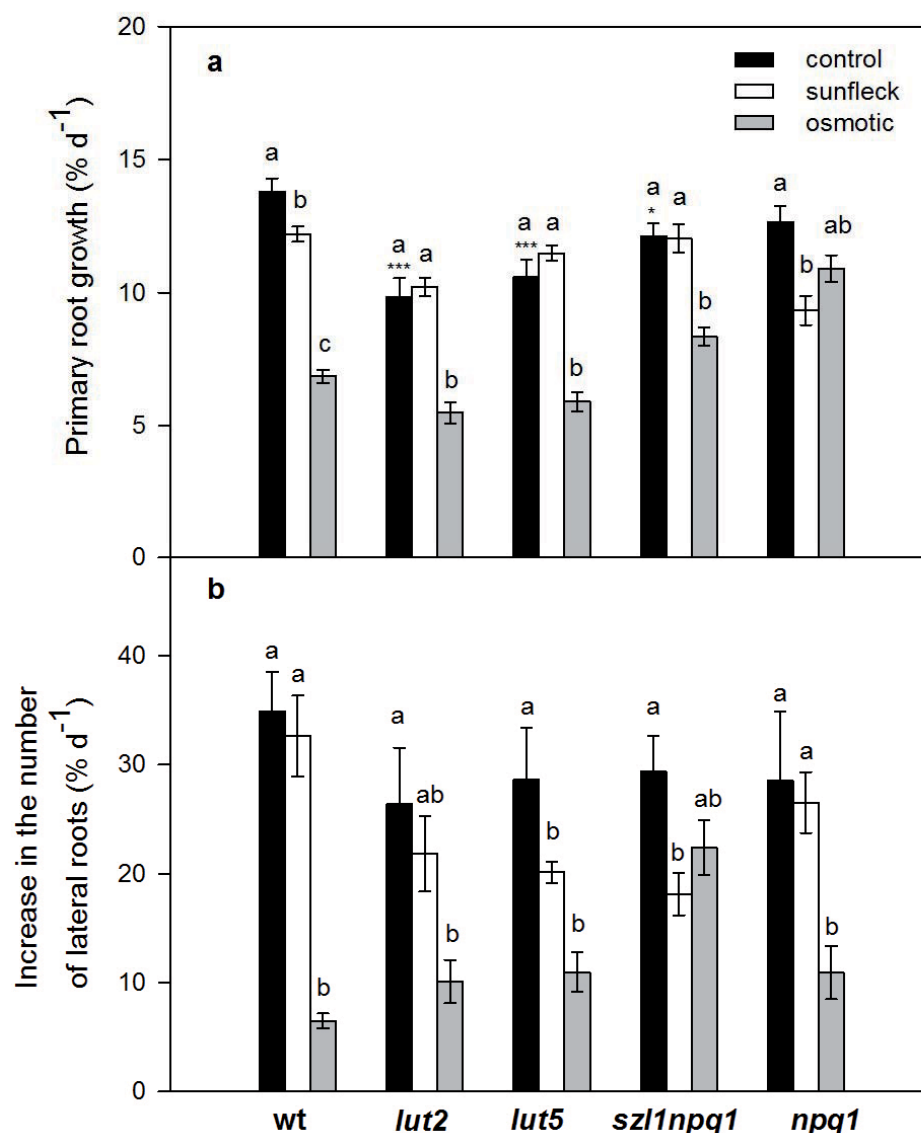


**Figure 3.2.7: Root growth analysis in wild type and mutants during the 5-day exposure to the control and sunfleck condition or 17-day cultivation in high-osmolarity medium containing 100 mM sorbit.** Growth of the primary root (a) and lateral roots (b) was calculated by comparing the length of the primary root and the number of lateral roots measured at the beginning (day 0, corresponding to the 12<sup>th</sup> day of cultivation for the osmotic stress experiment) and at the end of the experiment (day 5, corresponding to the 17<sup>th</sup> day of cultivation for the osmotic stress experiment) from control (closed bars), sunfleck (open bars) or osmotic stress (grey bars) plants. Values are means  $\pm$  S.E. (n=6-19). Significant differences (Tukey test of the Two-Way ANOVA) between the three treatments are marked with different letters for each plant; significant differences between wild type and mutants under the control condition are marked with "\*" (\*,  $P \leq 0.05$ ; \*\*\*,  $P \leq 0.001$ ).

Following the leaf growth analysis, the effects of sunflecks on seed production were examined under the control or sunfleck condition (Fig. 3.2.8). After bolting, inflorescence stems were covered with paper bags so that only rosette leaves and basal cauline leaves were directly exposed to the sunflecks (or the control light). In the control condition *szl1npq1* produced about 60% less seeds (in weight) than the other genotypes. The sunfleck treatment caused a severe and uniform reduction of seed yield in all plants, with the largest decrease found in *npq1* (Fig. 3.2.8).

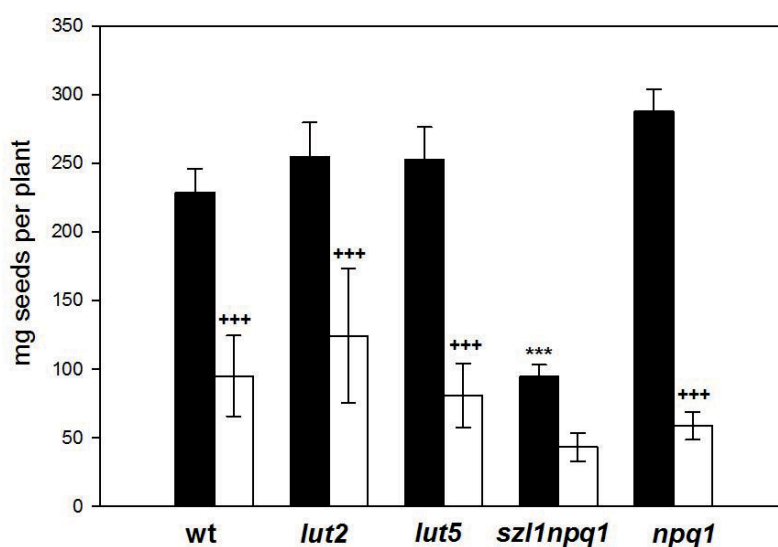


**Figure 3.2.8: Seed harvest of wild type and mutant plants grown under the control (closed bars) or sunfleck (open bars) condition.** Data are means  $\pm$  S.E. ( $n=3-10$ ). Significant differences (Tukey test of the Two-Way ANOVA) between the control and sunfleck treatments are marked with "+" for each plant; significant differences between wild type and mutants under the control condition are marked with "\*\*\*" (+++ and \*\*\*,  $P \leq 0.001$ ).

## 4 Discussion

### 4.1 Does ZEP synthesize Lx?

Operation of the Lx-cycle has been found widely and irregularly among different plant species (Matsubara *et al.* 2009), meaning that the ability to accumulate relatively high amounts of Lx has evolved independently among different plant taxa (García-Palzaola *et al.* 2004). The occurrence of the Lx cycle only in some higher plants and its different regulation in different species have been associated with variations in ZEP regulation (García-Palzaola *et al.* 2007). It has been shown that Lx, like A and V, is a substrate for VDE *in vitro* (Yamamoto and Higashi 1978, Matsubara *et al.* 2007), while the epoxidation reaction from L to Lx has been attributed to ZEP even if there has not been direct evidence of the involvement of this enzyme in the reaction. Matsubara *et al.* (2003) suggested that a mutation of the enzyme ZEP could be responsible for a different regulation and/or substrate specificity of the enzyme that increases its affinity for L, resulting in the formation of Lx. Furthermore, they excluded the possibility that the availability of L could be limiting for the synthesis of Lx in non-Lx species, based on the absence of Lx in the *A. thaliana* mutant *lutOE* which accumulates increased amounts of L at the expense of V due to overexpression of  $\epsilon$ -cyclase (Pogson and Rissler 2000). In the present work possible roles of the substrate specificity of ZEP and the availability of L in the occurrence of the Lx cycle were tested for the first time by heterologously expressing the ZEP isolated from *I. marginata*, a species which accumulates high levels of Lx in leaves (Matsubara *et al.* 2008).

A full-length cDNA clone encoding ZEP was isolated from leaves of *I. marginata*. The comparison of the predicted amino acid sequence of ImZEP1 with ZEP from other higher plants showed that ImZEP1 shares high sequence homology with other ZEP enzymes (Fig. 3.1.2) and thus can be identified as zeaxanthin epoxidase. The analysis of the amino acid sequence also revealed the presence of all four conserved motifs in ImZEP1 (Fig 3.1.2).

No Lx was detected when ImZEP1 was expressed in *A. thaliana szl1npq1* mutants accumulating extremely high levels of L (Fig. 3.1.12), while the ability of ImZEP1 to epoxidise Z to A and V could be clearly demonstrated in the transgenic lines with the *npq2* background (Fig.3.1.10). Hence, it

can be concluded that ImZEP1 is a functional ZEP in *A. thaliana* but does not synthesize Lx even when a large amount of L is available, indicating that Lx accumulation does not depend on the availability of L for the enzyme. Obviously, neither AtZEP (Matsubara *et al.* 2003) nor ImZEP1 (this study) utilizes overaccumulating L molecules as substrate. In leaves of *szl1npq1* mutants a substantial part of these extra L molecules are bound in the peripheral V1 xanthophyll-binding site and in the internal L2 binding site of the light harvesting antenna (Bassi R, personal communication), from which L can be released into the lipid phase of the thylakoid membrane to become accessible to the enzyme. In the case of VDE, such free xanthophylls in the lipid bilayer are considered as the substrate pool (Morosinotto *et al.* 2003, Jahns *et al.* 2009).

What could then be the cause of parallel operation of the two xanthophyll cycles in *I. marginata*? The presence of two ZEP isoforms may suggest possible involvement of the second isoform in operating the Lx cycle. In fact a partial sequence of the second isoform (*ImZep2*) has been isolated from leaves of *I. marginata* (Fig. 3.1.1), which was 100% identical to the partial sequence of *Zep2* previously found in *I. spectabilis* (Seltmann 2006). Although the low transcription level of *ImZep2* compared to *ImZep1* (Fig. 3.1.3) contrasts with high Lx contents of *I. marginata* leaves, it is possible that ImZEP2 has a higher affinity for L than ImZEP1 (or AtZEP) and can synthesize Lx. In the phylogenetic tree of Fig. 3.1.1, even though ZEPs of Lx species are grouped together with ImZEP1, ImZEP2 is positioned close to ZEP of *Cucumis sativus*, the first herbaceous non-parasitic species in which high amounts of Lx (20 mmol mol Chl<sup>-1</sup>) have been detected in leaves (Esteban *et al.* 2009). Further studies on ImZEP2 are necessary to clarify its role in the Lx biosynthesis and the Lx-cycle operation.

Different concentrations of Lx (when present) and diverse regulations of the Lx-cycle among various species (Matsubara *et al.* 2009; Esteban *et al.* 2008, 2009, 2010) suggest distinct regulation of the enzyme that catalyzes L epoxidation (presumably ImZEP2). Thus, in addition to the change in substrate specificity/affinity of the enzyme, regulation of the epoxidase activity could be influenced by specific environmental conditions (e.g. long exposure to shade environments) to give rise to different types of the Lx-cycle. Effects of environmental conditions on enzyme activity have been reported by Welsch and co-workers in their study on the *Sinapis alba* phytoene synthase (PSY), the first enzyme in the carotenoid biosynthetic pathway (Welsch *et al.* 2000). According to this study, far-red light illumination induce up-regulation of PSY at transcriptional and translational levels during de-etiolation of *S. alba* seedlings, but its activity depends on the

formation of thylakoids during the light-dependent chloroplasts development; the enzyme is therefore activated under irradiation with red or white light, which allows thylakoid formation during de-etiolation (Welsch *et al.* 2000).

## 4.2 Regulation of ImZEP activity

A splice variant of ZEP, completely missing an important domain (FHA domain), was found in *I. marginata* leaves (Fig. 3.1.4). It is unlikely that this splice variant is involved in the Lx-cycle because a similar splice variant of ZEP, lacking a large part of the FHA domain, has been found also in *A. thaliana* (AtZEPis2) (The Arabidopsis Information Resource; Niczyporuk 2009) which does not have the Lx-cycle. In other proteins the FHA domain is involved in phospho-dependent protein-protein interactions (Durocher *et al.* 2002), which is usually part of the mechanism of enzyme regulation. The function of the FHA domain in ZEP is not yet known and this question is certainly worth investigating.

It has been proposed that AtZEPis2 has reduced catalytic activity to epoxidise Z to A and V than the full-length variant AtZEP1; in fact the amount of AtZEPis2 increases in leaves during high-light exposure presumably to suppress ZEP activity (Niczyporuk 2009). The full length variant (AtZEPis1) has been found in the thylakoids (Niczyporuk 2009) to play a role in the V cycle. In a study on chloroplast proteomic, Joyard *et al.* (2009) have detected the presence of ZEP in both the inner envelope membrane of chloroplasts and in the thylakoids, while VDE is restricted to the thylakoid fraction (including lumen). Based on the localization of these and other enzymes in the carotenoid biosynthetic pathway, they postulated that the inner envelope membrane is the site of V (and other carotenoid) synthesis whereas in the thylakoids ZEP and VDE catalyze the opposite reactions of the V cycle. So far splicing-dependent differential localization of ZEP has not been reported.

In the western blot experiment, beside a clear band corresponding to the molecular weight of AtZEP, a weak second band, probably similar to AtZEPis2, was detected in wt plants, but not in the transgenic lines and their background plants *npq2* (Fig. 3.1.9). The accumulation of short variant is supposedly light regulated such that the protein level increases under high light (Niczyporuk 2009). As the growth light intensity was rather low, the wt plants may not have accumulated the ZEP short variant in high amounts. Interestingly, the ZEP protein (presumably the full-length variant) could be detected in *npq2* plants in which the epoxidation of Z is blocked in the V cycle as

well as in the carotenoid biosynthesis. This mutant was obtained by ethylmethane sulphonate-induced mutagenesis which causes mainly point mutations. Thus, it seems that the *npq2* mutation allows transcription (Nowicka *et al.* 2008) and translation of AtZEP to result in accumulation of inactive AtZEP proteins, and consequently, the inability to epoxidise Z. The results of the present study show that the *npq2* phenotype can be rescued by introducing *lmZEP1*, (Figs. 3.1.10, 3.1.13) indicating that the presence of the full-length *lmZEP1* can allow full epoxidation of Z to V and V-cycle operation.

It has been shown that Z epoxidation can be downregulated after exposure of plants to high-light conditions (Reinhold *et al.* 2008). The molecular basis of this downregulation is unclear, although Ebbert *et al.* (2000) have observed a correlation between dark-sustained D1/D2 phosphorylation and dark-sustained Z retention in *Monstera deliciosa* and spinach plants, suggesting that phosphorylation/de-phosphorylation of thylakoid proteins could be involved in the regulation of ZEP activity (Ebbert *et al.* 2000). Reinhold *et al.* (2008) further reported that the *stn7/stn8* mutant of *A. thaliana*, which lacks the thylakoid protein kinases STN7 and STN8 required for the phosphorylation of PSII proteins, still shows a light-dependent downregulation of ZEP activity. Therefore a direct modification of ZEP, instead of thylakoid protein phosphorylation, is most likely responsible for the regulation of ZEP.

For its activity ZEP requires molecular oxygen as a second substrate and other cofactors such as NADPH, FAD, ferredoxin and ferredoxin oxidoreductase (Siefermann and Yamamoto 1975; Büch *et al.* 1995, Bouvier *et al.* 1996). In addition, the *in-vitro* epoxidation system used by Bouvier *et al.* (1996) included also the thylakoid lipids MGDG and DGDG. Alteration in these enzyme cofactors or regulatory components may underlie the dark retention of Z and A in the transgenic line 20.72 having *lmZep1* gene insertion (Fig. 3.1.10). The insertion of the T-DNA in 20.72 may have disrupted or interfered with other genes affecting the regulation of ZEP activity. It should be noted, however, that the presence of a single T-DNA insertion was not unequivocally demonstrated in this line, since the segregation test carried out to select transgenic plants with single insertions was not accompanied by a southern blot experiment, which is a more precise analysis to check the insertion number. Nevertheless, a result similar to the observation in 20.72 has been published by Nowicka *et al.* (2008). They generated *A. thaliana* transgenic lines by homologous overexpression of AtZEP; in the obtained plants, however, the epoxidation reaction was not complete. It was assumed that the overexpression resulted in improper localization of ZEP, and thus disturbed

activity of the enzyme. The mechanism of ZEP downregulation remains to be elucidated in the future.

Notably, a trace amount of Lx was detected in the transgenic *A. thaliana* plants of Nowicka *et al.* (2008), which was interpreted as a change in the substrate specificity of ZEP in these transformants. In contrast to their report, however, none of the transgenic lines showed accumulation of Lx in the present study, including the line 34.25 having homologous expression of AtZEP. As neither ImZEP1 nor AtZEP was overexpressed in the transformed plants of this work (Fig. 3.1.9) despite the use of the 35S promotor (Table 2.1), it is difficult to compare these results with the observation by Nowicka *et al.* (2008).

#### 4.3 Effect of Z retention in the transgenic line 20.72

It is well-established that Z, together with the proton gradient across the thylakoid membrane ( $\Delta pH$ ) and the protonation-induced action of PsbS protein, plays an important role in the qE component of NPQ (Demmig-Adams *et al.* 1990; Gilmore and Yamamoto 1991), either acting indirectly as an allosteric effector enabling conformational changes of LHCs to bring about a dissipative state of the antennae (Horton *et al.* 2005) or being directly involved in the quenching process (Holt *et al.* 2005, Ahn *et al.* 2008).

In the  $\Delta pH$ -dependent process of quenching (qE), the quenching effect of Z is also dependent on the  $\Delta pH$ . There are cases, however, in which quenching is  $\Delta pH$ -independent, as it happens in cold-acclimated overwintering plants. Sustained downregulation of PSII complexes, associated with low PSII efficiency, is often correlated with Z+A retention in these plants (Matsubara *et al.* 2002, Adams *et al.* 2002). It has been suggested that reorganization of the photosynthetic apparatus may take place in the constitutive presence of de-epoxidised xanthophylls under low temperature (Ottander *et al.* 1995, Matsubara *et al.* 2002).

The sustained downregulation of PSII in overwintering plants may have something common with photoinhibition quenching (qI). Jahns and Mieke (1995) have found a kinetic correlation between the qI relaxation and the Z epoxidation in *Pisum sativum* plants, which is much faster than, but overall comparable with, the situation in overwintering eucalypt leaves during spring recovery (Gilmore and Ball 2000). The slowly relaxing component of NPQ, qI, involves at least two processes: The first step is thought to be reversible and occurs within about 1 h without any

obvious damage to PSII (Leitsch *et al.* 1994); the second step is accompanied by increasing damage to the PSII reaction center and can be reversed only by replacing the damaged D1 protein (Aro *et al.* 1993; Leitsch *et al.* 1994). The molecular mechanisms of qI as well as the exact role of Z therein are not yet fully understood.

The *npq2* mutants, which were used in this study to examine the catalytic activity of ImZEP1, constitutively accumulate Z due to the lack of ZEP activity. In agreement with previous studies (Kalituho *et al.* 2007), lower PSII efficiency and NPQ in comparison with wt were measured in dark-adapted leaves of *npq2* mutants or during the recovery phase following the high-light exposure (Figs 3.1.14; 3.1.15). This  $\Delta$ pH-independent quenching in *npq2* has been associated with conformational changes in LHC proteins caused by binding of Z, as is the case for the minor antenna complex CP26 (Dall'Osto *et al.* 2005). This mechanism may constitute a part of qI which does not involve PSII damage (Leitsch *et al.* 1994).

In the present study, the transgenic line 20.72 always retained a substantial amount of Z (ca. 20-25 mmol mol Chl<sup>-1</sup>) both before and after the high light treatment (Fig. 3.1.13), although the levels were much lower than in *npq2*. Contrary to *npq2* plants, however, the maximal photochemical efficiency of PSII in 20.72 was similar to that of wt prior to the high-light treatment; lower PSII efficiency was observed only in the late recovery phase of > 1 h (Fig. 3.1.14). The lack of constitutive PSII downregulation in 20.72 may be attributable to its lower Z amount compared to *npq2*, or the presence of A, V and N, all of which are absent in *npq2*. The exposure to high light and formation of  $\Delta$ pH may have induced conformational changes in the LHC proteins together with xanthophyll exchange to result in Z binding in the binding sites which are “active” in quenching. For example, replacement of V with Z in the allosteric site L2 has been shown to induce a conformational change in LHC proteins (Formaggio *et al.* 2001; Crimi *et al.* 2001). On the other hand, rapid NPQ relaxation found in 20.72 (Fig. 3.1.15) suggests that quenching of Fm' (or Fm) was not enhanced in this line compared to wt. A detailed analysis of carotenoid distribution within the thylakoid membranes, along with careful measurements of Fm and Fo quenching, could shed light on the unique behavior of PSII in 20.72 plants.

Finally, it is worth mentioning that the result of the leaf growth analysis in *npq2* mutants, showing comparable leaf RGR of 20-23% in wt and *npq2* (Fig. 3.1.16), is essentially similar to the one reported for leaf fresh weight by Dall'Osto *et al.* (2005); under a light intensity of ca. 120  $\mu$ mol photons m<sup>-2</sup> s<sup>-1</sup> (almost the same light intensity as used in this study), similar increase in leaf fresh

weight (500%) was found in *npq2* and wt plants after 3 weeks of cultivation. At a very low light intensity (ca. 20  $\mu\text{mol photons m}^{-2} \text{s}^{-1}$ ), however, impairment of growth was observed in the *npq2* mutants (Dall'Osto *et al.* 2005). Likewise, pronounced decrease in leaf growth of *npq2* at a very low light intensity (30  $\mu\text{mol photons m}^{-2} \text{s}^{-1}$ ) was also described in another study (Kalituho *et al.* 2006). In both studies the growth impairment at limiting light intensities was attributed to constitutive dissipation of absorbed light energy due to the constant presence of high levels of Z.

#### 4.4 Role of L and $\alpha$ -carotene in photoprotection under fluctuating light

In addition to Z, L also plays an important role in qE. Specifically, this xanthophyll seems to be involved in the rapid induction of NPQ, which was delayed markedly in the L-deficient mutants (*lut2*) on illumination (Pogson *et al.* 1998; Lokstein *et al.* 2002). Furthermore, accumulation of L in the absence of Z in the *szl1npq1* mutant can restore a large portion of NPQ that is absent in *npq1* (lacking Z), suggesting that additional L may be able to functionally replace Z for qE induction (Li *et al.* 2009). In agreement with these observations in the mutants and transgenic plants of *A. thaliana*, retention of L in the Lx cycle has been shown to enhance NPQ in the Lx-cycle plants (Matsubara *et al.* 2008, Esteban *et al.* 2010). Moreover, a recent study employing fluorescence lifetime measurements has indicated involvement of L in rapid de-excitation of Chl *a* molecules, which was represented by the appearance of a fluorescence lifetime pool centered at around 0.5 ns (Matsubara *et al.* 2011). Whether L plays a direct or an indirect role in qE is, however, still under debate (Li *et al.* 2009).

In this study the phenotyping experiments were conducted with the carotenoid mutants (*lut2*, *lut5*, *szl1npq1* and *npq1*) under sunfleck-induced photo-oxidative conditions to examine roles of L and  $\alpha$ -car in photoprotection and photoacclimation under fluctuating light. Under these conditions the V-cycle operates minimally and hence Z-dependent photoprotection, such as qE and ROS scavenging, is supposedly minimal (Alter *et al.* submitted). This provides a good experimental condition to assess the impact of L on photoprotection and plant performance, especially in dynamically changing light environments typically found in forest understory or inner canopy. As leaves of many shade-tolerant plants accumulate  $\alpha$ -car, the precursor of L, in low-light conditions (Thayer and Björkman 1990, Demmig-Adams and Adams 1992, Matsubara *et al.* 2009), the effects of  $\alpha$ -car were also studied in addition to the effects of L. Table 4.1 summarizes the changes observed in each genotype during the sunfleck treatment.

**Table 4.1 Summary of the sunfleck responses of different parameters in wt and the four carotenoid mutants of *A. thaliana*.**

|                             | wt                          | <i>lut2</i>                  | <i>lut5</i>                  | <i>szl1npq1</i>              | <i>npq1</i>                 |
|-----------------------------|-----------------------------|------------------------------|------------------------------|------------------------------|-----------------------------|
| <b>Pigments</b>             |                             |                              |                              |                              |                             |
| L                           | no change                   | ---                          | increase                     | increase                     | increase                    |
| V+A+Z                       | no change                   | no change                    | decrease                     | no change                    | increase                    |
| N                           | no change                   | no change                    | increase                     | increase                     | no change                   |
| $\alpha$ -car+ $\beta$ -car | no change                   | no change                    | no change                    | no change                    | no change                   |
| Chl                         | decrease                    | decrease                     | decrease                     | decrease                     | decrease                    |
| <b>PSII</b>                 |                             |                              |                              |                              |                             |
| Fv/Fm                       | no change                   | no change                    | no change                    | no change                    | no change                   |
| NPQ capacity                | increase                    | variable                     | increase                     | little change                | no change                   |
| PsbS                        | increase                    | variable                     | increase                     | increase                     | increase                    |
| <b>Growth</b>               |                             |                              |                              |                              |                             |
| Leaf RGR                    | no change                   | no change                    | no change                    | no change                    | no change                   |
| LMA                         | decrease                    | increase                     | decrease                     | no change                    | no change                   |
| Root RGR                    | decrease in<br>primary root | decrease in<br>lateral roots | decrease in<br>lateral roots | decrease in<br>lateral roots | decrease in<br>primary root |
| Seed harvest                | decrease                    | decrease                     | decrease                     | decrease                     | decrease                    |

#### 4.4.1 Responses of the pigment composition to fluctuating light

A marked response observed in all plants under the sunfleck-induced photooxidative condition was the decrease in Chl content (Fig. 3.2.2), as was also found in plants of *Silene dioica* under longer sunflecks of 15 min (Yin and Johnson 2000). In the present study, this decrease in Chl did not affect the Chl-based carotenoid composition in the sunfleck plants of wt (Fig. 3.2.1), indicating net degradation also for carotenoids. In contrast, the decrease in Chl was accompanied by an increase in L and N in *lut5* and *sz1npq1*, or L and V in *npq1* (Fig. 3.2.1).

Both *lut5* and *sz1* alleles are characterised by enhanced synthesis of  $\alpha$ -branch carotenoids (Fig. 3.2.1; Fiore *et al.* 2006; Kim and DellaPenna 2006; Li *et al.* 2009) as well as accumulation of  $\alpha$ -car. This kind of pigment phenotype is typically (but not exclusively) found in leaves of tropical plants under shade environments (Thayer and Björkman 1990; Matsubara *et al.* 2009). In *lut5*,  $\alpha$ -car undergoes higher turnover than  $\beta$ -car (Beisel *et al.* 2010) and leaves are slightly more sensitive to high light compared with wt (Kim *et al.* 2009). However, neither in *lut5* nor *sz1npq1* was the maximal PSII efficiency impaired by the sunfleck treatment (Fig. 3.2.3), suggesting that these plants could overcome the limited availability of  $\beta$ -branch carotenoids (V+A+Z and  $\beta$ -car) by, amongst other photoprotective mechanisms, increasing the levels of L and N (Fig. 3.2.1). L and N can contribute to photoprotection in thylakoid membranes: L through quenching of singlet and triplet Chl (Dall'Osto *et al.* 2006; Matsubara *et al.*, 2008; Li *et al.* 2009) and both through detoxification of ROS (Peng *et al.* 2006; Dall'Osto *et al.* 2007a). Furthermore, the sunfleck plants of *lut5* and *sz1npq1* had the lowest Chl contents (Fig. 3.2.2), or the smallest absorption cross section, indicating that they probably absorbed less light energy.

The *npq1* plants had a near-wt carotenoid composition in the control condition (Fig. 3.2.1). The major difference between wt and *npq1* resides in the inability of the latter to form Z through light-induced de-epoxidation of V, and hence to employ Z-dependent photoprotection (Fig. 3.2.1; Niyogi *et al.* 1998; Havaux & Niyogi 1999). Under non-stressful environments where the enzyme VDE is not active in wt, the *npq1* mutation is unlikely to have a drawback. By the same token, wt and *npq1* would display similar phenotypes under the sunfleck condition unless the treatment induces V de-epoxidation in wt. Based on the distinct changes in carotenoid composition of *npq1* and wt under the short sunflecks (Fig. 3.2.1), we suspect that the sunfleck treatment induced de-epoxidation of trace amounts of V to A and Z in wt. Probably, A and Z were converted back to V under low light during the sunfleck intervals so that they did not accumulate to a detectable level.

The absence of the V-cycle and associated photoprotection may have intensified photo-oxidative stress in *npq1* under the sunflecks.

Whereas most of the xanthophylls are bound in the antenna complexes, carotenes are bound in the core complex of PSII (Yamamoto and Bassi 1996). Among the mutants examined in this study, *lut2* had somewhat more  $\beta$ -car per Chl, whereas *szl1npq1* had very low carotene contents (Fig. 3.2.1b). Some of the carotene binding sites of the PSII core complex are unoccupied in *szl1npq1*, suggesting that xanthophylls cannot replace carotenes in these binding sites (Bassi R, personal communication). These genotype-specific carotene levels, including the presence of  $\alpha$ -car in *lut5* and *szl1npq1*, were not much affected by the sunfleck treatment (Fig. 3.2.1b). In other words, the specific ratios between carotenes and Chl were highly conserved in all cases, with or without sunflecks and regardless of genetic modifications in the carotenoid biosynthesis. Although photoacclimatory shift between  $\alpha$ -car (more in shade) and  $\beta$ -car (more in high light or sunflecks) is a common feature of leaves accumulating  $\alpha$ -car naturally (Thayer and Björkman 1990; Logan *et al.* 1997; Matsubara *et al.* 2009), the ratio between  $\alpha$ -car and  $\beta$ -car changed only marginally in the sunfleck plants of *lut5* and *szl1npq1* (Fig. 3.2.1b), indicating that these mutants are not able to adjust the balance between the two carotenes under photooxidative stress. Overall, the carotene balance in Arabidopsis leaves seems to be determined genetically rather than through chemical reactions (e.g. bleaching).

Together, the sunfleck-induced changes in leaf pigment composition of Arabidopsis carotenoid mutants can be described as parallel decrease in Chl and carotene contents (hence constant carotene:Chl ratio) combined with adjustment of xanthophyll levels which mostly results in their net increase relative to Chl. The xanthophyll species showing an increase in the sunfleck plants correspond largely to the balance between the two branches of the carotenoid biosynthetic pathway given by the specific mutations in these plants, which implies upregulation of xanthophyll synthesis under photo-oxidative stress.

#### 4.4.2 Effect of fluctuating light on PSII

When growing in the control condition, *lut2*, *lut5* and *npq1* had lower NPQ than wt in the initial phase of light induction (Fig. 3.2.4a, b, c and e), in agreement with the NPQ characteristics previously described in these plants (Niyogi *et al.* 1998; Pogson *et al.* 1998; Dall'Osto *et al.* 2007b). Only *szl1npq1* achieved somewhat higher NPQ in the initial phase (Fig. 3.2.4d), which has been attributed to the large pool of L accumulating in their leaves (Fig. 3.2.1a; Li *et al.* 2009). Rapid NPQ induction in the presence of additional L molecules has also been demonstrated in transgenic *Arabidopsis* plants having an extra pool of L at the expense of V (Pogson and Rissler 2000) as well as in species that are able to quickly synthesise L via light-induced de-epoxidation of Lx in the Lx cycle (Matsubara *et al.* 2008, 2011; Esteban *et al.* 2010).

Dynamic photoprotection by thermal energy dissipation, which is regulated by  $\Delta pH$ , plays a crucial role in plants exposed to short sunflecks (Alter *et al.* submitted). During the 7-d sunfleck treatment, the capacity for rapidly inducible and reversible component of NPQ (qE) increased in wt plants (Fig. 3.2.4f) concomitant with a significant increase in the PsbS protein level relative to Chl (Fig. 3.2.5). The PsbS is essential for the  $\Delta pH$ -dependent qE component of NPQ in higher plants (Li *et al.* 2000) and thus for plant fitness under fluctuating light environments (Külheim *et al.* 2002).

A similar but more pronounced NPQ enhancement was found in the sunfleck plants of *lut5* (Fig. 3.2.4h) which had a small NPQ capacity under the control condition (Fig. 3.2.4c; Dall'Osto *et al.* 2007b). The NPQ capacity of *lut5* may be limited, at least in part, by its small V+A+Z content (Fig. 3.2.1d) since the level of PsbS protein is comparable in *lut5* and wt (Fig. 3.2.5). The strong qE upregulation at diminishing V+A+Z in the sunfleck plants of *lut5* (Figs. 3.2.1d and 3.2.4h) could be explained by the increase in L and/or PsbS (Figs. 3.2.1a and 3.2.5). On the other hand, an analogous increase in L, together with a significant increase in V as well as PsbS, had no influence on NPQ in *npq1* plants (Fig. 3.2.4j). While this confirms the interplay between PsbS dosage and V-cycle de-epoxidation in controlling qE intensity (Li, *et al.* 2002), it raises a question as to the involvement of additional L in qE.

Furthermore, the present data also show that the extra pool of L does not enhance NPQ in the sunfleck plants of *npq1* (Figs. 3.2.1a and 3.2.4j) while the strong accumulation of L does restore rapid NPQ induction in *szl1npq1* having the *npq1* background (Fig. 3.2.4d and i; Li *et al.* 2009). The low Fv/Fm values (ca. 0.72) measured in *szl1npq1* under both conditions (Fig. 3.2.3) suggests qI by

photoinhibition or sustained downregulation of PSII. The extremely large pool of L (Fig. 3.2.1a; Li *et al.* 2009), replacing other xanthophylls in the antennae, may interfere with efficient photoprotection and/or PSII repair, leading to increased photoinhibition in these plants. Alternatively, some L molecules may "lock-in" PSII antenna complexes in a dissipative state to constitutively reduce PSII efficiency, as has been proposed for L molecules engaged in the Lx cycle (García-Plazaola *et al.* 2003; Matsubara *et al.* 2005). In contrast, the significant increase of L in *lut5* and *npq1* under the sunfleck condition did not result in lowering of Fv/Fm (Figs. 3.2.1a and 3.2.3). These contradictory observations concerning the effects of additional L on qE and qI have a striking resemblance to the ambivalent situation for quenching effects of L molecules in the Lx cycle (García-Plazaola *et al.* 2003; Matsubara *et al.* 2005, 2008, 2011). The inconsistency in the observations very likely arises from the existence of multiple L pools having different functions, depending on the localisation in the thylakoids. For example, substitution of V by L, or Lx by L, in the L2 binding site of recombinant antenna complexes of PSII results in fluorescence quenching (Formaggio *et al.* 2001; Matsubara *et al.* 2007). In the case of Lx-L substitution, however, this effect was not found in recombinant Lhcb1 or native LHCII trimers isolated from leaves of *I. sapindoides* (Matsubara *et al.* 2007).

The extra pool of L, which accumulated in leaves of *lut5* and *npq1* during the sunfleck treatment, was presumably not in the carotenoid binding sites or the antenna complexes involved in qE or qI. As for the missing effect on qE, this picture is reminiscent of the apparent lack of quenching effect by partial retention of Z in the transgenic line 20.72 (Fig. 3.1.15). Thus, both L and Z must be in the right place to influence qE. The additional L molecules in the sunfleck plants of *lut5* and *npq1* most likely served for other photoprotective purposes, such as quenching of Chl triplet (Dall'Osto *et al.* 2005) or scavenging of reactive oxygen species (Peng *et al.* 2006). Conversely, the lack of L in *lut2* (Fig. 3.2.1a) slows down the NPQ induction even in the presence of A and seems to cause erratic behaviour of the maximal NPQ (Fig. 3.2.4b and g) through destabilisation of LHCII trimers (Lokstein *et al.* 2002) and/or variable PsbS protein level (Fig. 3.2.5).

Notably, the plants of *sz1npq1* were unable to sustain high NPQ when measurements were conducted after long (overnight) dark adaptation; the NPQ level started to decline after 1 min of high light and only half of the initial qE remained at the end of the 5-min illumination (Fig. 3.2.4d and i). This peculiar pattern of NPQ induction is consistent with the role of L in NPQ formation, but contrasts with the rapid induction followed by maintenance of steady-state NPQ previously

reported in these plants (Li *et al.* 2009). The reason for these distinct observations of NPQ phenotype in *szl1npq1* is unknown, but it may reflect structural re-arrangement or instability in PSII. In *szl1npq1*, in which the levels of two minor antenna complexes CP29 and CP26 are reduced to 50% of the wt levels (Li *et al.* 2009), re-arrangement of PSII macro-structure through dissociation/re-association of antenna supercomplexes and/or resulting PSII re-distribution in the thylakoid membranes (Betterle *et al.* 2009) may be disturbed. The timing of NPQ decline corresponds to the onset of  $\Delta\text{pH}$  decrease due to photosynthetic induction (Walker 1981, Sivak *et al.* 1985), suggesting the high sensitivity of L-dependent quenching to  $\Delta\text{pH}$  in the *szl1npq1* plants. A similar observation of  $\Delta\text{pH}$ -dependent quenching by L has also been reported for *Persea americana* having the Lx-cycle (Matsubara *et al.* 2011).

#### 4.4.3 Effect of fluctuating light on growth

In parallel with the changes in pigment composition and PSII activity, growth responses to sunfleck-induced photooxidative stress were also investigated. The sunfleck treatment did not significantly affect the leaf RGR of the five genotypes (Fig. 3.2.6a). Besides the decrease in Chl content (Fig. 3.2.2), another distinctive response commonly observed in leaves under the short sunflecks is formation of flat lamina, instead of convex lamina seen under the control (i.e. low light) condition. While this change in leaf shape was uniformly found in all plants, it was accompanied by non-uniform changes in LMA (Fig. 3.2.6b). In a wide range of species, LMA is strongly influenced by the total irradiance received by leaves over the day (Poorter *et al.*, 2009); sun-exposed leaves usually have higher LMA than leaves growing in the shade (e.g. Matsubara *et al.*, 2009). In this study, the LMA values calculated from leaf dry mass and the *projected* leaf area are slightly overestimated for the control plants which had convex leaf lamina. The decrease in LMA found in the sunfleck plants of wt, and by tendency also *lut5*, may be a result of such overestimation of LMA in the control plants, or it may reflect enhanced photoprotective energy dissipation (Fig. 3.2.4f and h) during, and perhaps also between, the sunflecks, resulting in a reduced dry mass accumulation. The increasing LMA in *lut2* (Fig. 3.2.6b), or even no change of LMA in *szl1npq1* and *npq1*, means that their leaves became thicker and/or had higher dry mass density (e.g. more mesophyll or vascular cells per area) under the sunfleck condition. In particular, the marked LMA increase in *lut2* may suggest a link between leaf growth processes and  $\beta$ -branch carotenoids, especially V+A+Z (Fig. 3.2.1d), under photooxidative stress.

The growth analysis revealed different sensitivity to the sunfleck treatment also in the root system of the five genotypes, and further, between the primary and lateral roots within a genotype (Fig. 3.2.7). The primary root growth decreased in *wt* and *npq1* under the sunfleck condition, while *lut2*, *lut5* and *szl1npq1* responded mainly by reducing the number of lateral roots. Although root growth readily reacts to carbohydrate supply from the shoot (Yazdanbakhsh and Fisahn 2010) and therefore also to changes in light intensity (Nagel *et al.* 2006), the non-uniform patterns of sunfleck-induced root growth suppression observed in the different mutants seem to reflect altered carotenoid metabolism in roots, rather than variations in carbohydrate availability.

In plants two hormones are known to be derived from  $\beta$ -branch carotenoids and involved in stress responses: Absciscic acid (ABA) from 9'-*cis*-N or 9'-*cis*-V (Nambara and Marion-Poll 2005) and strigolactone (SL) from  $\beta$ -car (Schwartz *et al.* 2004). In addition to their roles in controlling aboveground growth, such as seed and bud dormancy by ABA (Koornneef *et al.* 2002; Horvath *et al.* 2003) and inhibition of shoot branching by SL (Gomez-Roldan *et al.* 2008; Umehara *et al.* 2008), both suppress formation of lateral roots, and in the case of SL it also promotes root hair elongation, under drought and osmotic stress (ABA) or phosphate deficiency (SL) (De Smet *et al.* 2006; Koltai 2011). Alteration in the carotenoid biosynthetic pathway may affect regulation of ABA or SL homeostasis in roots, as was found in carotenoid hydroxylase mutants having reduced leaf ABA content (Tian *et al.* 2004). In the present work, the plants with altered balance between  $\alpha$ - and  $\beta$ -branch carotenoids in leaves, albeit in the opposite directions (*lut2* with only  $\beta$ -branch carotenoids, *lut5* and *szl1npq1* more  $\alpha$ -branch carotenoids; Fig. 3.2.1), all showed somewhat lower RGR in the primary root than *wt* under the control condition and reduced formation of lateral roots under the sunfleck condition (Fig. 3.2.7). Although how sunflecks impinge on carotenoid metabolism in roots is not known, the patterns of root growth inhibition observed under the sunflecks and osmotic stress conditions were not identical (Fig. 3.2.7), suggesting distinct signaling pathways and/or agents.

As the primary impact of short sunflecks is photooxidative stress in leaves (Fig. 3.2.4), it is also possible that some signal travelled from shoot to root. Likewise, similar signals were possibly transported into inflorescence stems which were not directly exposed to the sunflecks, resulting in the generally reduced seed harvest in the sunfleck plants (Fig. 3.2.8). The effect on seed production was studied in a much longer term (many weeks) than for the photosynthetic and growth parameters (5-10 d). After long-term exposure to the sunfleck condition, earlier onset of

rosette leaf senescence and flowering was observed in all plants, which could have also contributed to the reduced seed yield. Interestingly, *szl1npq1* produced far less seeds than the other plants in the control condition, while a negative effect of the sunfleck treatment was still recognisable in these plants (Fig. 3.2.8). Compared with chloroplasts and leaves, much less is known about physiological functions and stress responses of carotenoid metabolism in roots and seeds (Howitt and Pogson, 2006). Whether stress signals of short sunflecks, affecting leaf and root growth (Figs. 3.2.6 and 3.2.7) as well as seed production (Fig. 3.2.8), are related to hormones (De Smet *et al.* 2006; Gomez-Roldan *et al.* 2008; Umehara *et al.* 2008; Koltai 2011) or photooxidative signals travelling from the leaves, as has been suggested for systemic acquired acclimation (Karpinski *et al.* 1999; Rossel *et al.* 2007; Szechyńska-Hebda *et al.* 2010), remains to be investigated.

## 5 Conclusion

The role of ZEP in the Lx-cycle was investigated in this thesis. The ZEP isoform 1 was isolated from *I. marginata* leaves and inserted in *A. thaliana npq2* mutants; no Lx was detected in the resulting transformed plants. The affinity of ZEP for L was tested *in vivo* by transforming *A. thaliana szl1npq1* mutants, which also gave no indication of L→Lx conversion by ZEP. Based on these observations, it can be concluded that ImZEP isoform 1 is not able to catalyze the epoxidation reaction from L to Lx. Further studies are necessary to prove the involvement in this reaction of a second isoform (ImZEP2) whose partial sequence has so far been obtained from leaves of two different *Inga* species (*I. marginata* and *I. spectabilis*).

Although no Lx was detected in the transformed plants, the functionality of ImZEP1 was demonstrated by the full epoxidation of Z to V and the operation of the V-cycle under high-light stress. The transgenic line 20.72, in which the impaired activity of ZEP results in retention of Z also in dark conditions, showed a lower PSII efficiency than wt and other transgenic lines in the late recovery phase after the treatment, but not at predawn before the treatment. This could suggest involvement of Z in the qI component of NPQ with the recovery kinetics of minutes to hours. The mechanism by which Z influences this qI component could be studied in the future by checking the carotenoid distribution within the thylakoid membranes of line 20.72.

Effect of the altered  $\alpha$ - and  $\beta$ - branch carotenoid composition was investigated in *A. thaliana* mutants under low-light condition and photooxidative stress caused by short sunflecks. Except for the much lower seed yield of *szlqnpq1*, the large variations in leaf carotenoid composition and NPQ capacity neither favour nor seriously penalise any of the mutants on a whole-plant level under the two conditions used, demonstrating the ability of these plants to cope with modifications in carotenoid metabolism to certain extent. While this ability may have allowed the natural occurrence of  $\alpha$ -car and Lx in leaves of some species, the conserved absence of these  $\alpha$ -branch carotenoids in other plants suggest selection pressure against mutations giving rise to accumulation of these pigments in their leaves. Further investigations are needed to elucidate the roles of the  $\alpha$ - and  $\beta$ -branch carotenoid metabolism in different cells and organs for plant acclimation and adaptation to variable and/or adverse environments.

## 6 Reference

- Adams III, W., Demmig-Adams, B., Rosenstiel, T., Brightwell, A., Ebbert, V. (2002).** Photosynthesis and photoprotection in overwintering plants. *Plant Biol.(Stuttg)*, 4, 545–557.
- Ahn, T. K., Avenson, T. J., Ballottari, M., Cheng, Y.-C., Niyogi, Krishna K, Bassi, Roberto, Fleming, Graham R. (2008).** Architecture of a charge-transfer state regulating light harvesting in a plant antenna protein. *Science (New York, N.Y.)*, 320(5877), 794-7.
- Alter P., Dreissen A., Luo, F., Matsubara, S. (submitted)** Acclimation responses of *Arabidopsis* to sunflecks: comparison of different sunfleck regimes and *Arabidopsis* accessions
- Amunts, A., Toporik, H., Borovikova, A., Nelson, N. (2010).** Structure determination and improved model of plant photosystem I. *The Journal of biological chemistry*, 285(5), 3478-86.
- Apel, K., Hirt, H. (2004).** Reactive oxygen species: metabolism, oxidative stress, and signal transduction. *Review Literature And Arts Of The Americas*, 55, 373-399.
- Aro, E. M., Virgin, I., Andersson, B. (1993).** Photoinhibition of Photosystem II. Inactivation, protein damage and turnover. *Biochimica et biophysica acta*, 1143(2), 113-34.
- Asada, K. (2000).** The water-water cycle as alternative photon and electron sinks. *Philosophical transactions of the Royal Society of London. Series B, Biological sciences*, 355(1402), 1419-31.
- Ausubel, F. M., Brent, R., Kingston, R.E., Moore, D.D., Seidman, J. G., Smith, J. A., Struhl, K. (2002).** Current protocols in molecular biology. John Wiley & Sons, Inc., New York
- Avenson, T. J., Ahn, T. K., Zigmantas, D., Niyogi, K. K., Li, Z., Ballottari, M., Bassi, R., Fleming, G. R. (2008).** Zeaxanthin radical cation formation in minor light-harvesting complexes of higher plant antenna. *The Journal of biological chemistry*, 283(6), 3550-8.
- Baroli, I., Do, A., Yamane, T., Niyogi, K. K. (2003).** Zeaxanthin accumulation in the absence of a functional xanthophyll cycle protects *Chlamydomonas reinhardtii* from photooxidative stress. *The Plant Cell Online*, 15, 992-1008.
- Bassi, R, Caffarri, S. (2000).** Lhc proteins and the regulation of photosynthetic light harvesting function by xanthophylls. *Photosynthesis research*, 64(2-3), 243-56.
- Beisel, K. G., Jahnke, S., Hofmann, D., Koppchen, S., Schurr, U., Matsubara, S. (2010).** Continuous Turnover of carotenenes and chlorophyll a in mature leaves of arabidopsis revealed by <sup>14</sup>CO<sub>2</sub> pulse-chase labeling. *Plant Physiology*, 152(4), 2188-2199.

- Betterle, N., Ballottari, M., Zorzan, S., de Bianchi, S., Cazzaniga, S., Dall'osto, L., Morosinotto, T., Bassi R. (2009).** Light-induced dissociation of an antenna hetero-oligomer is needed for non-photochemical quenching induction. *The Journal of biological chemistry*, 284(22), 15255-66.
- Bouvier, F., D'Harlingue, A., Hugueney, P., Marin, E., Marion-Poll, A., Camara, B. (1996).** Xanthophyll Biosynthesis: cloning, expression, functional reconstitution, and regulation of  $\beta$ -cyclohexenyl carotenoid epoxidase from pepper (*Capsicum annuum*). *The Journal of biological chemistry*, 271(46), 28861-28867.
- Bugos, R. C., Hieber, A. D., Yamamoto, H. Y. (1998).** Xanthophyll cycle enzymes are members of the lipocalin family, the first identified from plants. *The Journal of biological chemistry*, 273(25), 15321-4.
- Bungard, R. A., Ruban, A. V., Hibberd, J. M., Press, M. C., Horton, P., Scholes, J. D. (1999).** Unusual carotenoid composition and a new type of xanthophyll cycle in plants. *Proceedings of the National Academy of Sciences of the United States of America*, 96(3), 1135-9.
- Büch, K., Stransky, H., & Hager, A. (1995).** FAD is a further essential cofactor of the NAD(P)H and  $O_2$ -dependent zeaxanthin-epoxidase. *FEBS letters*, 376(1-2), 45-8.
- Crimi, M., Dorra, D., Böisinger, C. S., Giuffra, E., Holzwarth, A. R., Bassi, R. (2001).** Time-resolved fluorescence analysis of the recombinant photosystem II antenna complex CP29. Effects of zeaxanthin, pH and phosphorylation. *European journal of biochemistry / FEBS*, 268(2), 260-7.
- Dall'Osto, L., Caffarri, Stefano, Bassi, R. (2005).** A mechanism of nonphotochemical energy dissipation, independent from PsbS, revealed by a conformational change in the antenna protein CP26. *The Plant Cell Online*, 17(4), 1217.
- Dall'Osto, L., Lico, C., Alric, J., Giuliano, G., Havaux, M., Bassi, R. (2006).** Lutein is needed for efficient chlorophyll triplet quenching in the major LHCII antenna complex of higher plants and effective photoprotection in vivo under strong light. *BMC plant biology*, 6, 32.
- Dall'Osto, L., Cazzaniga, S., North, H., Marion-Poll, A., Bassi, R. (2007a).** The *Arabidopsis aba4-1* mutant reveals a specific function for neoxanthin in protection against photooxidative stress. *The Plant cell*, 19(3), 1048-64.
- Dall'Osto, L., Fiore, A., Cazzaniga, S., Giuliano, G., Bassi, R. (2007b).** Different roles of alpha- and beta-branch xanthophylls in photosystem assembly and photoprotection. *The Journal of biological chemistry*, 282(48), 35056-68.
- DellaPenna, D., Pogson, B. J. (2006).** Vitamin synthesis in plants: tocopherols and carotenoids. *Annual review of plant biology*, 57, 711-38.
- Demmig-Adams, B. (1990).** Carotenoids and photoprotection in plants: a role for the xanthophyll zeaxanthin. *Biochimica et Biophysica Acta*, 1020(1), 1-24.
- Demmig-Adams, B. (1992).** Photoprotection and other responses of plants to high light stress. *Annual Review of Plant*, 599-626.

- Demmig-Adams, B., Adams III, W.W.(1996a).** The role of xanthophylls cycle carotenoids in the protection of photosynthesis. *Trends Plant Sci.* 1, 21-26
- Demmig-Adams, B., Gilmore, A. (1996b).** Carotenoids 3: in vivo function of carotenoids in higher plants. *The FASEB journal*, 403-412.
- De Smet, I., Zhang, H., Inzé, D., Beeckman, T. (2006).** A novel role for abscisic acid emerges from underground. *Trends in plant science*, 11(9), 434-9.
- Dreuw, A., Fleming, G.R., Head-Gordon, M. (2003).** Chlorophyll fluorescence quenching by xanthophylls. *Physical Chemistry Chemical Physics*, 5(15), 3247–3256
- Dunn, S. D. (1986).** Effect of the modification of transfer buffer composition and the renaturation of proteins in gels on the recognition of proteins on western blots by monoclonal antibodies 1. *Analytical biochemistry*, 157, 144-153.
- Durocher, D., Jackson, S. P. (2002).** The FHA domain. *FEBS letters*, 513, 58-66.
- Ebbert, V., Demmig-Adams, B., Adams, W. W., Mueh, K. E., Staehelin, L. A. (2001).** Correlation between persistent forms of zeaxanthin-dependent energy dissipation and thylakoid protein phosphorylation. *Photosynthesis research*, 67(1-2), 63-78.
- Elhai, J., Wolk, C. P. (1988).** Conjugal transfer of DNA to cyanobacteria. *Methods in enzymology*, 167, 747-754.
- Esteban, R., Jiménez, M. S., Morales, D., Jiménez, E. T., Hormaetxe, K., Becerril, J. M., Osmond, B., García-Plazaola, J. I. (2008).** Short- and long-term modulation of the lutein epoxide and violaxanthin cycles in two species of the Lauraceae: sweet bay laurel (*Laurus nobilis* L.) and avocado (*Persea americana* Mill.). *Plant biology (Stuttgart, Germany)*, 10(3), 288-97.
- Esteban, R., Olano, J. M, Castresana, J., Fernández-Marín, B., Hernández, A., Becerril, J. M., García-Plazaola, J. I. (2009).** Distribution and evolutionary trends of photoprotective isoprenoids (xanthophylls and tocopherols) within the plant kingdom. *Physiologia plantarum*, 135(4), 379-89.
- Esteban R., Matsubara S., Jiménez M. S., Morales D., Brito P., Lozenzo R., Fernández-Marin B., Becerril J. M., García-Plazaola J. I. (2010).** Operation and regulation of the lutein epoxide cycle in seedlings of *Ocotea foetens*. *Functional Plant Biology* 37, 859-869.
- Finazzi, G., Rappaport, F., Furia, A., Fleischmann, M., Rochaix, J.-D., Zito, F., Forti, G. (2002).** Involvement of state transitions in the switch between linear and cyclic electron flow in *Chlamydomonas reinhardtii*. *EMBO reports*, 3(3), 280-5.
- Fiore, A., Dall’osto, L., Fraser, P. D., Bassi, R., Giuliano, G. (2006).** Elucidation of the beta-carotene hydroxylation pathway in *Arabidopsis thaliana*. *FEBS letters*, 580(19), 4718-22.
- Formaggio, E., Cinque, G., & Bassi, R. (2001).** Functional architecture of the major light-harvesting complex from higher plants. *Journal of molecular biology*, 314(5), 1157–1166.

- Frank, H. A., Cua, A., Chynwat, V., Young, A., Gosztola, D., Wasielewski, M. R. (1994).** Photophysics of the carotenoids associated with the xanthophyll cycle in photosynthesis. *Photosynthesis Research*, 41(3), 389–395.
- García-Plazaola, J. I., Hormaetxe, K., Hernández, A., Olano, J.M., Becerril, J.M. (2004).** The lutein epoxide cycle in vegetative buds of woody plants. *Functional plant biology*, 31(8), 815–823.
- García-Plazaola, J. I., Matsubara, S., Osmond, C. B.. (2007).** The lutein epoxide cycle in higher plants : its relationships to other xanthophyll cycles and possible functions. *Functional Plant Biology*, (34), 759-773.
- Gilmore, A. M., Ball, M C. (2000).** Protection and storage of chlorophyll in overwintering evergreens. *Proceedings of the National Academy of Sciences of the United States of America*, 97(20), 11098-101.
- Gilmore, A. M., Yamamoto, H.Y. (1991).** Zeaxanthin formation and energy-dependent fluorescence quenching in pea chloroplasts under artificially mediated linear and cyclic electron transport. *Plant physiology*, 96(2), 635..
- Gilmore, A. M., Yamamoto, H. Y. (1991).** Resolution of lutein and zeaxanthin using a non-endcapped, lightly carbon-loaded C18 high-performance liquid chromatographic column. *Journal of Chromatography A*, 543, 137-145.
- Gilmore, A. M., Yamamoto, H. Y. (1994).** Epoxidation of zeaxanthin and antheraxanthin reverses non-photochemical quenching of photosystem II chlorophyll a fluorescence in the presence of trans-thylakoid ApH. *FEBS Letters*, 350, 271-274.
- Gomez-Roldan, V., Fermas, S., Brewer, P. B., Puech-Pagès, V., Dun, E. A., Pillot, J.-P., Letisse, F., Matusova,R., Danoun, S., Portais, J.-C., Bouwmeester, H., Beécard, G., Beveridge, C.A., Rameau, C., Rochange, S.F. (2008).** Strigolactone inhibition of shoot branching. *Nature*, 455(7210), 189-94.
- Govindjee, Kern, J. F., Messinger, J., Whitmarsh, J. (2010).** Photosystem II. *Encyclopedia of Life Sciences (ELS)*, 1-15.
- Green, B. R., Durnford, D. G. (1996).** The chlorophyll-carotenoid proteins of oxygenic photosynthesis. *Annual review of plant physiology and plant molecular biology*, 47, 685-714.
- Hankamer, B., Barber, J., Boekema, E.J. (1997).** Structure and membrane organization of photosystem II in green plants. *Annual Review of Plant Biology*, 48(1), 641–671.
- Havaux, M., Niyogi, K K. (1999).** The violaxanthin cycle protects plants from photooxidative damage by more than one mechanism. *Proceedings of the National Academy of Sciences of the United States of America*, 96(15), 8762-7.
- Hieber, A. D., Bugos, R. C., Yamamoto, H. Y. (2000).** Plant lipocalins: violaxanthin de-epoxidase and zeaxanthin epoxidase. *Biochimica et biophysica acta*, 1482(1-2), 84-91.

- Heck, A. (2008).** Synthese heterologer Membranproteine und Carotinoide in dem phototrophen Bakterium *Rhodobacter capsulatus*. *Düsseldorf University dissertation*.
- Herrin, D. L., Smidt, G. W. (1988).** Rapid, reversible staining of northern blots prior to hybridization. *BioTechniques* 6, 196-200
- Hirschberg, J. (2001).** Carotenoid biosynthesis in flowering plants. *Current opinion in plant biology*, 4(3), 210-8.
- Holt, N. E., Fleming, G.R., Niyogi, K.K. (2004).** Toward an understanding of the mechanism of nonphotochemical quenching in green plants. *Biochemistry*, 43(26), 8281–8289.
- Horton, P., Wentworth, M., Ruban, A. (2005).** Control of the light harvesting function of chloroplast membranes: the LHCII-aggregation model for non-photochemical quenching. *FEBS letters*, 579(20), 4201–4206.
- Horvath, D. P., Anderson, J. V., Chao, W. S., Foley, M. E. (2003).** Knowing when to grow: signals regulating bud dormancy. *Trends in Plant Science*, 8(11), 534-540.
- Jahns, P., Mieke, B. (1996).** Kinetic correlation of recovery from photoinhibition and zeaxanthin epoxidation. *Planta*, 198(2), 202–210
- Jahns, P., Latowski, D., Strzalka, K. (2009).** Mechanism and regulation of the violaxanthin cycle: the role of antenna proteins and membrane lipids. *Biochimica et Biophysica Acta (BBA)-Bioenergetics*, 1787(1), 3–14.
- Jensen, P. E., Bassi, R., Boekema, E. J., Dekker, J. P., Jansson, S., Leister, D., Robinson, C., Scheller, H.V. (2007).** Structure, function and regulation of plant photosystem I. *Biochimica et biophysica acta*, 1767(5), 335-52.
- Jansen, M., Gilmer, F., Biskup, B., Nagel, K. A., Rascher, U., Fischbach, A., Briem, S., Dreissen, G., Tittmann, S., Braun, S., De Jaeger, I., Metzlaff, M., Schurr, U., Scharr, H., Walter, A. (2009).** Simultaneous phenotyping of leaf growth and chlorophyll fluorescence via GROWSCREEN FLUORO allows detection of stress tolerance in *Arabidopsis thaliana* and other rosette plants. *Functional Plant Biology*, 36(11), 902–914.
- Joyard, J., Ferro, M., Masselon, C., Seigneurin-Berny, D., Salvi, D., Garin, J., Rolland, N. (2009).** Chloroplast proteomics and the compartmentation of plastidial isoprenoid biosynthetic pathways. *Molecular plant*, 2(6), 1154-80.
- Kalituho, L., Rech, J., Jahns, P. (2007).** The roles of specific xanthophylls in light utilization. *Planta*, 225(2), 423-39.
- Karpinski, S., Reynolds, H., Karpinska, B., Wingsle, G., Creissen, G., Mullineaux, P. (1999).** Systemic Signaling and Acclimation in Response to Excess Excitation Energy in *Arabidopsis*. *Science*, 284(5414), 654-657.

- Katzke, N., Arvani, S., Bergmann, R., Circolone, F., Markert, A., Svensson, V., Jaeger, K.-E., Heck, A., Drepper, T. (2010). A novel T7 RNA polymerase dependent expression system for high-level protein production in the phototrophic bacterium *Rhodobacter capsulatus*. *Protein expression and purification*, 69(2), 137-46.
- Ke, B. (2001). Photosynthesis: an overview. In: Ke, B. *Photosynthesis Photobiochemistry and Photobiophysics*. Edited by Govindjee. pp. 1-46, Dordrecht: Kluwer Academic Publishers
- Kim, J., Smith, J. J., Tian, L., DellaPenna, D. (2009). The evolution and function of carotenoid hydroxylases in Arabidopsis. *Plant and Cell Physiology*, 50(3), 463.
- Kim, J., DellaPenna, D. (2006). Defining the primary route for lutein synthesis in plants: the role of Arabidopsis carotenoid beta-ring hydroxylase CYP97A3. *Proceedings of the National Academy of Sciences of the United States of America*, 103(9), 3474-9.
- Klipp, W., Masepohl, B., Pühler, A. (1987). Identification and mapping of nitrogen fixation genes of *Rhodobacter capsulatus*: duplication of a nifA-nifB region. *Journal of bacteriology*, 170(2), 693-9.
- Koltai, H. (2011). Strigolactones are regulators of root development. *New Phytologist*, 190(3), 545-549.
- Koornneef, M., Bentsink, L., Hilhorst, H. (2002). Seed dormancy and germination. *Current Opinion in Plant Biology*, 5(1), 33-36.
- Krause, G.H., Koroleva, O. Y., Dalling, J. W., Winter, K. (2001). Acclimation of tropical tree seedlings to excessive light in simulated tree-fall gaps. *Plant, Cell & Environment*, 24(12), 1345-1352.
- Krause, G., Vernotte, C. (1982). Photoinduced quenching of chlorophyll fluorescence in intact chloroplasts and algae. Resolution into two components. *Biochimica et Biophysica Acta (BBA)*, 679, 116-124.
- Külheim, C., Ågren, J., Jansson, S. (2002). Rapid regulation of light harvesting and plant fitness in the field. *Science (New York, N.Y.)*, 297(5578), 91-3.
- Laemmli, U. K. (1970). Cleavage of structural proteins during the assembly of the head of bacteriophage T4. *nature*, 227(5259), 680-685.
- Leitsch, J., Schnettger, B., Critchley, C. (1994). Two mechanisms of recovery from photoinhibition in vivo: reactivation of photosystem II related and unrelated to D1-protein turnover. *Planta*, 15-21.
- Li, X., Bjorkman, O., Shih, C., Grossman, A. (2000). A pigment-binding protein essential for regulation of photosynthetic light harvesting. *Nature*, 403, 391-395.
- Li, X. P., Phippard, A., Niyogi, K.K., Pasari, J. (2002). Structure-function analysis of photosystem II subunit S (PsbS) in vivo. *Functional Plant Biology*, 29(10), 1131-1139. CSIRO.

- Li, Z., Ahn, T. K., Avenson, T. J., Ballottari, M., Cruz, J. A., Kramer, D. M., Bassi, R., Fleming, G.R., Keasling, J.D., Niyogi, K.K. (2009). Lutein accumulation in the absence of zeaxanthin restores nonphotochemical quenching in the *Arabidopsis thaliana npq1* mutant. *The Plant cell*, 21(6), 1798-812.
- Logan, B. A., Barker, D. H., Demmig-Adams, B., Adams III, W. W. (1997). The response of xanthophyll cycle-dependent energy dissipation in *Alocasia brisbanensis* to sunflecks in a subtropical rainforest. *Functional Plant Biology*, 24(1), 27–33.
- Lokstein, H., Tian, L., Polle, J. E. W., DellaPenna, D. (2002). Xanthophyll biosynthetic mutants of *Arabidopsis thaliana*: altered nonphotochemical quenching of chlorophyll fluorescence is due to changes in Photosystem II antenna size and stability. *Biochimica et biophysica acta*, 1553(3), 309-19.
- Marin, E., Nussaume, L., Quesada, A., Gonneau, M., Sotta, B., Hugueney, P., Frey, A., Marion Poll, A. (1996). Molecular identification of zeaxanthin epoxidase of *Nicotiana plumbaginifolia*, a gene involved in abscisic acid biosynthesis and corresponding to the ABA locus of *Arabidopsis thaliana*. *The EMBO journal*, 15(10), 2331-42.
- Matsubara, S., Gilmore, A. M., Osmond, C. B. (2001). Diurnal and acclimatory responses of violaxanthin and lutein epoxide in the Australian mistletoe *Amyema miquelii*. *Australian Journal of Plant Physiology*, 28, 793-800
- Matsubara, S., Gilmore, A. M., Ball, M.C., Osmond, C.B., Anderson, J. M. (2002). Sustained downregulation of photosystem II in mistletoes during winter depression of photosynthesis. *Functional Plant Biology*, 29(10), 1157–1169.
- Matsubara, S., Morosinotto, T., Bassi, R., Christian, A.-L., Fischer-Schliebs, E., Lüttge, U., Orthen, B., Franco, A.C., Scarano, F. R., Förster, B., Pogson, B. J., Osmond, C. B. (2003). Occurrence of the lutein-epoxide cycle in mistletoes of the Loranthaceae and Viscaceae. *Planta*, 217(6), 868-79.
- Matsubara, S., Naumann, M., Martin, R., Nichol, C., Rascher, U., Morosinotto, T., Bassi, R., Osmond, C. B. (2005). Slowly reversible de-epoxidation of lutein-epoxide in deep shade leaves of a tropical tree legume may “lock-in” lutein-based photoprotection during acclimation to strong light. *Journal of experimental botany*, 56(411), 461-8.
- Matsubara, S., Morosinotto, T., Osmond, C. B., Bassi, R. (2007). Short- and long-term operation of the lutein-epoxide cycle in light-harvesting antenna complexes. *Plant physiology*, 144(2), 926-41.
- Matsubara, S., Krause, G. H., Seltmann, M., Virgo, A., Kursar, T. A., Jahns, P., Winter, K. (2008). Lutein epoxide cycle, light harvesting and photoprotection in species of the tropical tree genus *Inga*. *Plant, cell & environment*, 31(4), 548-61.
- Matsubara, S., Krause, G. H., Aranda, J., Virgo, A., Beisel, G. K., Jahns, P., Winter, K. (2009). Sun-shade patterns of leaf carotenoid composition in 86 species of neotropical forest plants. *Functional Plant Biology*, 36(1), 20.

- Matsubara, S., Chen, Y.-C., Caliendo, R., Govindjee, Clegg, R. M. (2011).** Photosystem II fluorescence lifetime imaging in avocado leaves: contributions of the lutein-epoxide and violaxanthin cycles to fluorescence quenching. *Journal of photochemistry and photobiology. B, Biology*, 104(1-2), 271-84.
- Merril, C. (1990).** Gel staining techniques. *Encyclopedia of Life Sciences*, 182(1939), 2943-2943.
- Miloslavina, Y., Wehner, A., Lambrev, P. H., Wientjes, E., Reus, M., Garab, G., Croce, R., Holzwarth, A. R.(2008).** Far-red fluorescence: a direct spectroscopic marker for LHCII oligomer formation in non-photochemical quenching. *FEBS letters*, 582(25-26), 3625-31.
- Morosinotto, T., Caffarri, S., Dall'osto, L., Bassi, R. (2003).** Mechanistic aspects of the xanthophyll dynamics in higher plant thylakoids. *Physiologia plantarum*, (119), 347-354.
- Mühlich M., Truhn D., Nagel K.A., Walter A., Scharr H., Ach T. (2008)** Measuring plant root growth. In *Lecture notes in computer science 5096* (ed G. Rigoll), pp. 497-506. Springer-Verlag, Heidelberg, Germany.
- Müller P., Li, X.P., Niyogi, K.K. (2001).** Non-photochemical quenching: a response to excess light energy. *Plant Physiol* 125, 1558-1566
- Nagel, K. A., Schurr, U., Walter, A. (2006).** Dynamics of root growth stimulation in *Nicotiana tabacum* in increasing light intensity. *Plant, cell & environment*, 29(10), 1936-45.
- Nagel, K. A., Kastenholz, B., Jahnke, S., van Dusschoten, D., Aach, T., Mühlich, M., Truhn, D., Scharr, H., Terjung, S., Walter, A., Schurr, U. (2009).** Temperature responses of roots: impact on growth, root system architecture and implications for phenotyping. *Functional Plant Biology*, 36(11), 947.
- Nakagawa, T., Kurose, T., Hino, T., Tanaka, K., Kawamukai, M., Niwa, Y., Toyooka, K., Matsuoka, K., Jimbo, T., Kimura, T. (2007).** Development of series of gateway binary vectors, pGWBs, for realizing efficient construction of fusion genes for plant transformation. *Journal of bioscience and bioengineering*, 104(1), 34-41.
- Nambara, E., Marion-Poll, A. (2005).** Absciscic acid biosynthesis and catabolism. *Annual review of plant biology*, 56, 165-85.
- Niczyporuk, S. (2009).** Untersuchungen zur Regulation der Zeaxanthin epoxidation in höheren Pflanzen. *Düsseldorf University dissertation*.
- Nilkens, M., Kress, E., Lambrev, P., Miloslavina, Y., Müller, M., Holzwarth, A. R., Jahns, P. (2010).** Identification of a slowly inducible zeaxanthin-dependent component of non-photochemical quenching of chlorophyll fluorescence generated under steady-state conditions in *Arabidopsis*. *Biochimica et biophysica acta*, 1797(4), 466-75
- Niyogi, K K, Grossman, A. R., Björkman, O. (1998).** *Arabidopsis* mutants define a central role for the xanthophyll cycle in the regulation of photosynthetic energy conversion. *The Plant cell*, 10(7), 1121-34.

- Niyogi, K. K. (1999).** Photoprotection revised: genetic and molecular approaches. *Annual review of plant physiology and plant molecular biology*, 50, 333-359.
- Nowicka, B., Strzalka, W., Strzalka, K. (2009).** New transgenic line of *Arabidopsis thaliana* with partly disabled zeaxanthin epoxidase activity displays changed carotenoid composition, xanthophyll cycle activity and non-photochemical quenching kinetics. *Journal of plant physiology*, 166(10), 1045-56.
- Osmond, C. B. (1994)** What is photoinhibition? Some insight from comparisons of shade and sun plants, in: Baker, N. R., Bowyer J. R. (Eds) *Photoinhibition of Photosynthesis: from molecular mechanisms to the field*. pp 1-24, Oxford
- Ottander, C., Campbell, D., Öquist, G. (1995).** Seasonal changes in photosystem II organisation and pigment composition in *Pinus sylvestris*. *Planta* 197, 176-183
- Pearcy, R. W. (1990).** Sunfleck and photosynthesis in plant canopies. *Annual Review of Plant Physiology and Plant Molecular Biology*, 41, 421-453
- Peng, C.-L., Lin, Z.-F., Su, Y.-Z., Lin, G.-Z., Dou, H.-Y., & Zhao, C.-X. (2006).** The antioxidative function of lutein: electron spin resonance studies and chemical detection. *Functional Plant Biology*, 33(9), 839.
- Pennington, T.D., Fernandes, E.C.M. (Eds) (1998).** The genus *Inga* utilization. Kew (RU). *The Royal Botanic Gardens*.
- Pfündel, E., Bilger, W.(1994).** Regulation and possible function of the violaxanthin cycle. *Photosynth. Res* 42, 89-109
- Pogson, B. J., McDonald, K. A., Truong, M., Britton, G., DellaPenna, D. (1996).** Arabidopsis carotenoid mutants demonstrate that lutein is not essential for photosynthesis in higher plants. *The Plant cell*, 8(9), 1627-39.
- Pogson, B. J., Niyogi, K. K., Björkman, O., DellaPenna, D. (1998).** Altered xanthophyll compositions adversely affect chlorophyll accumulation and nonphotochemical quenching in Arabidopsis mutants. *Proceedings of the National Academy of Sciences of the United States of America*, 95(22), 13324-9.
- Pogson, B. J., Rissler, H. M. (2000).** Genetic manipulation of carotenoid biosynthesis and photoprotection. *Philosophical transactions of the Royal Society of London. Series B, Biological sciences*, 355(1402), 1395-403.
- Poorter, H., Niinemets, Ü., Poorter, L., Wright, I. J., Villar, R. (2009).** Causes and consequences of variation in leaf mass per area (LMA): a meta-analysis. *New Phytologist*, 182(3), 565-588.

- Porra, R., Thompson, W., Kriedemann, P. (1989).** Determination of accurate extinction coefficients and simultaneous equations for assaying chlorophylls a and b extracted with four different solvents: verification of the concentration of chlorophyll standards by atomic absorption spectroscopy. *Biochimica et Biophysica Acta (BBA)-Bioenergetics*, 975(3), 384–394.
- Rabinowitch, H. D., Budowski, P., Kedar, N. (1975).** Carotenoids and epoxide cycles in mature-green tomatoes. *Planta*, 122(1), 91-97.
- Reinhold, C., Niczyporuk, S., Beran, K. (2008).** Short-term down-regulation of zeaxanthin epoxidation in *Arabidopsis thaliana* in response to photo-oxidative stress conditions. *Biochimica et Biophysica*, 1777, 462-469.
- Rochaix, J.-D. (2007).** Role of thylakoid protein kinases in photosynthetic acclimation. *FEBS letters*, 581(15), 2768-75.
- Rossel, J. B., Wilson, P. B., Hussain, D., Woo, N. S., Gordon, M. J., Mewett, O. P., Howell, K. A., Whelan, J., Kazan, K., J. Pogson, B. J. (2007).** Systemic and intracellular responses to photooxidative stress in *Arabidopsis*. *The Plant cell*, 19(12), 4091-110.
- Ruban, A. V., Berera, R., Iliaia, C., van Stokkum, I. H. M., Kennis, J. T. M., Pascal, A. A., van Amerongen, H., van Amerongen, H., Robert, B., Horton, P., van Grondelle, R. (2007).** Identification of a mechanism of photoprotective energy dissipation in higher plants. *Nature*, 450(7169), 575-8.
- Schreiber, U. (2004)** Pulse-Amplitude-Modulation (PAM) Fluorometry and Saturation Pulse Method: An Overview. In: G.C. Papageorgiou, Govindjee (Eds.), *Chlorophyll a Fluorescence - A Signature of Photosynthesis*, Springer, Dordrecht, pp. 279-319
- Schwartz, S. H., Qin, X., Loewen, M. C. (2004).** The biochemical characterization of two carotenoid cleavage enzymes from *Arabidopsis* indicates that a carotenoid-derived compound inhibits lateral branching. *The Journal of biological chemistry*, 279(45), 46940-5.
- Seltmann, M. (2006).** Untersuchungen der Biosynthese und der Funktion von Lutein-Epoxid in den Blättern von *Inga sapindoides*. *Düsseldorf University Diploma thesis*.
- Siefermann, D., Yamamoto, H.Y. (1975).** Properties of NADPH and oxygen-dependent zeaxanthin epoxidation in isolated chloroplasts. A transmembrane model for the violaxanthin cycle. *Arch of Bioch. And Bioph.* 171, 70-77
- Sirikhachornkit, A., Niyogi, K.K. (2010)** Antioxidants and photo-oxidative stress responses in plants and algae. in Rebeiz, C. A., Benning, C., Bohnert, H. J., Daniell, H., Hoober, J. K., Lichtenthaler, H. K., Portis, A. R., Trpathy, B. C. (Eds) *The Chloroplast - Basics and Applications*, Springer, Dordrecht pp. 379-396
- Sivak, M. N., Dietz, K.-J., Heber, U., Walker, D. A. (1985).** The relationship between light scattering and chlorophyll a fluorescence during oscillations in photosynthetic carbon assimilation. *Archives of Biochemistry and Biophysics*, 237(2), 513-519.

- Snyder, A. M., Clark, B. M., Bungard, R. A. (2005).** Light-dependent conversion of carotenoids in the parasitic angiosperm *Cuscuta reflexa* L. *Plant, Cell & Environment* 28, 1326-1333
- Straub, O., Pfander, H.(1987)** *Key to Carotenoids*. Edited by Pfander, H., Gerspacher, M., Rychener, M. & Schwabe, R. Birkhauser, Basel. pp. 11–218.
- Szechyńska-Hebda, M., Kruk, J., Górecka, M., Karpińska, B., Karpiński, S. (2010).** Evidence for light wavelength-specific photoelectrophysiological signaling and memory of excess light episodes in *Arabidopsis*. *The Plant cell*, 22(7), 2201-18.
- Thayer, S. S., Björkman, O. (1990).** Leaf xanthophyll content and composition in sun and shade determined by HPLC. *Photosynthesis Research*, 23(3), 331–343.
- Tian, Li, DellaPenna, D, Zeevaart, J. A. D. (2004).** Effect of hydroxylated carotenoid deficiency on ABA accumulation in *Arabidopsis*. *Physiologia Plantarum*, 122, 314-320.
- Triantaphylidès, C., Havaux, M. (2009).** Singlet oxygen in plants: production, detoxification and signaling. *Trends in plant science*, 14(4), 219-28.
- Umehara, M., Hanada, A., Yoshida, S., Akiyama, K., Arite, T., Takeda-Kamiya, N., Magome, H., Kamiya, Y., Shirasu, K., Yoneyama, K., Kyojuka, J., Yamaguchi, S. (2008).** Inhibition of shoot branching by new terpenoid plant hormones. *Nature*, 455(7210), 195-200.
- van Kooten O., Snell J.H.F. 1990.** The use of chlorophyll fluorescence nomenclature in plant stress physiology. *Photosynth. Res.*, 25, 147-150.
- Walker, D. (1981).** Secondary fluorescence kinetics of spinach leaves in relation to the onset of photosynthetic carbon assimilation. *Planta*, 153(3), 273–278.
- Wang, N., Fang, W., Han, H., Sui, N., Li, B., Meng, Q.-W. (2008).** Overexpression of zeaxanthin epoxidase gene enhances the sensitivity of tomato PSII photoinhibition to high light and chilling stress. *Physiologia plantarum*, 132(3), 384-96.
- Weaver, P. F., Wall, J. D., Gest, H. (1975).** Characterization of *Rhodopseudomonas capsulata*. *Archives of microbiology*, 105(3), 207-16.
- Welsch, R., Beyer, P., Hugueney, P, Kleinig, H., von Lintig, J. (2000).** Regulation and activation of phytoene synthase, a key enzyme in carotenoid biosynthesis, during photomorphogenesis. *Planta*, 211(6), 846-54.
- Wilson, K. J., Juan, P. M. (1989).** Protein and peptide purification. In *Protein sequencing, a practical approach*. Edited by J. B. C. Findley & M. L. Geisow. Oxford: IRL Press.
- Yamamoto, H., Nakayama, T. O. M., Chichester, C. (1962).** Studies on the light and dark interconversions of leaf xanthophylls. *Archives of Biochemistry and Biophysics*, 97(1), 168–173.
- Yamamoto, H.Y., Higashi, R. (1978).** Violaxanthin de-epoxidase: Lipid composition and substrate specificity. *Archives of Biochemistry and Biophysics*, 190(2), 514–522.

- Yamamoto H.Y., Bassi R. (1996)** Carotenoids: localization and function. In *Oxygenic Photosynthesis: The Light Reactions*. (eds D.R. Ort & C.F. Yocum), pp 539-563. Kluwer, Dordrecht.
- Yamamoto H.Y., Bugos R.C., Hieber A.D. (2004).** Biochemistry and molecular biology of the xanthophyll cycle. In: Frank H.A., Young A.J., Britton G., Cogdell R.J. (eds). *The photochemistry of carotenoids*. Dordrecht: Kluwer Academic Publishers. pp 293–303.
- Yanisch-Perron, C., Vieira, J., Messing, J. (1985).** Improved M13 phage cloning vectors and host strains: nucleotide sequences of the M13mp18 and pUC19 vectors. *Gene*, 33(1), 103-19
- Yazdanbakhsh, N., Fisahn, J. (2010).** Analysis of *Arabidopsis thaliana* root growth kinetics with high temporal and spatial resolution. *Annals of botany*, 105(5), 783-91.
- Yin, Z. H., Johnson, G. N. (2000).** Photosynthetic acclimation of higher plants to growth in fluctuating light environments. *Photosynthesis research*, 63(1), 97-107.
- Young, A. J. (1993).** Occurrence and distribution of carotenoids in photosynthetic systems. In: Young A. J. and Britton G. (eds) *Carotenoids in Photosynthesis*, pp16-71. Chapman and Hall, London

## 8 List of abbreviations

|                               |  |
|-------------------------------|--|
| $\alpha$ -car                 | $\alpha$ -carotene                               |
| $\beta$ -car                  | $\beta$ -carotene                                |
| A                             | Antheraxanthin                                   |
| ABA                           | Absciscic acid                                   |
| APS                           | Ammonium persulfate                              |
| APX                           | Ascorbate peroxidase                             |
| ATP                           | Adenosine triphosphate                           |
| AtZEP                         | <i>Arabidopsis thaliana</i> zeaxanthin epoxidase |
| BHL                           | Before high light                                |
| bp                            | Base pair  |
| CAT                           | Catalase   |
| cDNA                          | Complementary DNA                                |
| Chl                           | Chlorophyll                                      |
| $^1\text{Chl}^*$              | Chlorophyll singlet excited state                |
| $^3\text{Chl}^*$              | Chlorophyll triplet state                        |
| CT                            | Charge transfer                                  |
| d                             | Days   |
| DIG                           | Digoxigenin                                      |
| dNTPs                         | Deoxynucleotides                                 |
| dUTP                          | 2'-Deoxyuridine, 5'-Triphosphate                 |
| DGDG                          | Digalactosyldiacylglycerol                       |
| EDTA                          | Ethylenediaminetetraacetic acid                  |
| F <sub>m</sub>                | Maximal fluorescence in the dark adapted state   |
| F <sub>o</sub>                | Minimal fluorescence in the dark adapted state   |
| F <sub>v</sub>                | Variable fluorescence                            |
| FAD                           | Flavin adenine dinucleotide                      |
| FHA                           | Forkhead associated domain                       |
| GPX                           | Glutathione peroxidase                           |
| H <sub>2</sub> O <sub>2</sub> | Hydrogen peroxide                                |

|                |  |
|----------------|--|
| h              | Hour   |
| HL             | High light                                       |
| HPLC           | High performance liquid chromatography           |
| ICM            | Intra-cytoplasmic membranes                      |
| ImZEP          | <i>Inga marginata</i> zeaxanthin epoxidase       |
| IPTG           | Isopropyl $\beta$ -D-1-thiogalactopyranoside     |
| Kb             | Kilo base pair                                   |
| KDa            | Kilo Dalton                                      |
| L              | Lutein   |
| LB             | Luria Bertani                                    |
| LHC            | Light harvesting complex                         |
| LMA            | Leaf mass per area                               |
| Lx             | Lutein epoxide                                   |
| min            | Minutes  |
| MGDG           | Monogalactosyldiacylglycerol                     |
| MW             | Molecular weight                                 |
| N              | Neoxanthin                                       |
| NADPH          | Nicotinamide adenine dinucleotide phosphate      |
| NPQ            | Non photochemical quenching                      |
| O.D.           | Optical density                                  |
| $^1\text{O}_2$ | Singlet oxygen                                   |
| $\text{O}_2^-$ | Superoxide radical                               |
| $\text{OH}^*$  | Hydroxyl radical                                 |
| PCR            | Polymerase chain reaction                        |
| PS             | Photosystem                                      |
| PSY            | Phytoene synthase                                |
| PVDF           | Polyvinylidenfluorid                             |
| qE             | $\Delta\text{pH}$ -dependent thermal dissipation |
| qi             | Photoinhibition                                  |
| qT             | State transition                                 |
| R              | Recovery   |
| RACE-PCR       | Rapid amplification of cDNA ends - PCR           |

|          |  |
|----------|--|
| RGR      | Relative growth rate                       |
| rpm      | Revolutions per minute                     |
| ROS      | Reactive oxygen species                    |
| RT       | Room temperature                           |
| RT-PCR   | Reverse transcription-PCR                  |
| s        | Seconds                                    |
| S.E.     | Standard error                             |
| SDS      | Sodium dodecyl sulfate                     |
| SDS-PAGE | SDS-polyacrylamide gel electrophoresis     |
| SL       | Strigolactone                              |
| SOD      | Superoxide dismutase                       |
| T-DNA    | Transfer-DNA                               |
| TE       | Tris-EDTA                                  |
| TEMED    | Tetramethylethylenediamine                 |
| Tris     | Tris-(hydroxymethyl)aminomethane           |
| V        | Violaxanthin                               |
| VDE      | Violaxanthin de-epoxidase                  |
| v/v      | Volume to volume                           |
| w/v      | Weight to volume                           |
| wt       | Wild type                                  |
| X-Gal    | 5-bromo-4-chloro-indolyl-galactopyranoside |
| Z        | Zeaxanthin                                 |
| ZEP      | Zeaxanthin epoxidase                       |

## 9 Supplementary material

### 9.1 *ImZep1* cDNA sequence

```

1      CACCACAATG GCTTCCACCT TGTCTTACAG CTCTCTTAAT CCCTCAACGA CATCTTTCTC
61     AAGAACCAAT TTCTCAATTC CTACTTGTAAT ATATTTTTTCA TTGGATATTC CCCCCCTGG
121    AAGCAGAACA ATTAAGCATA TGAAGAAACT GCTGCCGATT ACAGCTGCGG TGGCAGAAGC
181    ACCACCTTCT GCTTCACCGT CAACACAAAC TTTGACTGAA AATCATGAGA ATCGAACTCC
241    TCGAAAGAAG ATTCGGATAC TTGTGGCAGG CGGTGGGATC GGTGGTTTGG TTTTGTCTCT
301    AGCTGCAAAG AGGAAAGGGT TTGAAGTTTT GGTGTTTGAG AAGGATTTGA GTGCTATAAG
361    GGGGGAGGGA CAGTACAGGG GTCCAATTCA GATACAGAGT AATGCATTAG CTGCTTTGGA
421    AGCTATAGAT CCGGAGGTTG CTGATGAAGT CATGAGGGTG GGTGTGTATA CGGGTGATAG
481    AATCAATGGA CTCGTTGACG GAGTTTCTGG TTCTTGGTAC GTCAAGTTTG ATACATTCAC
541    TCCTGCAGTG GAACGTGGGC TTCCAGTCAC GAGAGTTATA AGTCGAATGA CTTTACAAGA
601    GATACTTGCC TGTGCTGTTG GAGAAGATTC CATTATGAAT TCCAGTAATG TTGTTAATTT
661    TGTGGATGAC GGAAGCAAGG TAACAGTAGA GCTTGAGAAT GGTGAGAAAT ATGATGGTGA
721    TCTATTGGTT GGAGCAGATG GTATATGGTC CAAGGTGAGG AAAAATTTAT TTGGGCCAAC
781    AGAAGCAGTT TACTCTGGCT ACACTTGTTA CACTGGCATT GCAGATTTTG TTCCTGCTGA
841    CATTGAATCT GTTGGGTATC GAGTATTCTT GGGACACAAA CAATACTTTG TGTCTTCAGA
901    TGTGGTGGG GGAAGATGC AATGGTATGC ATTTTACAAT GAGCCACCTG GTGGTGTGTA
961    TGGCCCCCAT GGAAAAAAGG AAAGGCTCCT TCGAATATTT GAGGGCTGGT GTGATAATGT
1021   AATAGATCTA TTA CTTGCCA CGAACGAAGA GGCAATTCTG CGACGGGACA TATATGATAG
1081   GATACCCATA TTCACATGGG GAAAGGGTCG TGTGACCTTG CTTGGTGATT CTGTTTCATGC
1141   CATGCAACCA AATTTGGGGC AAGGAGGATG CATGGCTATT GAGGACAGTT ATCAGCTTGC
1201   GTGGGAATTG GATAATGCAT GGGAACGAAG TATAAAATCA GGGTCTCCAA TTGACATTGA
1261   TTCTTCCCTC AGGAGCTATG AGAGAGAGAG AGTACTGCGA GTTGCCATTA TTCACGGTTT
1321   GGCAAGAATG GCGGCTCTTA TGGCTTCCAC CTATAAGGCA TATCTTGGTG TTGGTCTTGG
1381   CCCTTTAGAG TTTTGTACCA AATTTTGAAT ACCACATCCT GGAAGAGTTG GAGGGAGGCT
1441   TGTAATTGAT AAGGTTATGC CTTTAATGTT AACTTGGGTC TTAGGTGGCA ATAGCTTCAA
1501   ACTTGAAGGC AGACCTGCAT GTTGCGAGCT CTCAGACAAA GCAAATGACC AGTTACCCAA
1561   ATGGTTTCAA GATGATGATG CACTAGAACG TGCTATTAAT GGAGAGTGGA CTCTATTACC
1621   ATGTGGGGAT GAAGCAGGAC TTTTGAAGCC TATATCGTTA AGTCAAGATG AGAATAAACC
1681   CTGCATAATT GGGAGCACCC AGCAAGAGGA CCATCTAAGC CGTTCAATTG TAATACCTTC
1741   ACCACAGGTT TCTCAGACAC ATGCTCGGAT TAACTACAAG GATGGTGCCT TCTTCCTGAC
1801   TGATTTGCGC AGTCAACATG GCACCTGGAT ATCTGACAAT GAAGGAAGGA GGTATCGGGT
1861   GCCTCCAAAT TATCCTACTC GTGTCCACCC CTCTGATTGT ATCGAATTTG GTTCTGATAA
1921   GGCTGCATTT CGTGTGAAGG TGACAAGGTC TGCTCCAAGA TATTCTGAGG AAGGAACATA
1981   GGTTTTACTG GAACGATGAC TCGAG

```

Start codon (ATG) and stop codon (TGA) are underlined

## 9.2 *ImZep1*\_splice cDNA sequence

```

1      CACCACAATG GCTTCCACCT TGTCTTACAG CTCTCTTAAT CCCTCAACGA CATCTTTCTC
61     AAGAACCAAT TTCTCAATTC CTACTTGTAAT ATATTTTTCAT TTGGATATTC CCCCCCTGG
121    AAGCAGAACA ATTAAGCATA TGAAGAAACT GCTGCCGATT ACAGCTGCGG TGGCAGAAGC
181    ACCACCTTCT GCTTCACCGT CAACACAAAC TTTGACTGAA AATCATGAGA ATCGAACTCC
241    TCGAAAGAAG ATTTCGATAC TTGTGGCAGG CGGTGGGATC GGTGGTTTGG TTTTGTCTCT
301    AGCTGCAAAG AGGAAAGGGT TTGAAGTTTT GGTGTTTGAG AAGGATTTGA GTGCTATAAG
361    GGGGGAGGGA CAGTACAGGG GTCCAATTCA GATACAGAGT AATGCATTAG CTGCTTTGGA
421    AGCTATAGAT CCGGAGGTTG CTGATGAAGT CATGAGGGTG GGTGTGATAA CGGGTGATAG
481    AATCAATGGA CTCGTTGACG GAGTTTCTGG TTCTTGGTAC GTCAAGTTTG ATACATTACAC
541    TCCTGCAGTG GAACGTGGGC TTCCAGTCAC GAGAGTTATA AGTCGAATGA CTTTACAAGA
601    GATACTTGCC TGTGCTGTTG GAGAAGATTC CATTATGAAT TCCAGTAATG TTGTTAATTT
661    TGTGGATGAC GGAAGCAAGG TAACAGTAGA GCTTGAGAAAT GGTGAGAAAT ATGATGGTGA
721    TCTATTGGTT GGAGCAGATG GTATATGGTC CAAGGTGAGG AAAAATTTAT TTGGGCCAAC
781    AGAAGCAGTT TACTCTGGCT ACACCTTGTTA CACTGGCATT GCAGATTTTG TTCTGCTGA
841    CATTGAATCT GTTGGGTATC GAGTATTCTT GGGACACAAA CAATACTTTG TGTCTTCAGA
901    TGTTGGTGGG GGAAGATGCA AATGGTATGC ATTTCACAAT GAGCCACCTG GTGGTGTGGA
961    TGGCCCCCAT GGAAAAAAGG AAAGGCTCCT TCGAATATTT GAGGGCTGGT GTGATAATGT
1021   AATAGATCTA TTACTTGCCA CGAACGAAGA GGCAATTCTG CGACGGGACA TATATGATAG
1081   GATACCCATA TTCACATGGG GAAAGGGTCG TGTGACCTTG CTGGTGATT CTGTTTATGC
1141   CATGCAACCA AATTTGGGGC AAGGAGGATG CATGGCTATT GAGGACAGTT ATCAGCTTGC
1201   GTGGGAATTG GATAATGCAT GGAACGAAG TATAAAATCA GGGTCTCCAA TTGACATTGA
1261   TTCTTCCCTC AGGAGCTATG AGAGAGAGAG AGTACTGCGA GTTGCCATTA TTCACGGTTT
1321   GGCAAGAATG GCGGCTCTTA TGGCTTCCAC CTATAAGGCA TATCTTGGTG TTGGTCTTGG
1381   CCCTTTAGAG TTTTGTGACCA AATTTTCAAT ACCACATCCT GGAAGAGTTG GAGGGAGGCT
1441   TGTAATTGAT AAGGTTATGC CTTTAATGTT AACTTGGGTC TTAGGTGGCA ATAGCTTCAA
1501   ACTTGAAGGC AGACCTGCAT GTTGCAGACT CTCAGACAAA GCAAATGACC AGTTACCCAA
1561   ATGGTTTCAA GATGATGATG CACTAGAACG TGCTATTAAT GGAGAGTGGA CTCTATTACC
1621   ATGTGGGGAT GAAGCAGGAC TTTTGAAGCC TATATCGTTA AGTCAAGATG AGAATAAACC
1681   CTGCATAATT GGGAGCACCC AGCAAGAGGA CCATCTAAGC CGTTCAATTG TAATACCTTC
1741   ACCACAGGTT TCTCAGACAC ATGCTCGGAT TATCCTACTC GTGTGAAGGT GACAAGGTCT
1801   GCTCCAAGAT ATTCTGAGGA AGGAACATAAG GTTTTACTTG AACGATTGACT CGAG

```

Start codon (ATG) and stop codon (TGA) are underlined

## 9.3 *ImZep2* partial cDNA sequence

```

1      ACCTGGTGGC ATGGATGGAA CCCACTATTA CATGGGTGTG ATCCCCTACC TGGTGGCATG
61     GATGCCCCC ATGGTAAAAA GGATAGGCTC TTGAAAATAT TTGAGGGTTG GTGTGATAAT
121    GTGATAGATT TGCTACTGAC CACAGATGAA GATTCCATTC TTCGACGTGA CATTATGAC
181    TAGGGAACCC ATA

```

## 10 List of tables and figures

|  |    |
|--|----|
| Figure 1.2.1: Photosystem II   | 2  |
| Figure 1.5.1: Xanthophyll biosynthetic pathway   | 7  |
| Figure 1.5.2: Xanthophyll binding sites in the LHCII of green plants                                 | 8  |
| Figure 1.7.1: Model of the lipocalin structure and sequence alignment of the three conserved motifs  | 12 |
| Table 2.1 List of vectors  | 14 |
| Table 2.2 Primer List  | 15 |
| Table 2.3 List of bacteria   | 16 |
| Table 2.4 List of plants   | 17 |
| Figure 2.2.1: <i>Rhodobacter capsulatus</i>  | 18 |
| Table 2.5 PCR program  | 22 |
| Table 2.6 Primer pairs   | 23 |
| Table 2.8 Program for real-time PCR  | 30 |
| Figure 3.1.1: Bioinformatical analysis of the partial amino acid sequence of ImZEP1 and ImZEP2       | 42 |
| Figure 3.1.2: Deduced amino acid sequence alignment of <i>Zep</i> from several plant species         | 43 |
| Figure 3.1.3: Gene expression level of <i>ImZep1</i> and <i>ImZep2</i> in <i>I. marginata</i> leaves | 45 |
| Figure 3.1.4: Alignment of the deduced amino acid sequence of <i>ImZep1</i> and <i>ImZep1_splice</i> | 46 |

|  |    |
|--|----|
| Figure 3.1.5: Real-time-PCR and western blot analysis of transformed <i>R. capsulatus</i>  | 48 |
| Figure 3.1.6: Western blot analysis of protein extracts from the transformed <i>E. coli</i> BL21(DE3)  | 49 |
| Figure 3.1.7: Morphology of <i>A. thaliana</i> wt (Col-0), <i>npq2</i> mutants and the transgenic lines 20.72, 24.75 and 34.25   | 51 |
| Figure 3.1.8: RT-PCR of <i>ImZep1</i> and <i>AtZep</i> transcripts in the transgenic lines   | 52 |
| Figure 3.1.9: Western blot analysis of ZEP protein   | 52 |
| Figure 3.1.10: HPLC chromatograms of leaf pigment extract from wt, <i>npq</i> and transformed plants   | 54 |
| Figure 3.1.11: RT-PCR of <i>ImZep1</i> transcript  | 57 |
| Figure 3.1.12: HPLC chromatograms of leaf pigment extracts from <i>szl1npq1</i> and 565.02 transgenic line (T1)  | 57 |
| Figure 3.1.13: Levels of N and the V-cycle pigments (V,A and Z) during the high-light treatment and subsequent recovery  | 59 |
| Figure 3.1.14: Quantum yield of PSII photochemistry in wt and <i>npq2</i> plants as well as the transgenic lines during the high-light treatment and subsequent recovery | 61 |
| Figure 3.1.15: Changes in NPQ in wt and <i>npq2</i> plants as well as the transgenic lines   | 62 |
| Figure 3.1.16: Leaf growth of wt and <i>npq2</i> plants as well as the transgenic lines  | 64 |
| Figure 3.2.1: Carotenoid composition in dark-adapted leaves of wild type, <i>lut2</i> , <i>lut5</i> , <i>szl1npq1</i> and <i>npq1</i> plants                             | 68 |
| Figure 3.2.2: Chlorophyll content of dark-adapted leaves of wild type and mutant plants harvested on day 7   | 70 |

|  |    |
|--|----|
| Figure 3.2.3: Maximal photosystem II efficiency (Fv/Fm) of dark-adapted leaves of wild type and mutant plants during 7-day exposure to the control or sunfleck condition   | 71 |
| Figure 3.2.4: Light induction and dark relaxation of non-photochemical quenching (NPQ) in wild type, <i>lut2</i> , <i>lut5</i> , <i>szl1npq1</i> and <i>npq1</i> plants during 7-day exposure to the control or sunfleck condition | 73 |
| Figure 3.2.5: Levels of PsbS protein in leaves of wild type and mutant plants  | 75 |
| Figure 3.2.6: Leaf relative growth rate (RGR) and leaf mass per area (LMA) of wild type and mutant plants during 10 days under the control or sunfleck condition   | 76 |
| Figure 3.2.7: Root growth analysis in wild type and mutants during the 5-day exposure to the control and sunfleck condition or 17-day cultivation in high-osmolarity medium containing 100 mM sorbit                               | 78 |
| Figure 3.2.8: Seed harvest of wild type and mutant plants grown under the control or sunfleck condition  | 79 |
| Table 4.1 Summary of the sunfleck responses of different parameters in wt and the four carotenoid mutants of <i>A. thaliana</i>  | 87 |

## Acknowledgements

I would like to thank Prof. Ulrich Schurr for giving me the opportunity to work on an interesting PhD project at the institute of plant sciences (IBG-2) as part of the Forschungszentrum Jülich and his continual support during all stages of this dissertation. I am also very grateful to Prof. Peter Jahns at the Heinrich Heine University of Düsseldorf, who kindly agreed to act as referee and commentator of my work.

Many thanks to Dr. Shizue Matsubara for her continuous presence and for being extremely helpful and understanding during the course of my PhD, trusting in my abilities and teaching me how to cope with the difficulties of science. I learned a lot from her and she will always be an example for my future science career.

Thanks to Prof. Roberto Bassi, Dr. Anika Wiese-Klinkenberg, Dr. Thomas Drepper, Dr. Achim Heck and Prof. Inga Janzik for their helpfulness and precious advices.

Thanks to all the colleagues at the IBG-2 institute for providing such a pleasant work environment.

I would have never reached this important goal of my life without the support of my family, grazie di cuore per essermi sempre vicini.

# Curriculum vitae

**ROSANNA CALIANDRO**

Current address: Wiesenstrasse 6g 52428 Juelich, Germany

Tel.: +49(0)17627587479

E-mail: rosanna.caliandro@gmail.com

Home address: via Robert Schuman 15/11 Bari, Italy

Born on/in: 02-Jan-1981 in Bari, Italy

Nationality: Italian

Marital status: Single

## CURRENT POSITION

Institute of Bio- and Geosciences (IBG): Plant Sciences

Forschungszentrum Juelich -- Heinrich-Heine University Duesseldorf

**PhD student in Biology**

**January 2008 – present**

PhD project

Investigation of the biosynthesis of lutein epoxide and the roles of  $\alpha$ -branch carotenoids in photoprotection and photoacclimation

**Dissertation defence: December 2011**

## EDUCATION

University of Bari, Italy

**Laurea (M.S. equivalent), Biological Sciences with specialization in Molecular Biology**

**July 2007**

Master degree thesis

Proteomic and functional analysis of water soluble protein fraction extract from *Rhodobacter sphaeroides* cells grown in presence of cobalt ions

## TECHNICAL COMPETENCES AND SKILLS

### Molecular biology and biochemical techniques

- Genomic DNA and RNA extraction from leaves (*Arabidopsis thaliana* and *Inga marginata*)
- cDNA synthesis
- RT-PCR
- RACE PCR
- Agarose gel electrophoresis
- Cloning of cDNA sequences in GATEWAY TOPO TA and pUC vectors as well as expression vectors (GTEWAY; pRhot-vector, specific for *R.sphaeroides* )
- Southern and northern blotting
- Bioinformatic analysis of gene and protein sequences
- Protein extraction from leaves (*A. thaliana*)
- SDS-PAGE and western blotting
- Two-dimensional gel electrophoresis
- *Agrobacterium*-mediated plant transformation by floral dip method
- Preparation of selective plates and isolation of transformants

### Microbiological techniques

- Preparation of *Escherichia coli*, *Rhodobacter sphaeroides* and *A. tumefaciens* bacterial cultures
- Transformation of *E. coli*
- Isolation of plasmidic DNA from *E. coli*
- Transformation of *Agrobacterium* by freeze-thaw method
- Transformation of *R. sphaeroides* by using biparental conjugation
- Protein extraction form *R. sphaeroides* and *E. coli*
- Genomic DNA and RNA extraction from *R. sphaeroides*

### Analytical techniques

- Photosynthetic pigment extraction from leaves (*A. thaliana*, *I. marginata* and *Persea americana*)
- Separation and analysis of photosynthetic pigments by HPLC

### Phenotyping of *A. thaliana* plants

- Leaf growth analysis by using a method based on chlorophyll fluorescence images

- Analysis of root growth and architecture based on images of roots growing inside agarose plates
- Determination of photosystem II activities by chlorophyll a fluorescence analysis

#### Computational skills

Familiar with the following software:

- Microsoft office
- SigmaPlot
- DNAMAN
- Empower (HPLC software of Waters)

#### Supervisory experience:

Supervised two students during their internship and a bachelor student

### CONFERENCES AND WORKSHOPS

Participation in the **Symposium on Plant Responses to Light Stress** organized by the IBG-2 Institute of Plant Sciences of Forshcungszentrum Juelich **March 2009**

Participation in the **Expresso Workshop on Protein Expression** organized by the Institute for Molecular Enzyme Technology of Heinrich-Heine University Duesseldorf **April 2010**

Poster presentation at the **15th International Congress on Photosynthesis** in Beijing organized by the International Society of Photosynthesis Research **August 2010**

Participation in the **Symposium “Assimilating Photosynthesis –Quintessence of Life’s Variations and Vital Inefficiencies”** organized by the IBG-2 Institute of Plant Sciences of Forshcungszentrum Juelich **April 2011**

Participation to the international botanical congress **Botanikertagung 2011** in Berlin organized by the German Botanical Society **September 2011**

### MEMBERSHIPS

Member of the International Society of Photosynthesis Research **2010-2011**

## PRESENTATIONS

Oral presentation at the **Symposium on Plant Responses to Light Stress** in Juelich. Title of the talk:  
**"Molecular Characterization of Zeaxanthin Epoxidase from *Inga marginata*"** **March 2009**

Poster presentation at the **15th International Congress on Photosynthesis** in Beijing.  
Title of the poster: **"Roles of the  $\alpha$ -branch Carotenoids in Photoprotection and Photoacclimation under Fluctuating Light"** **August 2010**

Co-author of the oral presentation **"Fluorescence Lifetime Imaging (FLI), Non-Photochemical Quenching (NPQ) and Photosynthesis: Avocado Leaves"** held by Prof. Govindjee (University of Illinois) at the **International Workshop "Mechanisms of Non-Photochemical Quenching"** in Passau **April 2011**

Poster presentation at the **Botanikertagung 2011** in Berlin. Title of the poster: **"Investigation of the role of zeaxanthin epoxidase in the lutein epoxide cycle"** **September 2011**

## PUBLICATIONS

Matsubara S., Chen Y.-C., **Caliandro R.**, Govindjee, Clegg R.M. (2011) "Photosystem II fluorescence lifetime imaging in avocado leaves: Contributions of the lutein-epoxide and violaxanthin cycles to fluorescence quenching". *Journal of Photochemistry and Photobiology B: Biology*  
doi:10.1016/j.photobiol.2011.01.003

**Caliandro R.**, Nagel K.A., Kastenholz BJ, Bassi R., Pogson BJ, Schurr U. Matsubara S.  
"Effects of altered  $\alpha$ - and  $\beta$ -branch carotenoid biosynthesis on acclimation of *Arabidopsis* to photo-oxidative stress induced by short sunflecks" (submitted)

## LANGUAGES

**Italian:** mother tongue

**English:** fluent

**German:** basic knowledge